
# UNIVERSITÀ DEGLI STUDI DI ROMA "TOR VERGATA"

FACOLTA' DI INGEGNERIA

DOTTORATO DI RICERCA IN INGEGNERIA AMBIENTALE

XXIV CICLO

# Development of risk assessment models and tools for the management of contaminated sites

Iason Verginelli

A.A. 2010/2011

Tutor: Prof. Renato Baciocchi

Coordinatore: Prof. Renato Gavasci

| | |
|---|---|
| Title of dissertation: | Development of risk assessment models and tools for the management of contaminated sites |
| Author: | Iason Verginelli |
| Tutor: | Renato Baciocchi |
| Coordinator: | Renato Gavasci |
| Research institution: | Università degli studi di Roma "Tor Vergata"<br>Facoltà di Ingegneria |
| Course: | Dottorato in Ingegneria Ambientale (XXIV ciclo) |
| Research period: | October 2008 – October 2011 |

# ABSTRACT

In the last decades soil and groundwater contamination caused by abandoned waste disposal sites and industrial activities has become a key environmental issue in most of advanced countries. Risks for human health, as a result of toxic chemicals introduced into the environment, are in fact a matter of main concern to modern society and the effective management of environmental contamination problems has become an important environmental priority of both national and European policies. In this framework, the management of contaminated sites often relies on a risk-based corrective action (RBCA) approach, where the actual pollution of the site is evaluated depending on the effective risk posed to the human health or environment. For instance, this is the case of the Italian regulatory approach, where the guidelines for risk assessment application developed by the national environmental agency (ISPRA) are based on the RBCA procedure. According to this approach, environmental management decisions and remedial actions that are taken at a site, are evaluated and prioritized based on the actual reduction in risk that would result from their implementation. This result is achieved by assessing the potential risks that chemicals at a site may pose to human health and the environment. The main strength of the RBCA procedure relies in its capacity of evaluating risks to human health through relatively simple fate and transport and exposure models. However, such models are usually based on very simplifying assumptions. Among these, a key one consists in neglecting natural attenuation processes taking place in the subsurface, that several experimental and field studies in the last decades have shown to be particularly relevant. These processes, acting without human intervention, can in fact lead to a significant reduction of the mass, toxicity, mobility, volume and concentrations of contaminants, that are not accounted for in the RBCA risk procedure, possibly inducing an overestimation of risks. The main focus of this Ph.D. thesis was to analyze these issues, by developing different alternative modeling approaches accounting for the key natural attenuation processes

occurring in the subsurface, which were applied to different contamination scenarios. In particular, the attention was focused on vapor intrusion of volatile organic compounds (VOC) from contaminated soil and groundwater into indoor environments, transport and natural attenuation of contaminants in groundwater and leaching of contaminants to groundwater from dissolved plumes located in the unsaturated zone. In addition, in order to highlight the relevance of the different attenuation processes occurring in the subsurface and to assess the feasibility for their inclusion in the risk assessment procedures, the developed models were applied to several contamination scenarios and compared with the results obtained applying the traditional ASTM-RBCA approach. The obtained results showed that in many cases the standard RBCA approach may lead, for some types of constituents and soils, to extremely conservative results in terms of risk. On the contrary, the developed models have provided more realistic results with respect to the ASTM-RBCA procedure and thus may represent a simple but meaningful integration of the traditional approach, since they keep its original simplicity, but allow to overcome its limitations in correctly managing risk for specific site conditions.

Finally, another aspect addressed concerned the use of a suitable software for the application of the risk-assessment procedure to contaminated sites. As a matter of fact, in Italy there are different risk assessment softwares available but none of these fully applies the RBCA procedure defined by the national guidelines issued by ISPRA. To overcome this limitation, a new software called Risk-net, integrally based on the ISPRA guidelines for risk analysis, was developed. The software has been validated by the Reconnet network and is now available for free on the website of the network: www.reconnet.net.

# SOMMARIO

La contaminazione nei terreni e nelle acque sotterranee causata dallo smaltimento di rifiuti abbandonati e da attività industriali è diventata negli ultimi decenni una questione di fondamentale importanza nella maggior parte dei paesi industrializzati. Infatti i rischi per la salute umana causati da sostanze chimiche tossiche introdotte nell'ambiente risultano una delle principali fonti di preoccupazione per la società moderna e pertanto la corretta ed efficace gestione dei problemi di contaminazione ambientale è diventata una priorità nelle politiche nazionali ed europee. In questo contesto, la gestione dei siti contaminati prevede spesso un approccio basato sull'analisi di rischio (RBCA), in cui l'inquinamento riscontrato in un sito viene valutato sulla base dei rischi per la salute umana o l'ambiente. Questo ad esempio è il caso dell'approccio normativo italiano, in cui le linee guida di riferimento per l'applicazione dell'analisi di rischio, sviluppate dall'Istituto Superiore per la Protezione e la Ricerca Ambientale (ISPRA), applicano l'approccio RBCA ai siti interessati dal rilascio di contaminanti. Secondo tale approccio, la gestione e le eventuali azioni correttive da intraprendere in un sito, vengono orientate sulla base della effettiva riduzione del rischio che deriverebbe dalla loro attuazione. Questo viene fatto mediante una valutazione dei potenziali rischi per la salute umana e l'ambiente associati alle diverse sostanze chimiche riscontrate nel sito. La principale peculiarità della procedura RBCA consiste nella sua capacità di valutare i rischi per la salute umana attraverso l'utilizzo di modelli di trasporto ed esposizione relativamente facili da applicare. Tuttavia tali modelli si basano spesso su ipotesi di base estremamente semplificative trascurando la maggior parte dei processi di attenuazione naturale che avvengono nel sottosuolo che diversi studi sperimentali e di campo negli ultimi decenni hanno dimostrato essere particolarmente rilevanti. Questi processi, che agiscono senza intervento umano, possono infatti condurre ad una riduzione della massa, tossicità, mobilità, volume e concentrazione dei contaminanti e pertanto non

tenerne conto nella valutazione dei rischi può condurre ad una significativa sovrastima degli effettivi impatti.

L'obiettivo principale del dottorato è stato quello di analizzare e approfondire tali tematiche attraverso lo sviluppo di modelli di trasporto che tenessero conto dei processi chiave di attenuazione naturale che avvengono generalmente nel sottosuolo. In particolare, l'attenzione si è focalizzata sul processo di intrusione all'interno degli edifici di composti organici volatili (VOC) derivanti da suoli e acque sotterranee contaminate, sul trasporto e attenuazione di contaminanti nelle acque sotterranee e sulla lisciviazione dei contaminanti da suolo insaturo in falda. Inoltre, al fine di evidenziare la rilevanza dei diversi processi di attenuazione considerati e al fine di valutare la fattibilità di un loro inserimento nelle procedure di analisi di rischio, i modelli sviluppati sono stati applicati a diversi scenari di contaminazione e confrontati con i risultati ottenuti applicando il tradizionale approccio ASTM-RBCA. Le elaborazioni effettuate hanno mostrato che in molti casi l'approccio standard può condurre, per alcuni tipi di sostanze e terreni, a risultati estremamente conservativi in termini di rischio. Viceversa, i modelli sviluppati hanno fornito risultati più realistici rispetto alla procedura ASTM-RBCA e possono quindi rappresentare una semplice ma significativa integrazione dell'approccio tradizionale, in quanto mantengono la semplicità originale prevista nella procedura di analisi di rischio, ma permettono di superarne alcuni limiti ai fini di una più accurata valutazione e gestione del rischio.

Infine, un altro aspetto affrontato ha riguardato l'utilizzo di un software idoneo per l'applicazione della procedura di analisi di rischio prevista in Italia. A livello nazionale non è infatti disponibile uno strumento che consenta di applicare integralmente la procedura definita nelle linee guida ISPRA (2008). Per superare questa limitazione, in questo lavoro è stato sviluppato un nuovo software, chiamato Risk-net, progettato al fine di applicare tutti i calcoli necessari per il processo di pianificazione definito dall'ISPRA (2008). Il software è stato validato dalla rete Reconnet ed è ora disponibile gratuitamente sul sito della rete: www.reconnet.net.

# ACKNOWLEDGMENTS

I gratefully acknowledge my tutor, Renato Baciocchi, for his interest as well as qualified and very useful advices and support during the project.
Also, I would like to thank Giovanni Grillo, formerly eni researcher, and Eugenio Sordini and Felicia Massetti of eni for having introduced me to the topic of natural attenuation.
I would like to acknowledge Simona Berardi of Higher Institute for Workers Safety and Health (ISPESL, now INAIL), Laura D'Aprile of National Higher Institute for Environmental Research (ISPRA), Andrea Forni of SGM Ingegneria, Antonio Traversa of Regional Environmental Agency of Lazio region (ARPA Lazio), Andrea Sconocchia of Regional Environmental Agency of Umbria region (ARPA Umbria) and Igor Villani of Province of Ferrara for the useful advices for the refinement of the Risk-net software.
Last but not least, I would like to thank my family for their constant support and encouragement during this research program.

This research was partially funded by eni refining & marketing division (Rome).

# TABLE OF CONTENTS

# INTRODUCTION

## RISK ASSESSMENT TO CONTAMINATED SITES

In most of industrialized countries, the management of contaminated sites often relies on a risk-based approach, where the actual pollution of the site is evaluated depending on the effective risk posed to the human health or environment. Namely, in the case of a potentially contaminated site, investigation typically follows a stepwise approach starting with a preliminary screening investigation followed by a site-specific risk-based assessment (Provoost et al. 2006). In this context, risk assessment results a very useful tool, because it gives a rational and objective starting point for priority setting and decision making (Ferguson et al. 1998). In fact, even though the use of predetermined guideline values is simple and less expensive than more elaborate site-specific assessment methods, its exclusive application would result in a poor site-specificity and consequently could lead to extremely conservative clean-up actions. In this view, a combined approach, using predetermined screening values to simplify the preliminary stages of decision making and then site-specific risk assessment to evaluate clean-up levels in later stages of an investigation, is generally considered the most appropriate (Ferguson et al. 1998).

The most acknowledged technical and scientific references for the risk-assessment approach are the ASTM Risk-Based Corrective Action (RBCA) standards for evaluating petroleum sites (E 1739-95) and chemical release sites (E 2081-00). The procedure outlined in these documents is based on the information collected during the contaminated site investigation, which are used to evaluate the potential effects on the health of exposed receptors and on the environment, allowing to assess whether a particular site requires remedial action and eventually the specific risk-based remediation goals. Namely the risk is defined by using site-specific data concerning

receptors, exposure potential, site hydrogeology and the type, amount, and toxicity of the chemicals of concern.

The ASTM RBCA is based on a "tiered" approach to risk and exposure assessment, where each tier refers to a different level of complexity (Figure I.1). Namely in Tier 1, aimed to the definition of the contamination screening values, only on-site receptors are considered, transport of contaminants is described through simple analytical models and conservative default values are used for all hydro-geological, geometrical and exposure data, without requiring any site characterization.

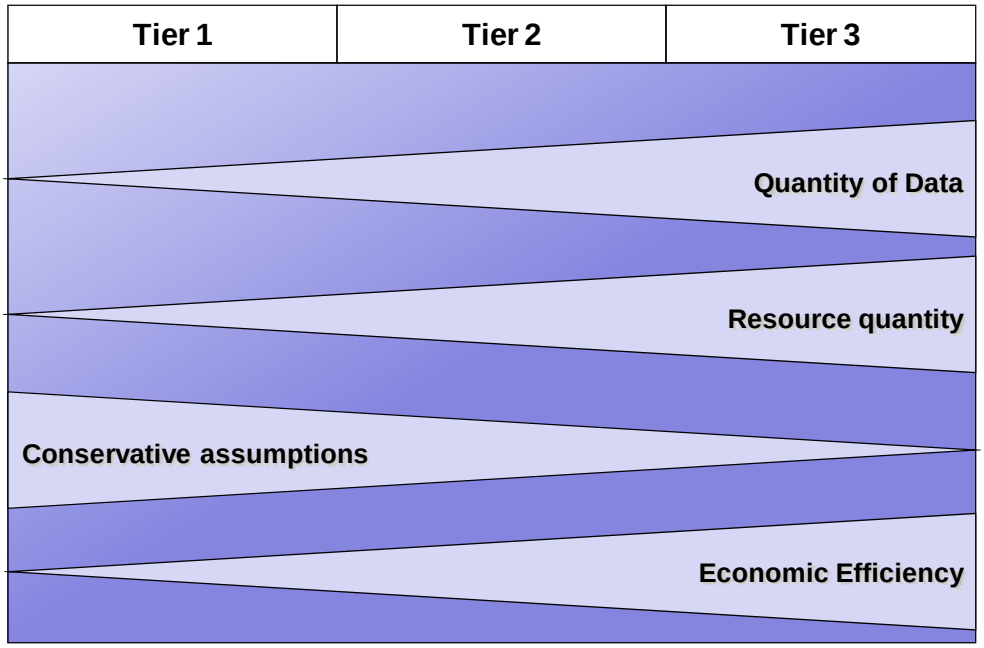


**Figure I.1.** Risk assessment level characterization.

In Tier 2, aimed to evaluate site-specific target levels, off-site receptors are included in the conceptual model, all input data should possibly be site-specific, whereas the models used to describe contaminants transport are still analytical. Finally, fate and transport modeling in Tier 3 application usually involves the use of numerical models which can simulate time-dependent constituent migration under conditions of spatially-varying properties of the environmental media through which migration is occurring. In Italy the risk analysis procedure is performed using the Tier 2 conditions, that represent a

reasonable compromise between the need for a detailed site assessment and the advantage of handling a rather simple and easy-to-use management tool. In addition, data collection for fate and transport models in Tier 2 application is typically limited to relative economically or easily to obtain site-specific data. Most of the data collected for this application are related to the geometric description of the area, to the physical properties of the environmental media through which migration is occurring and to constituent concentrations in source areas. Therefore, only in very specific situations, where a more detailed description of the contaminant transport through numerical models is required, risk analysis is performed following the Tier 3 approach.

## RISK CALCULATION

In this framework, the risk for human health correlated to the exposure to a given contaminant, is calculated applying the following general equation:

$$R = E \cdot T \tag{I.1}$$

Where $T$ is the contaminant toxicity. The individual risk is defined as the risk for human health associated to a specific exposure route and to a single contaminant. Its determination is performed in a different way, depending on the type of contaminant's effects (carcinogenic or toxic), that the given compound may have on the human health receptor (U.S.EPA, 1989). Namely, in the case of carcinogenic compounds:

$$R = E \cdot SF \tag{I.2}$$

Where $R$ is the life-long probability of incremental cancer case occurrence, caused by exposure to the contaminant, $SF$ (slope factor) is the probability of incremental cancer case occurrence per unit dose, $E$ is the exposure, averaged to a lifetime exposure duration ($AT$ = 70 years).
For toxic, non-carcinogenic effects:

$$HQ = E / RfD \tag{I.3}$$

where $HQ$ is the so-called "Hazard Quotient", defined as the ratio between the actual exposure to a given contaminant and the corresponding maximum allowable or

reference dose, *RfD* (Reference Dose), i.e. the daily exposure rate that does not induce adverse effects on humans during the entire life-time; and *E* is the daily chronic contaminant exposure rate. The latter one is the product of the contaminant's concentration at the point of exposure, $C_{poe}$, with the effective exposure rate, *EM*, that may correspond to the daily ingested soil amount, inhaled air volume or ingested water volume, per unit body weight, depending on the exposure pathway considered:

$$E = EM \cdot C_{poe} \tag{I.4}$$

The estimation of the effective exposure rate requires evaluating the daily dose of the contaminated matrix that is assumed by the human receptors identified in the conceptual model (D'Aprile et al. 2008).

The effective exposure rate, *EM,* depends on the ingestion or inhalation rate, *CR*, the Exposure Frequency, *EF*, the Exposure Duration, *ED*, the Body Weight, *BW*, and the Averaging Time, *AT*. The general form of the equation used to estimate this parameter is as follows:

$$EM = \frac{CR \cdot EF \cdot ED}{BW \cdot AT} \tag{I.5}$$

The concentration at the point of exposure, $C_{poe}$, is estimated introducing the appropriate transport factor, *FT*:

$$C_{poe} = FT \cdot C_s \tag{I.6}$$

The transport factor, *FT*, accounts for the physical and chemical properties of the contaminant, the mechanism of the contaminant's release to the different environmental compartments, the physical and chemical properties of the environmental matrix through which migration occurs and the interactions between the contaminant and the matrix along the migration pathway.

By setting the total risk for carcinogenic effects at a target risk level (e.g. TR = $10^{-6}$ for carcinogenic contaminants and THI = 1 for non carcinogenic contaminants) it is possible to solve the above equations for the concentration term, obtaining the risk-based clean-up goals:

$$CSR = \frac{C_{poe}}{FT} = \frac{E}{EM \cdot FT} = \frac{TR}{SF \cdot EM \cdot FT} \qquad \text{for carcinogenic contaminants} \qquad \text{(I.7)}$$

$$CSR = \frac{Cpoe}{FT} = \frac{E}{EM \cdot FT} = \frac{THI \cdot RfD}{EM \cdot FT} \qquad \text{for non carcinogenic contaminants} \qquad \text{(I.8)}$$

Where *TR* is the target Risk for the single constituent and *THI* the Target Hazard Index. The above calculations should be applied for each contaminant, medium and land-use combination and involves identifying the different appropriate exposure pathways and routes (e.g. residential ingestion of soil) and exposure parameters (e.g. 1 mg/day of soil ingested). To this end, a conceptual site model should be developed. The definition of conceptual model is used to identify all potential or suspected sources of contamination, types and concentrations of contaminants detected at the site, potentially contaminated media and potential exposure pathways, including receptors (see Fig. I.2).

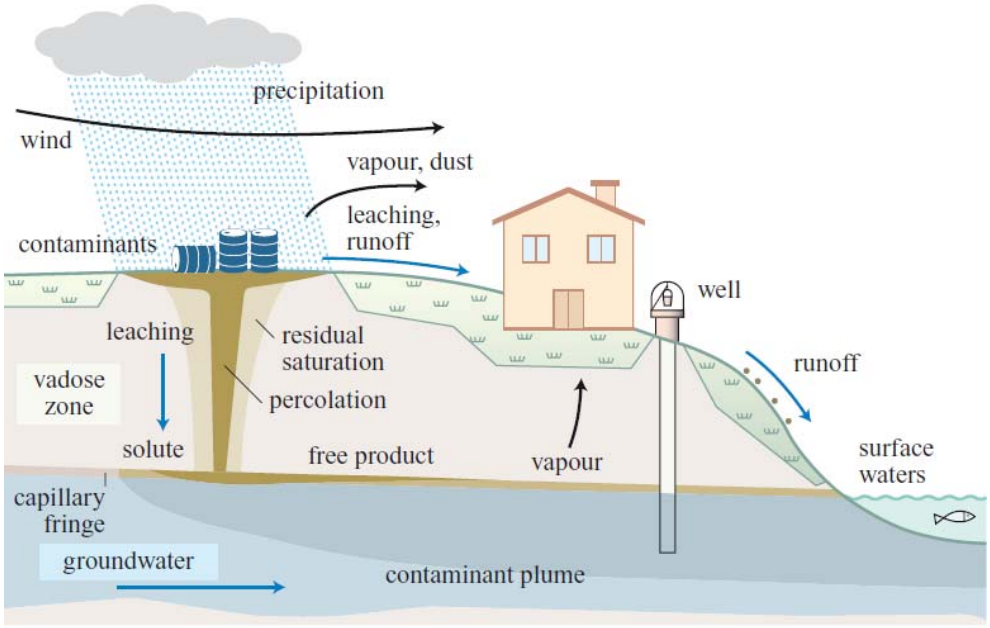


**Figure I.2.** A graphical representation of a conceptual site model (Grillo and Pedroni, 2007).

The migration pathways usually considered in the RBCA approach are:

From Surface Soil
- Outdoor volatilization
- Indoor volatilization
- Outdoor particulate emission
- Indoor particulate emission
- Leaching to groundwater

From Subsurface Soil
- Outdoor volatilization
- Indoor volatilization
- Leaching to groundwater

From Groundwater
- Outdoor volatilization
- Indoor volatilization
- Groundwater transport

The exposure pathways usually considered are:

- Dermal contact with soil
- Ingestion of soil
- Inhalation of vapors in outdoor environments
- Inhalation of vapors in indoor environments
- Inhalation of particulate matter in outdoor environments
- Inhalation of particulate matter in indoor environments
- Inhalation of particulate matter in outdoor environments
- Inhalation of particulate matter in indoor environments
- Ingestion of water

## AIMS AND CONTENTS OF THIS THESIS

Despite the risk-based approach for the management of contaminated sites has clear advantages, the experience and the better understanding of the different natural processes occurring in the subsurface gained over the years have highlighted some critical issues of the Tier 2 RBCA application. The purpose of this research was to analyze these problems and provide, where possible, alternative solutions.

Specifically, a preliminary study was designed to evaluate the consistency of the combined use of predetermined guideline, defined by the Italian law, and risk-based clean-up values (not reported in this thesis, for more information see the supporting documentation in the attached CD).

Afterwards, the core of the research, discussed in this thesis, was addressed to evaluate the fate and transport models used in the Tier 2 risk-assessment procedure. In fact, it is well known that the ASTM fate and transport models in many cases result too simplified as they neglect several natural attenuation processes occurring in the subsurface. Natural Attenuation refers to naturally-occurring processes in soil and groundwater environments that act without human intervention (U.S.EPA, 1999) and that can be particularly effective in reducing the mass, toxicity, mobility, volume and concentrations of contaminants. These natural processes include biological degradation, volatilization, dispersion, dilution, and sorption of the contaminant onto the organic matter and clay minerals in the soil (Mulligan and Yong, 2004). In the last decades several studies have demonstrated the occurrence of natural attenuation by studying the attenuation in the unsaturated zone (Lundegard and Johnson 2006; Johnson et al. 2006; Kastanek et al. 1999), the evolution of the plume length (Shih et al. 2004; Newell and Connor, 1998; Prommer et al. 2002, Kao and Prosser, 2001), the mass reduction (Christensen et al. 2000), the geochemical processes (Cozzarelli et al. 2001) and the vertical vapors profiles (Hers et al. 2000; Roggemans et al. 2000; Hohener et al. 2003)
As a results, the application of the ASTM models, which neglect almost all the processes described above, can lead in many cases to a significant overestimation of constituent concentrations at the point of exposure (i.e. conservative predictions of constituent migration and attenuation) and consequently of the risk-based site-specific clean up-levels. To overcome this limitation, in this work different alternative modeling approaches accounting for the key natural attenuation processes occurring in the subsurface, while keeping the analytical form required for the RBCA Tier 2 application, were developed. Namely the attention was focused on the main critical migration pathways generally observed in contaminated sites. In this view, alternative analytical models were developed for vapor intrusion of volatile organic compounds (VOC) from contaminated soil and groundwater into indoor environments (**Section 1**), transport and natural attenuation of contaminants in groundwater (**Section 2**) and leaching of contaminants to groundwater from dissolved plumes located in the unsaturated zone (**Section 3**). In addition, in order to highlight the relevance of the different attenuation processes occurring in the subsurface and to assess the feasibility for their inclusion in the risk assessment procedures, the developed models were applied to several

contamination scenarios and compared with the results obtained applying the traditional ASTM-RBCA approach.

Last but not least, another aspect addressed concerned the use of a suitable software for the application of the risk-assessment procedure to contaminated sites. As a matter of fact, in Italy there are different risk assessment softwares available (e.g. the American softwares RBCA ToolKit and RISC and the Italian ones GIUDITA and ROME) but none of these fully applies the RBCA Tier 2 procedure defined by the national guidelines issued by ISPRA according to the Italian law (D.Lgs 152/06 and D.Lgs 04/08). To overcome this limitation a new software, called Risk-net, was developed. This software was designed to complete all calculations required for the ISPRA (2008) guidelines for risk analysis, allowing to assess the potential effects on the health of exposed receptors and on the environment and, eventually, the specific risk-based remediation goals. Risk-net has been validated by the Reconnet network (Italian network for the management and remediation of contaminated sites) and is now available for free download from the website of Reconnet: www.reconnet.net. In **Section 4** a general description of the Risk-net software design, followed by a description of the main features and detailed information on modeling and calculation procedures is reported.

# SECTION 1

# VAPOR INTRUSION FROM HYDROCARBON CONTAMINATED SOURCES

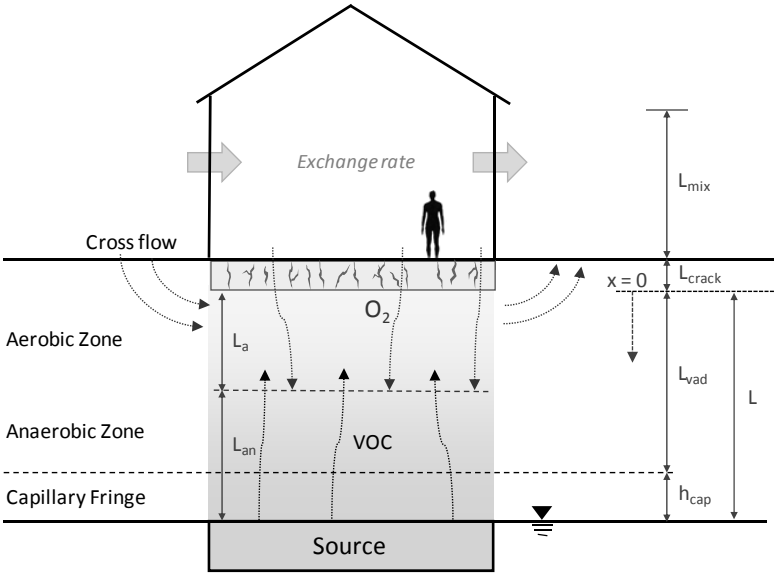


*This chapter is partially taken from:*

*Verginelli I., Baciocchi R. (2011). Modeling of vapor intrusion from hydrocarbon-contaminated sources accounting for aerobic and anaerobic biodegradation. Journal of Contaminant Hydrology 126 (3–4), 167–180.*

## BACKGROUND

Natural attenuation can significantly influence the potential impact of petroleum hydrocarbon releases, by reducing, mainly through biodegradation processes, the mass, mobility and concentration of contaminants. These processes can be particularly effective in attenuating petroleum hydrocarbon vapors, either from groundwater or unsaturated soil sources.

Nevertheless, most risk assessment procedures do not include vapor degradation as a standard feature for developing clean-up levels (e.g. ASTM, 2000). This assumption can lead to an overestimation of the overall human health risk, since vapor intrusion to indoor air is one of the most important exposure pathways at many contaminated sites impacted by volatile compounds (Hers et al., 2003). Consequently the significance of this pathway is the subject of intense debate (Johnson et al., 1998) and in the last years this issue has been the focus of a number of studies. Actually this topic has been addressed since the 1980s, initially with the emphasis placed on assessing impacts of naturally occurring radon intrusion (e.g. Nazaroff et al., 1997; Robinson et al., 1997; Garbesi and Sextro, 1989). In this framework, Johnson and Ettinger (1991) developed an analytical model which is still now the most widely used algorithm for assessing the vapors intrusion to enclosed spaces (Tillman and Weaver, 2006).

However several field investigations have shown that the J&E model often overpredicts the indoor concentration of contaminants at sites impacted by petroleum hydrocarbon compounds (Johnson et al., 2002; Provoost et al., 2007). This is especially related to the fact that the J&E algorithm does not include biodegradation, which the field studies have shown to be particularly effective in attenuating vapors (Roggemans et al., 2001; Fischer et al., 1996; Luo et al., 2009; DeVaull et al., 2002; Lahvis et al., 1999; Dawson and McAlary, 2009; Lundegard et al., 2008).

A range of numerical (e.g. Abreu and Johnson, 2006; Hers et al., 2000; Bozkurt et al., 2009; Yu et al., 2009) and analytical (e.g. Johnson et al.; 1998; DeVaull, 2007; Davis et al. 2009; Parker, 2003; McHugh et al. 2006; Verginelli et al., 2010; Mills et al., 2007) models including aerobic biodegradation were developed to overcome this limitation. These models differ by the underlying assumptions and the conditions at which they can be applied. For instance, some models describe the transient behavior of the vapor

intrusion process (e.g. Mills et al., 2007; McHugh et al., 2006), other the spatial variability (Abreu et al., 2009), the non-homogeneous soil conditions (Bozkurt et al., 2009), the oxygen-limited biodegradation (e.g. DeVaull, 2007; Verginelli et al., 2010) or the volatilization from soil contaminated by NAPL (Parker, 2003). Recently API developed a user-friendly software called "BioVapor" (API, 2009) which implements the oxygen-limited biodegradation model developed by DeVaull (2007).

All these models account just for the aerobic reaction whereas anaerobic biodegradation is always neglected. However, as reported by Foght (2008) and Haeseler et al. (2010), in the last decades several studies have demonstrated that many aromatic hydrocarbons such as benzene, toluene, ethylbenzene and xylene (BTEX) and some polycyclic aromatic hydrocarbons (PAHs) can be completely degraded under anaerobic conditions. In fact these experimental and field studies have shown that, under oxygen deficiency, anaerobic bacteria can use nitrate, sulfate, iron, manganese and carbon dioxide as their electron acceptors and break down organic chemicals into smaller compounds (see Table 1.1) even though with usually much slower rates than the aerobic reaction (Schreiber et al., 2004). Besides, anaerobic biodegradation can potentially take place near the vapor source zone where the oxygen concentration may result below the minimum one required to sustain aerobic biodegradation (Boopathy, 2004; Dou et al., 2008; Lee et al., 2001; Johnson et al., 2006; Molins et al., 2010; Bekins et al., 2005; Gray et al., 2010; Salminen et al., 2004). This is somehow confirmed by the frequent methane detection at sites where petroleum hydrocarbons have been released into the subsurface (e.g. Lundegard et al., 2006; Lundegard et al., 2008; Hers et al., 2000), indicative of anaerobic biotransformation under methanogenic conditions (Bekins et al., 2005; Gray et al., 2010).

To assess how anaerobic biodegradation might influence the attenuation of vapors in the sub-soil, in this chapter a 1-D vapor intrusion model including both aerobic and anaerobic biodegradation is proposed. To evaluate the availability of oxygen in the subsurface, the transport of oxygen and its consumption (resulting from the different sources of oxygen demand) has been included in the model. In the case of anaerobic reaction under methanogenic conditions, the model accounts for the generation of methane which leads to a further oxygen demand (due to aerobic biodegradation of methane) in the vadose zone.

**Table 1.1.** Stoichiometric mineralisation equations and mass ratios for aerobic and anaerobic biodegradation (Haeseler et al., 2010)

| Stoichiometric mineralisation equation | Stochiometric Mass Ratio |
|---|---|
| **Aerobic Conditions** | |
| $C_nH_m + \left(n + \frac{m}{4}\right)O_2 \rightarrow \frac{m}{2}H_2O + nCO_2$ | $\gamma_{O_2} = \left(n + \frac{m}{4}\right) \cdot MW_{O_2} / MW_{C_nH_m}$ |
| **Denitrifying conditions** | |
| $C_nH_m + \left(\frac{2}{3}n + \frac{m}{6}\right)NO_3 \rightarrow \left(\frac{1}{3}n + \frac{m}{12}\right)N_2 + \frac{m}{2}H_2O + nCO_2$ | $\gamma_{NO_3} = \left(n + \frac{m}{4}\right) \cdot MW_{NO_3} / MW_{C_nH_m}$ |
| **Sulfate reducing conditions** | |
| $C_nH_m + \left(\frac{2}{5}n + \frac{m}{10}\right)SO_4 \rightarrow \left(\frac{2}{5}n + \frac{m}{10}\right)H_2S + \left(\frac{2}{5}m - \frac{2}{5}n\right)H_2O + nCO_2$ | $\gamma_{SO_4} = \left(\frac{2}{5}n + \frac{m}{10}\right) \cdot MW_{SO_4} / MW_{C_nH_m}$ |
| **Methanogenic conditions** | |
| $C_nH_m + \left(n - \frac{m}{4}\right)H_2O \rightarrow \left(\frac{n}{2} - \frac{m}{8}\right)CO_2 + \left(\frac{n}{2} + \frac{m}{8}\right)CH_4$ | $\varphi_{CH_4} = \left(\frac{1}{2}n + \frac{1}{8}m\right) \cdot MW_{CH_4} / MW_{C_nH_m}$ |

The features of this model, as reported in Table 1.2, allow to use it as a screening tool to identify under which site conditions the attenuation of biodegradable compounds is likely to be significant.

**Table 1.2.** Model Features.

| Feature | J&E 1991 | Johnson et al. 1998 | Bio-Vapor 2009 | This Work |
|---|---|---|---|---|
| Steady-state transport | **V** | **V** | **V** | **V** |
| Diffusion in the vadose zone | **V** | **V** | **V** | **V** |
| Diffusion and Advection in the building zone | **V** | **V** | **V** | **V** |
| Cross flow under foundations | --- | --- | **(*)** | **V** |
| Capillary fringe attenuation factor | --- | --- | **(*)** | **V** |
| Background indoor concentration | --- | --- | **V** | --- |
| Multi-component contamination | --- | --- | **V** | **V** |
| Aerobic Biodegradation (pseudo 1st-order) | --- | **V** | **V** | **V** |
| Aerobic layer thickness | --- | **(*)** | **V** | **V** |
| Baseline soil respiration | --- | --- | **V** | **V** |
| Oxygen vertical and lateral transport | --- | --- | **(*)** | **V** |
| Anaerobic Biodegradation (pseudo 1st-order) | --- | --- | --- | **V** |
| $CH_4$ Production (methanogenic bio) | --- | --- | --- | **V** |
| $O_2$ consumption due to $CH_4$ production | --- | --- | --- | **V** |

## MODELING

The indoor concentration resulting from the vapor intrusion process can be influenced by several factors such as the vapor source type (e.g., soil or groundwater), the source concentration, the source position relative to the building, the contaminant biodegradability, the physical characteristics of the soil (e.g., moisture, porosity), the building and foundation characteristics, the convective-advective factors (e.g. temperature-pressure differences, heating, ventilation, wind speed) and other minor factors (Abreu and Johnson, 2005; Patterson and Davis, 2009).

A schematic representation of the scenario considered in this work is reported in Fig.1.1.

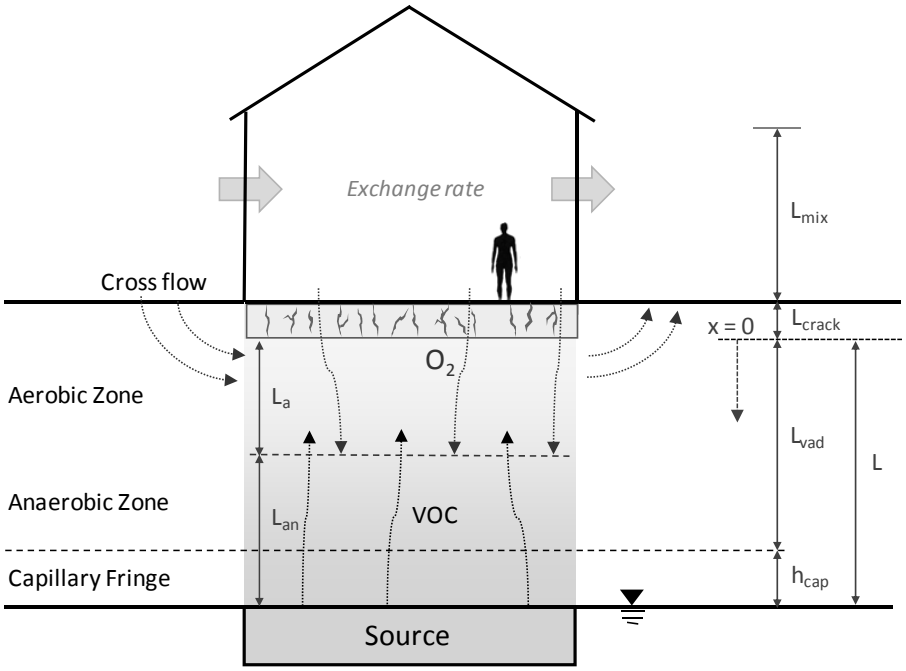


**Figure 1.1.** Conceptual Model. The symbol x represents the spatial variable and is positive with increasing depth. The origin of x is at the bottom of the building.

**Governing Equations**

The reactive transport of VOC vapors and oxygen has been described by two coupled diffusion-advection differential equations with reaction terms at steady-state:

$$\begin{cases} D_v^{eff} \dfrac{d^2C_v}{dx^2} - v_D \cdot \dfrac{dC_v}{dx} - R_v(C_v, C_{O_2}) = 0 \\ D_{O_2}^{eff} \dfrac{d^2C_{O_2}}{dx^2} - v_D \cdot \dfrac{dC_{O_2}}{dx} - R_{O_2}(C_v, C_{O_2}) = 0 \end{cases} \tag{1.1}$$

where the subscripts $v$ and $O_2$ refer to the vapor phase contaminant and to oxygen, respectively. $C$ is the concentrations of the species in the soil-gas phase, $R$ the reaction rates, $v_D$ the Darcy velocity and $D^{eff}$ the effective porous medium diffusion coefficients which can be estimated by using the Millington and Quirk (1961) expression:

$$D^{eff} = D_{air} \cdot \frac{\theta_a^{10/3}}{\theta_e^{2}} + \frac{D_{wat}}{H} \cdot \frac{\theta_w^{10/3}}{\theta_e^{2}} \tag{1.2}$$

where $D_{air}$ and $D_{wat}$, are the diffusion coefficients in water and in air respectively, $\theta_e$ the porosity, $\theta_a$ and $\theta_w$ the air and water-filled porosity respectively and $H$ the dimensionless Henry's law constant.

The reaction rates $R$ in the soil matrix were assumed to be first-order in $C_v$:

$$\begin{cases} R_v(C_v, C_{O_2}) = \begin{cases} \alpha_a \cdot C_v & for \quad C_{O_2} \geq C_{O_2,tresh} \\ \alpha_{an} \cdot C_v & for \quad C_{O_2} < C_{O_2,tresh} \end{cases} \\ R_{O_2}(C_v, C_{O_2}) = \begin{cases} \gamma \cdot R_v(C_v, C_{O2}) & for \quad C_{O_2} \geq C_{O_2,tresh} \\ 0 & for \quad C_{O_2} < C_{O_2,tresh} \end{cases} \end{cases} \tag{1.3}$$

where $C_{O2,tresh}$ represents the oxygen threshold concentration required to sustain aerobic biodegradation. Some studies suggest that aerobic biodegradation of hydrocarbons stops, or slows down to very low rates, when oxygen soil gas concentration falls below approximately 2% v/v (Roggemans et al., 2001).

In the case of aerobic biodegradation, the oxygen reaction term, $R_{O2}$, is related to $R_v$ by the stoichiometric mass ratio ($\gamma$) between oxygen and the compound(s) of concern (see Table 1.1).

Since biodegradation is commonly assumed to take place in the water phase of the unsaturated soil porosity, the kinetic rate constants for the aerobic or the anaerobic reaction, $\alpha_i$, can be expressed, assuming linear equilibrium partitioning, as follows:

$$\alpha_i = \frac{\lambda_i \cdot \theta_w}{H} \tag{1.4}$$

where the subscript $i$ refers either to aerobic ($a$) or to anaerobic ($an$) biodegradation, respectively.

$\lambda$ is the intrinsic degradation rate constant, $\theta_w$ the water-filled porosity of the soil and $H$ the dimensionless Henry's law constant.

It is worth noting that in this work a first-order kinetics was considered. As shown in previous studies (e.g. Johnson et al., 2002; DeVaull, 2007), this assumption usually describes correctly the biodegradation process up to high contaminant concentration, when hydrocarbon-degrading microbes may result rate-limiting, as reported by Hers et al. (2000) who estimated BTX zero-order mineralisation rates between 0.6 and 1.4 mg/l/h.

**Model Derivation**

To solve the two coupled differential equations (Eq. 1.1), the whole domain was divided into regions characterized by different behaviors. For each region the differential equations were separately integrated by imposing the boundary conditions at the interfaces, allowing to obtain the expressions for the vapor phase concentration and flux profile along each zone summarized in Table 1.3.

The expressions for the unknowns needed to solve the equations reported in Table 1.3 ($C_a$, $C_0$ and $C_{indoor}$) were derived by equating the fluxes at the interface between the contiguous layers. The expressions obtained are reported in the following.

**Table 1.3.** Model derivation.

| | |
|---|---|
| **ANAEROBIC ZONE (L < x < $L_a$)** | |
| Assumptions | $\begin{cases} R_v = \dfrac{\lambda_{an} \cdot \theta_{an}}{H} \cdot C_v \\ v_D = 0 \end{cases}$ |
| Boundary Conditions | $\begin{cases} C(L) = C_{source,sg} \\ C(L_a) = C_a \end{cases}$ |
| Concentration Profile | $\begin{cases} C(x) = C_a \cdot \dfrac{\sinh\left(k_{an} \cdot (L-x)\right)}{\sinh\left(k_{an} \cdot L_{an}\right)} + C_{source,sg} \cdot \dfrac{\sinh\left(k_{an} \cdot (x-L_a)\right)}{\sinh\left(k_{an} \cdot L_{an}\right)} \\ C(x) = C_a + \dfrac{C_a - C_i}{L_a - L} \cdot (x - L_a) \qquad \left(R_v = 0\right) \end{cases}$ |
| Flux Profile | $\left\{ \Phi_{an}(x) = D_{an} \cdot k_{an} \left[ C_i \cdot \dfrac{\cosh\left(k_{an} \cdot (x-L_a)\right)}{\sinh\left(k_{an} \cdot L_{an}\right)} - C_a \cdot \dfrac{\cosh\left(k_{an} \cdot (L-x)\right)}{\sinh\left(k_{an} \cdot L_{an}\right)} \right] \right.$ |
| Fluxes at the interfaces | $\begin{cases} \Phi_{an}(L_a) = D_{an} k_{an} \left[ \dfrac{C_{source,sg}}{\sinh\left(k_{an} \cdot L_{an}\right)} - \dfrac{C_a}{\tanh\left(k_{an} \cdot L_{an}\right)} \right] \\ \Phi_{an}^{\lambda_{an}=0}(L_a) = D_{an} \cdot \dfrac{C_i - C_a}{L - L_a} \qquad \left(R_v = 0\right) \end{cases}$ |
| **AEROBIC ZONE (0 < x < $L_a$)** | |
| Assumptions | $\begin{cases} R_v = \dfrac{\lambda_a \cdot \theta_a}{H} \cdot C_v \\ v_D = 0 \end{cases}$ |
| Boundary Conditions | $\begin{cases} C(L_a) = C_a \\ C(0) = C_0 \end{cases}$ |
| Concentration Profile | $\left\{ C(x) = C_0 \cdot \dfrac{\sinh\left(k_a \cdot (L_a - x)\right)}{\sinh(k_a \cdot L_a)} + C_a \cdot \dfrac{\sinh(k_a \cdot x)}{\sinh(k_a \cdot L_a)} \right.$ |
| Flux Profile | $\left\{ \Phi_a(x) = k_a \cdot D_a \cdot \left( C_a \cdot \dfrac{\cosh(k_a \cdot x)}{\sinh(k_a \cdot L_a)} - C_0 \cdot \dfrac{\cosh\left(k_a \cdot (L_a - x)\right)}{\sinh(k_a \cdot L_a)} \right) \right.$ |
| Fluxes at the interfaces | $\begin{cases} \Phi_a(L_a) = k_a \cdot D_a \cdot \left( \dfrac{C_a}{\tanh(k_a \cdot L_a)} - \dfrac{C_0}{\sinh(k_a \cdot L_a)} \right) & (x = L_a) \\ \Phi_a(0) = k_a \cdot D_a \cdot \left( \dfrac{C_a}{\sinh(k_a \cdot L_a)} - \dfrac{C_0}{\tanh(k_a \cdot L_a)} \right) & (x = 0) \end{cases}$ |

| BUILDING ZONE (x < 0) | |
|---|---|
| Assumptions | $\begin{cases} R_v = 0 \\ v_D = Q_s \,/\, A_b \end{cases}$ |
| Boundary Conditions | $\begin{cases} C(0) = C_0 \\ C(-L_{crack}) = C_{indoor} \end{cases}$ |
| Concentration Profile | $\begin{cases} C(x) = C_0 - (C_0 - C_{indoor}) \cdot \dfrac{\exp\left(-\zeta \cdot x / L_{crack}\right)}{\exp\left(-\zeta\right) - 1} \end{cases}$ |
| Flux Profile | $\begin{cases} \Phi_{cracks}(x) = \dfrac{Q_s}{A_b} \cdot \left[ C_0 - \left(C_0 - C_{indoor}\right) \cdot \dfrac{\exp\left(-\zeta \cdot x / L_{crack}\right)}{\exp\left(-\zeta\right) - 1} \right] \end{cases}$ |
| Fluxex at the interfaces | $\begin{cases} \Phi_{cracks}(0) = \dfrac{Q_s}{A_b} \cdot \left( C_0 - \dfrac{C_0 - C_{indoor}}{\exp(-\zeta) - 1} \right) & (x = 0) \\ \Phi_{cracks}(-L_{crack}) = \dfrac{Q_s}{A_b} \cdot \left( C_0 - \dfrac{C_0 - C_{indoor}}{1 - \exp(\zeta)} \right) & (x = -L_{crack}) \\ \Phi_{mix} = L_{mix} \cdot ER \cdot C_{indoor} \end{cases}$ |

***Concentration at the aerobic to anaerobic interface***

The concentration $C_a$ at the aerobic to anaerobic interface ($x = L_a$) was obtained by imposing the continuity of the two fluxes at the interface ($\Phi_{an} = \Phi_{a,}$ see Table 1.3):

$$C_a = \frac{C_{source,sg}}{\cosh\left(k_{an} \cdot L_{an}\right) + \left( \dfrac{k_a \cdot D_a}{\tanh(k_a \cdot L_a)} - \dfrac{k_a \cdot D_a}{\alpha_R \cdot \sinh(k_a \cdot L_a)} \right) \cdot \dfrac{sinh\left(k_{an} \cdot L_{an}\right)}{k_{an} \cdot D_{an}}} \tag{1.5}$$

With:

$$\alpha_R = \cosh(k_a L_a) + \frac{\sinh(k_a L_a)}{k_a \cdot D_a \cdot \left(R_{crack} + R_{mix}\right)} \tag{1.6}$$

In the case of negligible anaerobic biodegradation contribution (i.e. $\lambda_{an} = 0$) Eq. (1.5) reduces to:

$$C_a(\lambda_{an}=0)=\frac{C_{source,sg}}{1+\left(\frac{k_a\cdot D_a}{\tanh(k_a\cdot L_a)}-\frac{k_a\cdot D_a}{\alpha_R\cdot\sinh(k_a\cdot L_a)}\right)\cdot\frac{L_{an}}{D_{an}}} \tag{1.7}$$

$L_a$ and $L_{an}$ are the aerobic and anaerobic layer thickness, respectively. $k_a$ and $k_{an}$ are parameters which give an indication of biodegradation relevance relative to diffusion, in terms of the inverse of the diffusive-reaction length:

$$k_i=\sqrt{\frac{\lambda_i\cdot\theta_w}{H\cdot D_i}} \tag{1.8}$$

where the subscript $i$ refers to aerobic ($a$) and anaerobic ($an$) biodegradation respectively.

$D_i$ is the effective diffusivity coefficient and is equal to:

$$D_i=\begin{cases}D_{an}=\dfrac{L_{an}}{\dfrac{h_{cap}}{D_{cap}^{eff}}+\dfrac{L_{an}-h_{cap}}{D_{soil}^{eff}}} & \text{Groundwater source}\\ D_a=D_b=D_{soil}^{eff} & \text{Soil source}\end{cases} \tag{1.9}$$

With reference to Eq. (1.9) it should be noted that the expression for groundwater sources does not account for groundwater fluctuations although seasonal changes in groundwater levels may be considerable and may lead to significant difference in the diffusion coefficient. For this reason, it has also been proposed to use an empirical attenuation factor between the groundwater source concentration and the deep soil gas concentration above the capillary fringe; a default value of 0.1 is suggested in BioVapor (2009).

$R_{mix}$ representing the dilution factor due to air building exchange ($ER$):

$$R_{mix}=\frac{1}{L_{mix}\cdot ER} \tag{1.10}$$

where $L_{mix}$ is the enclosed space volume/infiltration area ratio.

$R_{crack}$ represents the attenuation contribution of cracks:

$$\begin{cases} R_{crack} = \left( R_{mix} + \vec{i}\,\frac{A_b}{Q_s} \right) \cdot \left( \exp(\vec{i} \cdot \xi) - 1 \right) & (\Delta p \neq 0) \\ R_{crack} = \frac{L_{crack}}{D_{crack}^{eff} \cdot \eta} & (\Delta p = 0) \end{cases} \tag{1.11}$$

With:

$$\xi = \frac{Q_s}{A_b} \cdot \frac{L_{crack}}{D_{crack}^{eff} \cdot \eta} \tag{1.12}$$

$L_{crack}$ is the foundation thickness, $A_b$ the foundation area in contact with soil, $\eta$ the foundation crack fraction, $Q_s$ the convective flow rate from the soil into the building and $i$ the versor of the advective flow depending on the pressure difference ($\Delta p$) between the soil and the building and is equal to i =1 in the case of positive building pressure (i.e. $\Delta p > 0$) and to i = -1 for negative building pressure ($\Delta p < 0$).

The overall convective flow rate from the soil into the building, $Q_s$, can be calculated as the sum of the vertical pressure-driven advection flow ($Q_{s/b}$) and the cross-flow due to wind loading ($Q_{cross}$):

$$Q_s = Q_{s/b} + \vec{i} \cdot Q_{cross} \tag{1.13}$$

An expression for the derivation of $Q_{s/b}$ is given by Johnson and Ettinger (1991):

$$Q_{s/b} = \frac{2\pi |\Delta p| \cdot k_v \cdot X_{crack}}{\mu \cdot \ln\left( \frac{2Z_{crack}}{r_{crack}} \right)} \tag{1.14}$$

With:

$$r_{crack} = \frac{\eta \cdot A_b}{X_{crack}} \tag{1.15}$$

where $k_v$ is the soil permeability to vapor flow, $\mu$ the vapor viscosity, $X_{crack}$ the foundations perimeter and $Z_{crack}$ the foundations depth.

It is worth noting that Eq. (1.14) can lead, in some cases, to unreliable prediction of the effective convective flow (Johnson, 2002). For instance, Hers et al. (2003) observed that the model predictions were both higher and lower than the measured values even though overall were within one order of magnitude of the measured values. Moreover Hers et al. (2003) suggest that a typical range for house on coarse-grained soil is on the order of 1 to 10 L/min.

The resulting pressure difference between the soil and the building, leading to soil-gas migration by convection, can be induced by temperature effects, wind interaction with the building and the operation of heating, ventilation and air-conditioning systems (Robinson et al., 1997).

The pressure difference due to temperature gradient between the soil and the building can be estimated as follows:

$$\Delta p = \rho \cdot g \cdot \left( \frac{T_{indoor} - T_{soil}}{T_{indoor}} \right) \cdot H_{building} \tag{1.16}$$

where $\rho$ is the density of outdoor air, $g$ the acceleration due to gravity, $H_{building}$ the height of building and $T_{indoor}$ and $T_{soil}$ the indoor and outdoor temperature respectively.

Generally residential buildings are under negative pressure due to kitchen and bathroom ventilation and indoor heating (McHugh and McAlary, 2009). On the contrary buildings or offices with ventilation and air-conditioning systems are typically designed to operate under positive pressure (McHugh et al., 2006).

However in most buildings pressure fluctuates in response to changes in wind, air conditioning and weather (Patterson and Davis, 2009). To account for this bi-directional flow across the building foundation, McHugh et al. (2006) proposed a model describing the pressure difference ($\Delta p$) as a periodic sinusoidal pressure gradient, with a frequency of pressure cycles of two hours.

Concerning the cross-flow, an expression for the derivation of $Q_{cross}$ (see Eq. 1.13) is given by Fisher et al. (1996):

$$Q_{cross} = v_{cross} \cdot W_{sub} \cdot Z_{sub} \tag{1.17}$$

where $W_{sub}$ is the average cross-sectional length under the building, $Z_{sub}$ the depth of the subslab region and $v_{cross}$ the resulting upwind-downwind velocity in the subsoil:

$$v_{cross} = \frac{k_v}{\mu} \cdot \frac{\Delta P_{wind}}{L_{sub}} \tag{1.18}$$

$L_{sub}$ is the length of the building in the direction of the wind and $\Delta P_{wind}$ the difference between the dynamic air pressure associated with wind acting on windward side and rear side house walls, which may be both evaluated as suggested by Krylov et al. (1998):

$$P_{wind} = \frac{1}{2} \cdot \rho \cdot v_{wind}{}^2 \cdot k_{wind} \tag{1.19}$$

where $v_{wind}$ is the wind speed and $k_{wind}$ a position-dependent coefficient in the range - 1 to + 1, which describes the distribution of wind-induced pressure over house walls. For a simplified one-dimensional picture of dynamic pressure distribution, Krylov et al. suggest to use $k_{wind}$ = 0.915 for the windward side of the house and $k_{wind}$ = - 0.8 for the roof, rear and side walls of the house (corresponding to suction).

***Concentration at the bottom of the basement***

The concentration, $C_0$, at the bottom of the basement ($x$ = 0) was obtained imposing the continuity of the two fluxes at the interface ($\Phi_{a,} = \Phi_{cracks,}$, see Table 1.3):

$$C_0 = \frac{C_a}{\alpha_R} \tag{1.20}$$

with $C_a$ and $\alpha_R$ defined as in Eq. (1.5) and (1.6) respectively.

***Indoor Concentration***

Finally using the expression derived for the flow through the foundations ($\Phi_{cracks}$ at $x$ = - $L_{crack}$ reported in Table 1.3) and accounting for the vapors dilution due to building air exchange rate ($\Phi_{mix}$), the indoor concentration, $C_{indoor}$, can be calculated as:

$$C_{indoor} = C_0 \cdot \frac{R_{mix}}{R_{crack} + R_{mix}} \tag{1.21}$$

with $C_0$ defined as in Eq. (1.20) and $R_{mix}$ and $R_{crack}$ calculated with Eqs. (1.10) and (1.11) respectively.

**Aerobic layer thickness**

The last unknown parameter, required as input in the model, is the aerobic layer thickness, $L_a$, which depends upon the oxygen demand related to the aerobic biodegradation reaction and to the baseline soil respiration. Assuming that in the anaerobic layer the oxygen concentration is constant and equal to the minimum required to sustain aerobic biodegradation ($C_{O2,tresh}$), the downward diffusive flow at the aerobic to anaerobic interface ($x = L_a$) can be set equal to zero. Consequently, the aerobic layer thickness, $L_a$, can be calculated by iteratively solving Eq. (1.22) which corresponds to the condition that the oxygen flux migrating into the subsurface equals the total oxygen demand rate:

$$\Phi_{O_2}(L_a) - R_{O_2}(L_a) = 0 \tag{1.22}$$

The oxygen flux that migrates in the subsurface ($\Phi_{O2}$) can be calculated as the sum of three contributions related to the vertical convective flux rate, to molecular diffusion through the foundations and the subsoil and to the lateral airflow under the building:

$$\begin{cases} \Phi_{O_2}(L_a) = \dfrac{D_{O2} \cdot \left(C_{O_2,amb} - C_{O_2,tresh}\right)}{L_{crack} + L_a} + \left(v_{cross} + \dfrac{Q_{s/b}}{A_b}\right) \cdot C_{O_2,amb} & (\Delta p > 0) \\ \Phi_{O_2}(L_a) = \dfrac{D_{O2} \cdot \left(C_{O_2,amb} - C_{O_2,tresh}\right)}{L_{crack} + L_a} + v_{cross} \cdot C_{O_2,amb} - \dfrac{Q_{s/b}}{A_b} \cdot C_{O_2,0} & (\Delta p < 0) \end{cases} \tag{1.23}$$

$D_{O2}$ is the overall effective oxygen diffusivity coefficient and is equal to:

$$D_{O2} = \frac{L_{crack} + L_a}{\dfrac{L_{crack}}{D^{eff}_{O_2,crack} \cdot \eta} + \dfrac{L_a}{D^{eff}_{O_2,soil}}} \tag{1.24}$$

with $D_{O2,crack}$ and $D_{O2,soil}$ representing the effective oxygen diffusion coefficients through the foundations and the vadose zone respectively.

The oxygen demand rate, $R_{O2}(L_a)$, can be calculated accounting for the contribution due to aerobic biodegradation of the $n$ degradable compounds and for the baseline oxygen respiration rate:

$$R_{O_2}(L_a) = \sum_{i=1}^{n} \gamma_i \cdot D_{a,i} \cdot k_{a,i} \cdot \left(C_{a,i} + C_{0,i}\right) \left( \frac{\cosh(k_{a,i} \cdot L_a) - 1}{\sinh(k_{a,i} \cdot L_a)} \right) + \rho_s \cdot L_a \cdot \Lambda_{base} \tag{1.25}$$

where $\gamma$ is the stoichiometric mass ratio between oxygen and the i-th compound, $\Lambda_{base}$ the zero-order baseline soil oxygen respiration term (DeVaull, 2007) and $\rho_s$ the soil density.

In the case of negligible anaerobic biodegradation, the overall oxygen consumption can be estimated by using Eq. (1.25), but with the concentration $C_a$ (at $x=L_a$) and $C_o$ (at $x=0$) calculated with Eq. (1.7) and Eq. (1.20) respectively.

**Methane Generation**

As discussed in the introduction, at sites where petroleum hydrocarbons have been released, methane is frequently detected (e.g. Lundegard et al., 2006; Lundegard et al., 2008; Hers et al., 2000; McAlary et al., 2007) as a result of the methanogenic biodegradation of other hydrocarbons (see Table 1.1). In this case, Eq. (1.25) shall be modified by adding a term accounting for the oxygen demand related to its consumption, which can be estimated as follows:

$$R_{O_2,CH_4} = \sum_{i=1}^{n} \gamma_{CH_4,i} \cdot D_{a,CH_4} \cdot k_{a,CH_4} \cdot \left(C_{a,CH_{4,i}} + C_{0,CH_4,i}\right) \left( \frac{\cosh(k_{a,CH_4} \cdot L_a) - 1}{\sinh(k_{a,CH_4} \cdot L_a)} \right) \tag{1.26}$$

The methane flux at the aerobic to anaerobic interface ($x=L_a$) can be estimated as the sum of the diffusive flux migrating from the source plus the stoichiometric methane generated in the anaerobic zone from the VOC compound(s) undergoing methanogenic anaerobic biodegradation:

$$\Phi_{CH_4}(L_a) = D_{CH4} \cdot \left( \frac{C_{source,sg,CH_4} - C_{a,CH_4}}{L - L_a} \right) + \sum_{i=1}^{n} \frac{\Phi_{VOC,i}^{\lambda b=0}(L_a) - \Phi_{VOC,i}(L_a)}{\varphi_{CH_4}} \quad (1.27)$$

where $\varphi_{CH4}$ is the stoichiometric mass ratio between methane and the *i-th* compound and $D_{CH4}$ the effective diffusivity coefficient of methane in the anaerobic zone.

The methane concentration, $C_{a,CH4}$, at the aerobic to anaerobic interface ($x=L_a$) to be used in Eq. (1.26) can be estimated, as discussed for the other compounds, by imposing the continuity of the two fluxes at the interface:

$$C_{a,CH4} = \frac{\frac{D_{an,CH_4}}{L_{an}} C_{source,sg,CH_4} + \sum_{i=1}^{n} \frac{\Phi_{VOC,i}^{\lambda_{an}=0}(L_a) - \Phi_{VOC,i}(L_a)}{\varphi_{CH4,i}}}{\frac{D_{an,CH_4}}{L_{an}} + \frac{k_a \cdot D_{a,CH_4}}{\tanh(k_{a,CH_4} \cdot L_a)} - \frac{k_{a,CH_4} \cdot D_{a,CH_4}}{\alpha_{R,CH_4} \cdot \sinh(k_{a,CH_4} \cdot L_a)}} \quad (1.28)$$

The other terms of Eq. (1.26) can be calculated as discussed for the other compounds.

**Source Concentration**

The model requires, as input, the source concentration in the soil-gas phase, $C_{source,sg}$. If site-specific data are not available, the source concentration in the soil-gas phase can be derived from the liquid-phase concentration, $C_{source,w}$, through the Henry's law, i.e. assuming a linear equilibrium partitioning:

$$C_{source,sg} = C_{source,w} \cdot H \quad (1.29)$$

In the case of vapors originating from soil, the source concentration in the vapor phase can be calculated from the total soil concentration, $C_{source,tot}$, assuming again a linear equilibrium partitioning:

$$C_{source,sg} = C_{source,tot} \cdot \frac{\rho_s \cdot H}{\theta_w + H \cdot \theta_a + \rho_s \cdot K_{oc} \cdot f_{oc}} \quad (1.30)$$

where $K_{oc}$ is the chemical-specific organic carbon partition coefficient, $f_{oc}$ the organic carbon fraction in soil, $\theta_a$ the air-filled porosity and $\rho_s$ the bulk soil density.

In saturation conditions (i.e. $C_{source,w} > S$ and $C_{source,tot} > C_{sat}$ for groundwater and soil source respectively) the concentration in the soil gas should be set equal to:

$$C_{source,sat,sg} = S \cdot H \tag{1.31}$$

where $S$ is the contaminant solubility.
$C_{sat}$ is the saturation concentration in the soil:

$$C_{sat} = S \cdot \frac{\theta_w + H \cdot \theta_a + \rho_s \cdot K_{oc} \cdot f_{oc}}{\rho_s} \tag{1.32}$$

In the case of a mixture, the effective solubility of each compound, $S_{mix,i}$, can be calculated as suggested by DeVaull (API, 2009):

$$S_{mix,i} = \frac{C_{source,w,i}}{\sum_{i=1}^{n} \frac{C_{source,w,i}}{S_i}} \tag{1.33}$$

It is worth noting that some studies have demonstrated that the equilibrium partitioning based on Henry's law is a poor predictor of the relationship between VOC concentrations measured in groundwater and deep soil gas (McHugh and McAlary, 2009).

## RESULTS AND DISCUSSION

The developed model was solved analytically and used to assess under which site conditions biodegradation is expected to play a significant role in attenuating degradable vapors migrating from source to enclosed spaces and to evaluate the contribution of the aerobic and anaerobic attenuation pathways. To this end, solutions have been calculated, using representative parameter ranges and values (Table 1.4 and Table 1.5).

**Table 1.4.** Model Input Parameters (unless otherwise noted in figures).

| Parameter | Units | Value |
|---|---|---|
| Soil bulk density ($\rho_s$) | g/cm$^3$ | 1.7 |
| Soil porosity ($\theta_e$) | - | 0.35 |
| Soil moisture content ($\theta_w$) | - | 0.10 |
| Organic fraction ($f_{oc}$) | - | 0.01 |
| Toluene source concentration ($C_{source,sg}$) | g/m$^3$ | 10 |
| Source Depth ($L$) | m | 3 |
| Volume air exchanges ($ER$) | h$^{-1}$ | 0.5 |
| Building volume to foundation area ratio ($L_{mix}$) | m | 2 |
| Foundations thickness ($L_{crack}$) | m | 0.15 |
| Foundation area ($A_b$) | m$^2$ | 100 (10x10) |
| Convective flow rate from the soil into the building ($Q_s$) | L/min | 3 |
| Lateral pressure difference ($\Delta p_{wind}$) | Pa | 1 |
| Soil permeability to vapor flow ($k_v$) | m$^2$ | $10^{-11}$ |
| Vapor viscosity ($\mu$) | Pa s | $1.8 \cdot 10^{-5}$ |
| Water content of the foundation cracks ($\theta_{w\ crack}$) | - | 0.12 |
| Air content of the foundation cracks ($\theta_{a\ crack}$) | - | 0.26 |
| Foundation perimeter ($X_{crack}$) | m | 40 |
| Foundation crack fraction ($\eta$) | - | 0.0001 |

The foundation crack fraction, $\eta$, was set equal to 0.0001, that is much lower than the ASTM (2000) standard value ($\eta$ = 0.01). The choice of this value is in line with the

results based on measurements of air-entry rates for radon, which provided a range between 0.001 and 0.0001 (e.g. Nazaroff, 1992; Revzan et al., 1991).

The convective flow rate, $Q_s$, was set equal to 3 L/min which is representative of the range suggested by Hers et al. (2003). The aerobic and anaerobic biodegradation rate constants used as reference value in this work are the geometric mean, obtained through a detailed statistical analysis of several field and laboratory studies, by DeVaull (2007) and Aronson and Howard (1997) respectively.

**Table 1.5a.** Chemico-physical properties of the compounds of concern.

| Compound | $MW$ | $H$ | $D_{wat}$ | $D_{air}$ | $\lambda_a$ (a) | $\lambda_{an}$ (b) | $\gamma$ | $\varphi$ |
|---|---|---|---|---|---|---|---|---|
| | g/mole | - | $cm^2/s$ | $cm^2/s$ | $h^{-1}$ | $h^{-1}$ | $g_{O2}/g_{CH}$ | $g_{CH}/g_{CH4}$ |
| Benzene | 78.1 | 0.228 | $9\cdot10^{-6}$ | 0.088 | $7.9\cdot10^{-1}$ | $1.9\cdot10^{-4}$ | 3.07 | 0.77 |
| Toluene | 92.1 | 0.272 | $9\cdot10^{-6}$ | 0.087 | $7.9\cdot10^{-1}$ | $1.55\cdot10^{-2}$ | 3.13 | 0.78 |
| Etilbenzene | 106.2 | 0.323 | $8\cdot10^{-6}$ | 0.075 | $7.9\cdot10^{-1}$ | $5.4\cdot10^{-3}$ | 3.16 | 0.79 |
| Xylenes | 106.2 | 0.314 | $8\cdot10^{-6}$ | 0.087 | $7.9\cdot10^{-1}$ | $1.25\cdot10^{-3}$ | 3.16 | 0.79 |
| Other hydrocarbons aliphatic(c) | 100 | 75 | $7\cdot10^{-6}$ | 0.07 | 71 | $1.2\cdot10^{-3}$ (d) | 0.48 | 0.54 |
| Other hydrocarbons aromatic(c) | 100 | 0.3 | $7\cdot10^{-6}$ | 0.07 | $7.9\cdot10^{-1}$ | $5.6\cdot10^{-3}$ | 0.42 | 0.52 |

*(a) DeVaull, 2007*
*(b) Aronson and Howard, 1997*
*(c) API (2009)*
*(d) Siddique et al.,2008*

**Table 1.5b.** Chemico-physical properties of oxygen and methane.

| **Oxygen** | | |
|---|---|---|
| Diffusion Coefficient in air ($D_{air}$) | $cm^2/s$ | 0.219 |
| Diffusion Coefficient in water ($D_{wat}$) | $cm^2/s$ | $1.97\cdot10^{-5}$ |
| Baseline $O_2$ respiration rate ($\Lambda_{base}$) | $mg_{O2}/g_{oc}/h$ | $7\cdot10^{-6}$ |
| Ambient air concentration ($C_{O2,amb}$) | $g/m^3$ | 279 |
| Threshold concentration ($C_{O2,tresh}$) | $g/m^3$ | 27.9 |
| **Methane** | | |
| Diffusion Coefficient in air ($D_{air}$) | $cm^2/s$ | 0.1 |
| Diffusion Coefficient in water ($D_{wat}$) | $cm^2/s$ | $1\cdot10^{-5}$ |
| Aerobic biodegradation constant ($\lambda_a$) | $h^{-1}$ | 82 (a) |

*(a) DeVaull, 2007*

The model was first applied to the case of soil contamination by toluene only, allowing to assess the effect of the main site-specific parameters (Fig.1.2) and the role played by methanogenic anaerobic biodegradation (Fig.1.3) on the attenuation factor. Finally, the attenuation factor of toluene in different hydrocarbon mixtures was evaluated, assuming or neglecting anaerobic biodegradation under methanogenic conditions (Fig.1.4).

Fig.1.2 reports the attenuation factor ($\alpha = C_{indoor} / C_{source,sg}$) for toluene as a function of different site parameters, calculated with the model described in this chapter assuming that anaerobic reaction is occurring under methanogenic conditions. The contribution of anaerobic biodegradation to the overall attenuation is highlighted by comparing the model results with those obtained assuming just aerobic biodegradation (i.e. $\lambda_{an} = 0$) and those obtained applying the Johnson & Ettinger (1991) model which neglects both aerobic and anaerobic biodegradation. Fig.1.2 also reports the aerobic layer thickness, $L_a$, calculated assuming just aerobic biodegradation (indicated as $L_a1$) or both aerobic and anaerobic biodegradation ($L_a2$). For reference, the results were also compared with those obtained with the commercial software BioVapor (API, 2009), using the parameters reported in Table 1.4 and Table 1.5. The BioVapor simulations were run by directly specifying, as boundary condition for oxygen, the depth of the aerobic zone (reported in Fig.1.2 as $L_a1$) obtained using the equations discussed in the previous paragraphs.

The results hereby presented, separately discuss the influence of the different parameters analyzed on the attenuation factor.

**Source Concentration**

Fig.1.2a reports the predicted attenuation factor, $\alpha$, as a function of the soil-gas source concentration which was varied in the range of 0.01 to 100 g/m$^3$.The results obtained with the developed model, reported in the figure, show that aerobic biodegradation has a rather important effect on the attenuation factor for low to intermediate source concentration values. Namely, for quite low source concentration (1 g/m$^3$ in the specific case), the aerobic zone extends deeply ($L_a1$=194 cm against $L$=300 cm), with a reduction of the attenuation factor of several orders of magnitude with respect to the Johnson & Ettinger model (J&E). An increase of the source concentration leads to a corresponding decrease of the aerobic zone depth ($L_a1$ values reported in Fig.1.2a), until

the downward oxygen flux becomes too low to sustain the biodegradation of the gradually increasing contaminant upward flux, which is the case for $C_{source,sg}$ equal or above 10 g/m$^3$ in Fig.1.2a.

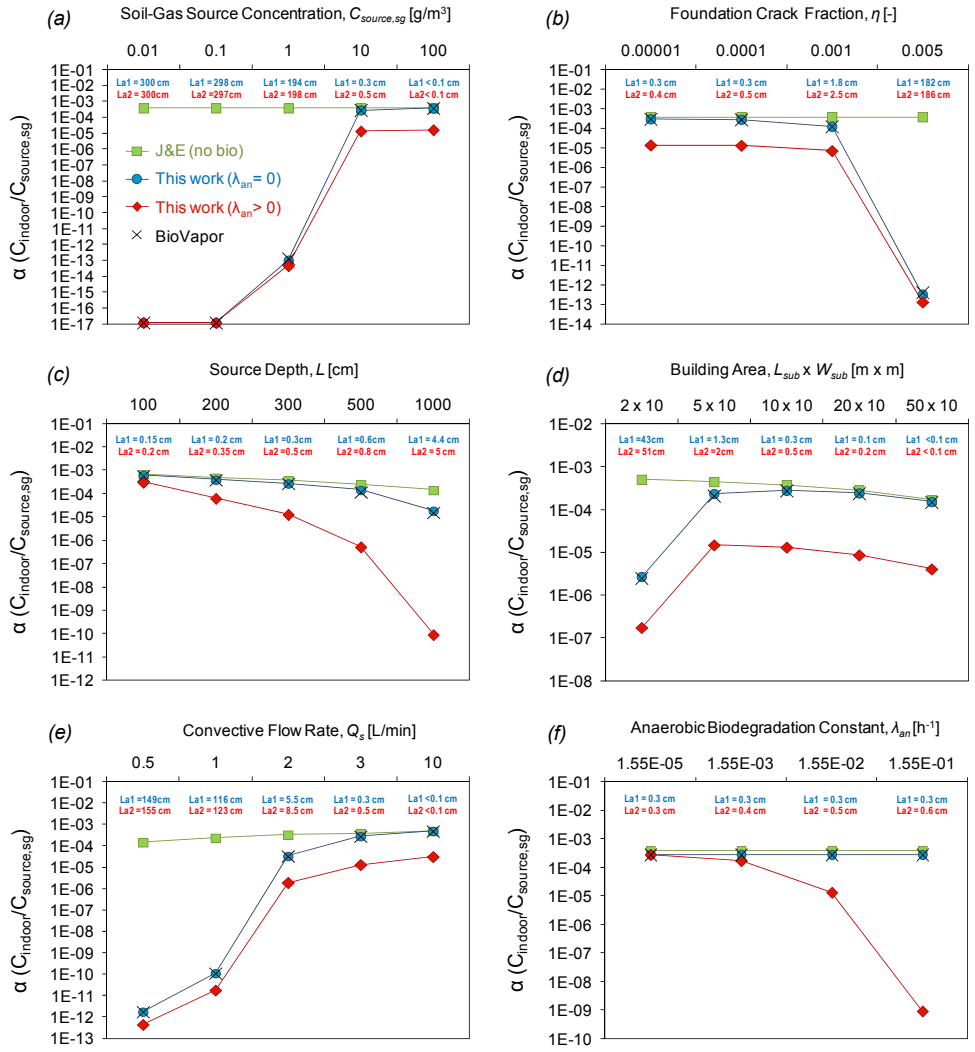


**Figure 1.2**. Toluene Attenuation factor vs.: (a) soil-gas source concentration, (b) foundation crack fraction (c) source depth, (d) building area, (e) convective flow rate, (f) anaerobic biodegradation constant; (♦) results obtained with the developed biodegradation model assuming anaerobic reaction occurring under methanogenic conditions; (●) results obtained assuming negligible anaerobic reaction; (■) results obtained with the Johnson & Ettinger model assuming no biodegradation; (X) results obtained with the BioVapor Software. La2 and La1 are the aerobic layer thickness calculated, neglecting or including anaerobic biodegradation.

The same results obtained with the developed model accounting just for aerobic biodegradation were also given by the BioVapor tool, provided that the aerobic layer thickness calculated by the developed model was used as input to BioVapor. The results of the model obtained accounting for both aerobic and anaerobic biodegradation, also shown in Fig.1.2a, are basically the same of those obtained considering aerobic biodegradation only, as long as low source concentration values are considered (below 1 $g/m^3$ in the specific case). On the contrary, an increasing influence of anaerobic biodegradation on the attenuation factor is observed for higher source concentration values, with one order of magnitude difference with respect to the results obtained neglecting this attenuation process.

**Foundation crack fraction**

Fig.1.2b reports the predicted attenuation factor, $\alpha$, as a function of the foundation crack fraction ($\eta$) which represents the ratio of the area of cracks to the total exposed area. The results obtained show that the overall attenuation is strongly influenced by the value of this parameter. With reference to the case of negligible anaerobic biodegradation (i.e. $\lambda_{an} = 0$) it can be noticed that the aerobic biodegradation is effective in reducing $\alpha$ only above a threshold crack fraction value below which a stepwise increase of α to the J&E one is observed (in this case for $\eta < 0.001$). For such low $\eta$ values, the oxygen diffusive flux through the cracks is dramatically reduced, so that biodegradation of the vapor flux (although also reduced) is not sustained anymore (e.g. for $\eta = 0.001$ $L_a1 = 1.8$cm). In this case, the oxygen replenishment results just from the lateral airflow transport.

The results obtained accounting for anaerobic biodegradation (i.e. $\lambda_{an} > 0$) show basically the same trend although, the attenuation factor is generally lower with respect to the one provided by the model accounting for aerobic biodegradation only, with differences up to one order of magnitude, when very low values of the foundation crack fraction ($\eta$ <0.001 in the specific case) are considered. On the contrary, for high values of $\eta$ (in the specific case for $\eta$ =0.005), a downward extension of the aerobic layer is observed (e.g. for $\eta$ =0.005 $L_a1$=182 cm against $L$= 300 cm) and the model accounting for both aerobic and anaerobic biodegradation provide basically the same results of those obtained considering just aerobic biodegradation.

**Source Depth**

Fig.1.2c shows the influence of source depth on the attenuation factor. With reference to this figure it can be noticed that, in this specific case, for shallow sources the different models provide basically the same results (e.g. see $L$ = 100 cm). An increase of the source depth leads to a gradual reduction up to one order of magnitude of the attenuation factor calculated assuming just aerobic biodegradation with respect to the Johnson & Ettinger model (J&E). The results obtained also suggest that taking anaerobic biodegradation in account (i.e. $\lambda_{an} > 0$) would lead to a remarkable further attenuating effect up to several order of magnitude (e.g. see $L \geq 500$ cm).

**Building Area**

Fig.1.2d reports the predicted attenuation factor for different dimensions of the building (in the range of 20 to 500 $m^2$). The results obtained show that the size of the building significantly influences the attenuation of the vapors. Namely, for small building size (e.g. 20 $m^2$) the J&E model provides results up to several orders of magnitude higher than those obtained applying the biodegradation model. In this case, the lateral flow is significant and leads to a large oxygen supply in the subsoil with a consequent downward extension of the aerobic zone layer (e.g. $L_a1$= 43cm against $L$= 300 cm). On the contrary, larger building sizes lead to a reduction of the influence of the lateral transport resulting in a gradual increase of the $\alpha$ calculated assuming just aerobic biodegradation to the values provided by the J&E model. For these scenarios, the results obtained with the model accounting for both aerobic and anaerobic biodegradation (i.e. $\lambda_{an} > 0$), suggest that anaerobic biodegradation may be important, leading to a reduction of the attenuation factor up to one order of magnitude.

**Soil-Building Pressure**

The results reported in Fig.1.2e give an indication of the dependence of the attenuation factor on the convective flow rate, $Q_s$. The flow rate has been varied from 0.5 to 10 L/min i.e. within the range suggested by Hers et al. (2003). The results obtained show, as expected, that the increase of $Q_s$ leads to a corresponding significant increase of $\alpha$ resulting from higher vapors flow rates entering into the building. Fig.1.2e also shows that, in this specific case, the aerobic biodegradation (i.e. $\lambda_{an} = 0$) results are significant

for flow rates up to 3 L/min, above which the $\alpha$ obtained becomes close to the J&E one. This does not apply to the case of both aerobic and anaerobic biodegradation in which case, even for higher flow rates, a slightly lower $\alpha$ than the one resulting from the J&E model is obtained.

**Anaerobic Biodegradation Constant**

Fig.1.2f reports the predicted attenuation factor as a function of the anaerobic biodegradation constant. The results obtained show that the attenuation factor is relatively sensitive to $\lambda_{an}$ for values higher than $1.55 \cdot 10^{-3}$ $h^{-1}$ (e.g. see $\lambda_{an}$ = 0.155 $h^{-1}$ in Fig.1.2f) under which the anaerobic biodegradation contribution becomes negligible and the same results of those obtained assuming just aerobic biodegradation are observed. It is worth noting that $\lambda_{an} = 1.55 \cdot 10^{-3}$ $h^{-1}$ is 10 fold lower than the geometric mean of the anaerobic biodegradation constant obtained through a detailed statistical analysis of several field and laboratory studies, by Aronson and Howard (1997). For higher values of $\lambda_{an}$ a rapid decrease by several orders of magnitude of the attenuation factor in the case of anaerobic biodegradation is observed (e.g. see the case of $\lambda_{an}$ =0.155 $h^{-1}$).

**Methane Generation**

Fig.1.3 reports the predicted attenuation factor (Fig.1.3a and Fig.1.3c) and the corresponding calculated aerobic layer thickness (Fig.1.3b and Fig.1.3d) as a function of the source concentration for two values of the anaerobic biodegradation constant, considering or neglecting methane generation from anaerobic methanogenic biodegradation (the other inputs are reported in Table 1.4 and Table 1.5). With reference to these figures, it can be noticed that for low source concentrations, the methane generation term does not affect the attenuation factor α. Besides, the result is independent of the concentration, since oxygen rich conditions are established down to the source depth (i.e. $L_a/L$ = 1, see Fig.1.3b and Fig.1.3d). For intermediate to high source concentrations, the occurrence of anaerobic biodegradation under methanogenic conditions can lead, especially for high values of the anaerobic biodegradation constant ($\lambda_{an}$ = 0.015 $h^{-1}$, Fig.1.3c and Fig.1.3d), to a significant increase of α with respect to the attenuation under denitrifying or sulfate reducing conditions. For higher concentrations the results of the two models (methanogenic and non-methanogenic conditions),

approach each other, with the attenuation factor α resulting once again independent of the source concentration due to oxygen depletion immediately beneath the building ($L_a/L = 0$, see Fig.1.3b and Fig.1.3d).

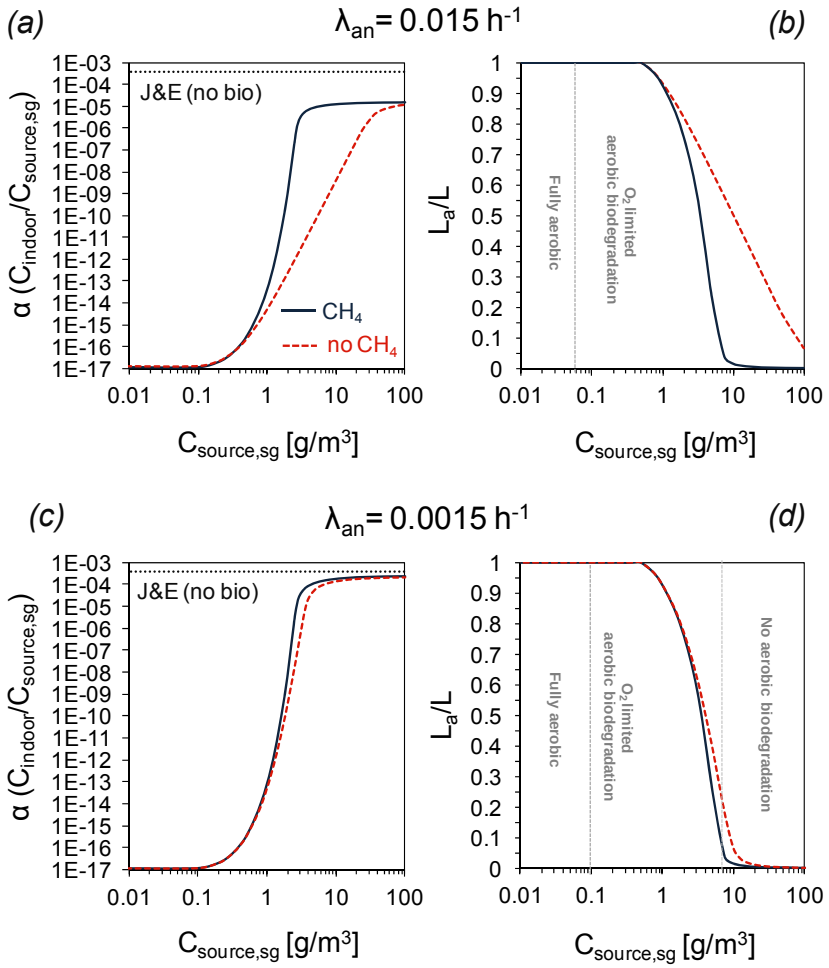


**Figure 1.3**. Toluene attenuation factor and normalized aerobic layer depth vs. soil-gas source concentration for two values of the anaerobic biodegradation constant: methanogenic anaerobic biodegradation (continuous line); non-methanogenic anaerobic biodegradation (dashed lines). For reference the results obtained by the Johnson & Ettinger model are also shown.

These results, which are more evident for high values of the anaerobic biodegradation constant, are due to the fact that under methanogenic conditions, the anaerobic reaction leads to methane generation. The methane produced in the anaerobic zone migrates upward in the vadose zone, leading to a further oxygen demand, due to oxidation of

methane, with a consequent reduction of the layer thickness where aerobic biodegradation occurs.

**Table 1.6**. Vapor phase composition.

| **Compound** | **Pure Toluene** *(Fig.1.4a)* | **BTEX mixture** *(Fig.1.4b)* | **Fresh Gasoline** *(Fig.1.4c)* | **Weathered Gasoline** *(Fig.1.4d)* |
|---|---|---|---|---|
| | Vapor phase mass fraction | | | |
| Benzene | --- | 2.5E-01 | 2.3E-03 | 1.6E-02 |
| Toluene | 1.0E+00 | 2.5E-01 | 4.8E-03 | 4.9E-02 |
| Etilbenzene | --- | 2.5E-01 | 2.0E-04 | 2.0E-04 |
| Xylenes | --- | 2.5E-01 | 2.4E-03 | 1.7E-02 |
| Total BTEX [(a)] | 1.0E+00 | 1.0E+00 | 9.7E-03 | 8.2E-02 |
| Other hydrocarbons – aliphatic [(a)] | --- | --- | 9.9E-01 | 9.1E-01 |
| Other hydrocarbons – aromatic [(a)] | --- | --- | 1.5E-03 | 7.5E-03 |

*(a) API (2009)*

**Mixture of Hydrocarbons**

The previous results showed the influence of the different site-specific parameters on the overall attenuation assuming a soil contaminated by toluene only, although in typical contamination scenario it is more common to find a mixture of hydrocarbons. This scenario can be readily simulated with the model presented in this chapter. Fig.1.4 reports an example of the different behavior, in terms of the toluene attenuation factor (calculated considering both aerobic and methanogenic anaerobic biodegradation) as a function of the source concentration, assuming a soil contaminated by toluene only (Fig.1.4a), by a BTEX mixture (Fig.1.4b), by Fresh Gasoline (Fig.1.4c) and by Weathered Gasoline (Fig.1.4d). The vapor phase mass fractions assumed for the simulation are reported in Table 1.6. The other inputs are reported in Table 1.4 and Table 1.5.

As expected, the results obtained show that the predicted toluene attenuation factor, calculated at the same toluene source concentration, is typically higher when toluene is present as one of the components of a hydrocarbon mixture, either it is a BTEX mix or a gasoline one. Such a behavior is particularly relevant for intermediate to high source concentrations. Namely, in this specific case, an increase of the attenuation factor, in the case of toluene only, is observed for toluene concentration ($C_{source,sg}$) above 0.1 g/m$^3$,

whereas for a Fresh Gasoline source this conditions is reached for $C_{source,sg}$ > 0.003 g/m$^3$. Indeed, the presence of a mixture of hydrocarbons increases the oxygen demand and thereby reduces the thickness of the layer where aerobic biodegradation occurs. Furthermore, in this case (i.e. methanogenic anaerobic biodegradation) the presence of a mixture causes an increase of methane production which, as described above, leads to an higher oxygen consumption in the aerobic zone with a consequent further reduction of the aerobic biodegradation pathway.

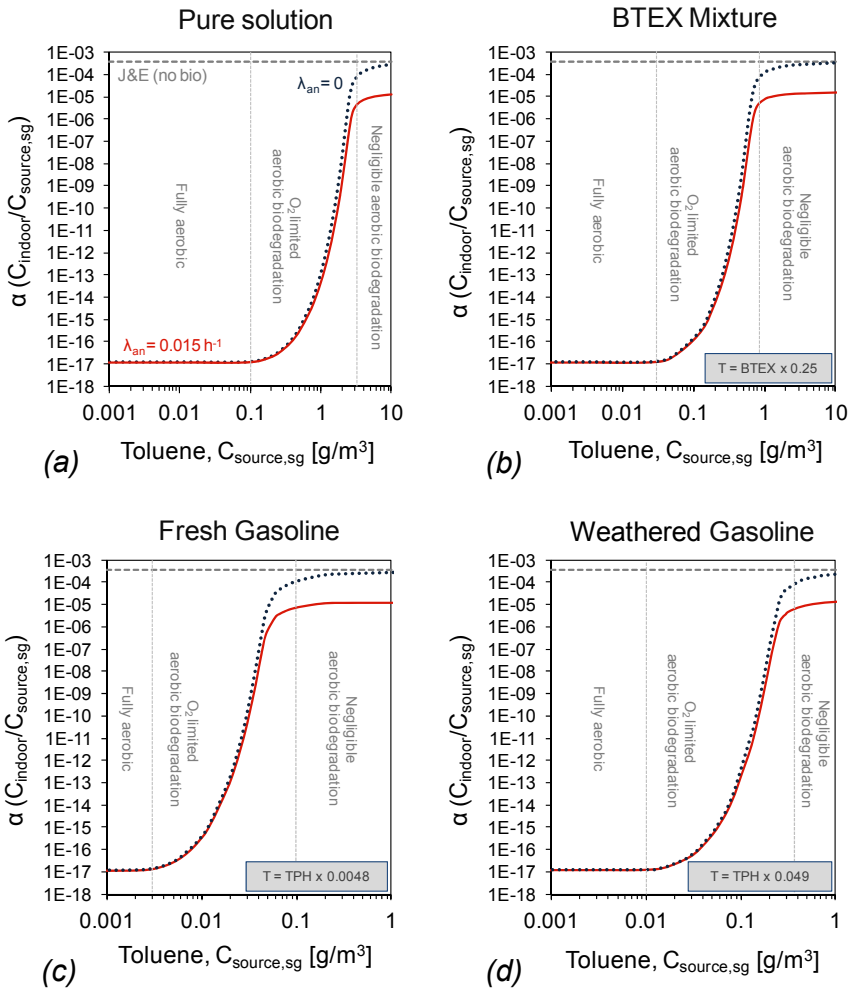


**Figure 1.4.** Toluene attenuation factor vs. toluene soil-gas source concentration in the case of a soil contaminated by (a) Toluene, (b) BTEX, (c) Fresh Gasoline and (d) Weathered Gasoline source. Aerobic and methanogenic anaerobic biodegradation (continuous line); Aerobic and negligible anaerobic reaction (dashed lines). For reference the results obtained by the Johnson & Ettinger model also reported.

# SECTION 2

# EXPOSURE DURATION TO CONTAMINATED GROUNDWATER

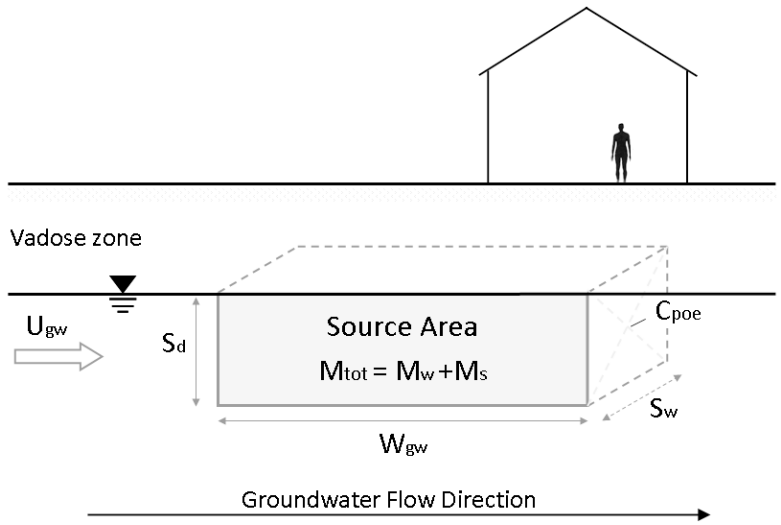


*This chapter is partially taken from:*

*Baciocchi R., Berardi S., Verginelli I. (2010). Human Health Risk Assessment: models for predicting the Effective Exposure Duration of On-Site Receptors Exposed to Contaminated Groundwater. Journal of Hazardous Materials 181(1–3), 226–233.*

## BACKGROUND

Among the different simplifying assumption of Tier 2 ASTM-RBCA models, a key one consists in considering a constant concentration value for the contamination source throughout the entire exposure period of a generic receptor. This approach is somehow mitigated in the case of vapour volatilization from soil, by introducing a limit on the maximum amount of contaminant that can be generated by the contamination source, whereas no mention to this issue is given in the ASTM-RBCA guidelines for contamination source in groundwater, neither for volatilization, nor for migration in the saturated zone. This assumption may lead, for some types of constituents and soils, to extremely conservative results in terms of risk as the source reduction due to the various attenuation processes may occur and have a significant influence on contaminant concentrations. As a matter of fact, several studies have shown that natural attenuation (NA) can be particularly effective in reducing the mass, toxicity, mobility, volume and concentrations of contaminants (Azadpour-Keeley et al. 2007; Johnson et al. 2006; Lundegard et al. 2006; Khan and Husain, 2001; Rugner et al. 2006). NA refers to naturally-occurring processes in soil and groundwater environments that act without human intervention (U.S.EPA 1999). These natural processes include biological degradation, volatilization, dispersion, dilution, and sorption of the contaminant onto the organic matter and clay minerals in the soil (Mulligan and Yong, 2004). Recent studies have demonstrated the occurrence of natural attenuation in groundwater by studying the evolution of the plume length (Shih et al. 2004; Newell and Connor, 1998; Prommer et al. 2002) and the mass reduction (Christensen et al. 2000), the geochemical processes (Cozzarelli et al. 2001). Various commercial packages are available for simulating these processes. The analytical models BIOSCREEN (U.S.EPA, 1996) and BIOCHLOR (U.S.EPA, 2000) allow to simulate the NA for petroleum fuel and chlorinated solvents, respectively. The Domenico analytical transport model (Domenico, 1987) is the basis for these models and includes the assumption that the source concentration does not change with time. On the other hand, the RBCA ToolKit (Connor et al. 2007) and the $RISC_4$ (Spence and Walden, 2001) packages account for the decrease in exposure concentration due to volatilization, biodegradation and leaching for contaminated soil and due to dissolution and biodegradation in the case of groundwater source. In addition

numerical models such as BIOPLUME III 2-D (Rifai et al. 2000), MODFLOW (Harbaugh et al. 2000) coupled with RT3D (Clement, 1997) and FEFLOW (Wasy, 2006) allow to simulate this process.

It is worth noting that all these models simulate a transient condition and thus the risk is not calculated using the usual equations of a Tier 2 framework but rather as the sum of the incremental risk values associated to each exposure interval.

Hence in this work a model to overcome the limitation of the ASTM-RBCA one, but keeping its original simplicity (Tier 2 framework), was developed. This model accounts for source attenuation, through a simple material balance, identifying the time required for depletion and consequently the effective exposure duration. The only source attenuation mechanism included in this work relies on run-off by groundwater flow, which is assumed to be dominant with respect to volatilization. Although biodegradation may some times contribute significantly to source depletion, it is not considered here, since it would require a level of characterization, that is usually not available when performing a Tier 2 risk analysis. The results provided by the proposed model are then compared with those obtained through the traditional ASTM-RBCA approach, a model based on the source depletion algorithm of the RBCA ToolKit software and a commercial numerical model (FEFLOW), allowing to assess its feasibility for inclusion in risk analysis procedures.

## MODELING

The analytical Fate and Transport models included in the ASTM-RBCA standard are based on the following assumptions (ASTM, 1999):

- Constant source concentration;
- Fixed Exposure Duration (for instance for industrial receptors, ED= 25 years).

This assumption, which relies on considering a time-independent source-area concentration, may often result in too conservative results, since the groundwater flow usually and actually leads to a gradual run-off of the source concentration until its complete depletion. The main parameters that influence the source run-off are the site hydro-geological characteristics (e.g., hydraulic gradient and soil texture) and the contaminant's properties (e.g., partition coefficient). This means that in practice, also the exposure duration will not be fixed, but will depend on the time required for the complete source depletion.

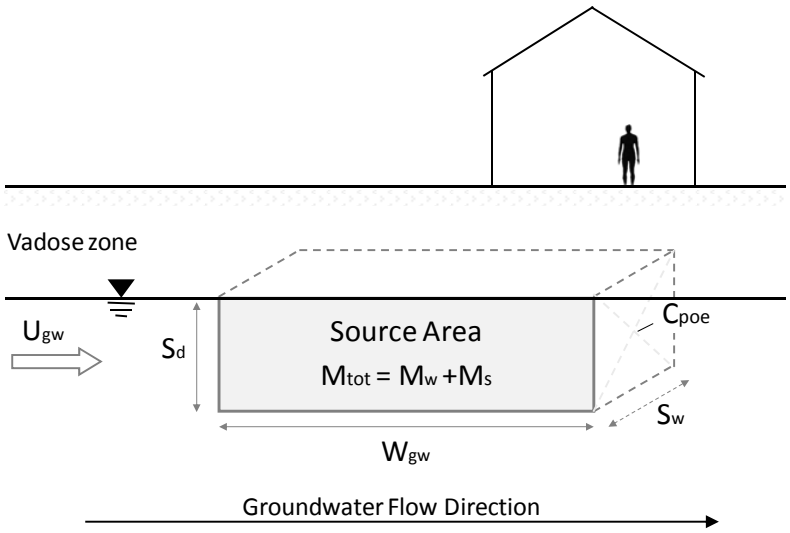


**Figure 2.1.** Conceptual Model.

Since the model proposed by the ASTM-RBCA standard is not suitable for describing these effects, two alternative analytical models are described in this chapter that take into account source depletion:

1. A simple model, properly developed in this work, based on the same equation given above for risk calculation, but which accounts for source depletion using a material balance approach to evaluate the period of exposure, assuming constant source concentration until complete depletion by groundwater run-off;
2. A model based on the source depletion algorithm included in RBCA ToolKit, assuming variable concentration over time. In this case the total risk is calculated as the sum of the incremental risk values associated to each exposure interval.

The derivation of both analytical models is described in the following section, which is followed by a section where the details of the numerical model used for comparison are summarized.

## Analytical models

### *Exposure-Duration model*

Let us assume the conceptual model shown in Fig.2.1 with a contamination source located in the aquifer (contaminated groundwater).

Assuming that no NAPL is present, the contaminant's total mass $M_{tot}$ (Eq. 2.1), can be expressed as the sum of the mass in the dissolved phase $M_w$ (Eq. 2.2) and the mass in the soil sorbed one $M_s$ (Eq. 2.3):

$$M_{tot} = M_w + M_s \tag{2.1}$$
$$M_w = V \cdot C_w \cdot \theta_e \tag{2.2}$$
$$M_s = V \cdot \rho_s \cdot C_s \cdot (1 - \theta_e) \tag{2.3}$$

Where $V$ is the total source volume, $C_w$ and $C_s$ the average source concentration in water and soil, and $\theta_e$ the effective soil porosity.

The concentration in the soil sorbed phase can be expressed, assuming a linear equilibrium, in terms of the concentration in the dissolved phase through the partition coefficient $K_d$:

$$C_s = C_w \cdot K_d \tag{2.4}$$

Hence, replacing Eqs. (2.1) – (2.3) into Eq. (2.4), the total mass $M_{tot}$ can be expressed as:

$$M_{tot} = M_w + M_s = V \cdot C_w \cdot [\theta_e + \rho_s \cdot K_d \cdot (1 - \theta_e)] \quad (2.5)$$

The time needed to achieve complete source depletion $t_d$, can be calculated by imposing the condition that the mass transported by groundwater flow $M_{transp}$, is equal to the total mass initially present $M_{tot}$ :

$$M_{transp} = M_{tot} \quad (2.6)$$

Making the simplifying but conservative assumption that the groundwater flow does not affect the constant source concentration during the run-off process, the transported mass can be defined as:

$$M_{transp} = t \cdot Q \cdot C_w \quad (2.7)$$

Replacing Eq. (2.7) into Eq. (2.6) and properly manipulating Eq. (2.7), it is then possible to evaluate the time required for the complete source depletion $t_d$:

$$t_d = M_{tot} / (Q \cdot C_w) \quad (2.8)$$

In the framework of the Risk Analysis approach, this time can be considered as the effective exposure duration $ED_{eff}$.

Making reference to the conceptual model reported in Fig.2.1, the terms of the latter equation can be expressed as:

$$Q = U_{gw} \cdot S_w \cdot S_d \quad (2.9)$$

$$U_{gw} = K_s \cdot i \quad (2.10)$$

$$V = W_{gw} \cdot S_w \cdot S_d \quad (2.11)$$

Replacing Eqs. (2.9), (2.10) and (2.11) in Eq. (2.8), the following equation for the estimation of average exposure duration is obtained:

$$ED_{eff} = W_{gw} \cdot [\theta_e + \rho_s \cdot K_d \cdot (1 - \theta_e)] / (K_s \cdot i) \quad (2.12)$$

It is worth noting that in this model the average exposure duration does not depend on the initial source concentration but only on the hydro-geological characteristics and on the contaminant's properties.

Thus, the proposed approach for the estimation of the effective exposure duration can be summarized as follows. The exposure duration is the minimum value between the one provided by Eq. (2.12) and the one set by the RBCA approach, i.e.:

$$\begin{cases} ED = \mathrm{ED}_{\mathrm{eff}} & \text{when } \mathrm{ED}_{\mathrm{eff}} < 25\,years \\ ED = 25\,years & \text{when } \mathrm{ED}_{\mathrm{eff}} \geq 25\,years \end{cases} \tag{2.13}$$

It is worth noting that the value provided by this model does not match the actual time required for the source depletion, but it is rather an hypothetical period of exposure obtained assuming the source concentration constant until complete depletion.

***Source-Depletion model***

Differently from the assumption made in the model discussed above, the source concentration actually decreases with time, thus also affecting the rate of the run-off process and consequently the time to achieve complete source depletion.

The change of total source mass *dM* can be calculated differentiating Eq. (2.5):

$$dM = V \cdot \left[\theta_e + \rho_s \cdot K_d \cdot (1-\theta_e)\right] \cdot dC \tag{2.14}$$

As seen before, the time needed to achieve complete source depletion $t_d$, corresponds to the condition that the transported mass is equal to the total mass initially present (Eq. 2.6). In this case the effective transported mass can be expressed by differentiating Eq. (2.7):

$$M_{transp} = Q \cdot C_w(t) \cdot dt \tag{2.15}$$

Equating Eqs. (2.14) and (2.15) provides:

$$Q \cdot C_w(t) \cdot dt = V \cdot \left[\theta_e + \rho_s \cdot K_d \cdot (1-\theta_e)\right] \cdot dC \tag{2.16}$$

This differential equation can be manipulated and integrated assuming $C_w = C_0$ at $t=0$ :

$$-\int_{C_0}^{Cw(t)} dC / C_w(t) = Q / \left[V \cdot \theta_e + V \cdot \rho_s \cdot K_d \cdot (1-\theta_e)\right] \cdot \int_0^t dt \tag{2.17}$$

Whose solution is:

$$\ln(C_w(t) / C_0) = - Q \cdot t / \left[V \cdot \theta_e + V \cdot \rho_s \cdot K_d \cdot (1-\theta_e)\right] \tag{2.18}$$

Then solving Eq. (2.18) for the concentration in dissolved phase $C_w(t)$ and replacing the equation parameters given in Eq. (2.9), (2.10) and (2.11), the source concentration at time $t$, $C_w(t)$ is given by:

$$C_w(t) = C_0 \cdot \exp\left[-K_s \cdot i \cdot t / [\theta_e \cdot W_{gw} + \rho_s \cdot W_{gw} \cdot K_d \cdot (1-\theta_e)]\right] \tag{2.19}$$

This equation is equal to the following one, provided by RBCA ToolKit:

$$C_w(t) = C_0 \cdot \exp(-\gamma \cdot t) \tag{2.20}$$

provided that γ is equal to:

$$\gamma = Q \cdot (A + B) \tag{2.21}$$

with $A$ defined as:

$$A = 1 / [\theta_e \cdot W_{gw} + \rho_s \cdot W_{gw} \cdot K_d \cdot (1-\theta_e)] \tag{2.22}$$

and assuming $B = 0$, i.e. neglecting biodegradation.

It is worth pointing out that in the RBCA ToolKit formulation the groundwater concentration and the initial mass of contaminant are both required as user input. In our model, the mass of contaminant is calculated as a function of the groundwater concentration, always assuming linear equilibrium between the liquid and the soil phase, allowing to provide only the groundwater concentration as user input.

Finally, it is worth to underline that the two analytical models discussed in this section correspond to two limiting ideal models that can be used to describe mass transport in porous media: the source-depletion model corresponds to a plug flow model, whereas the exposure-duration model to a perfectly well mixed one.

**Numerical model**

The FEFLOW software (Finite Element subsurface FLOW) version 5.3x was used in this work. This version allows to simulate 2D and 3D fluid flow, mass and heat transport problems in a saturated media, in unsaturated media and also in variable saturation media (Wasy, 2006). In this work the simulations were performed using the following main settings:

- Two dimensional modeling;
- Triangular discretization (Tmesh method);
- Saturated media (groundwater);
- Transient conditions (flow and transport);
- Automatic time stepping schemes based on forward Euler/backward Euler method;
- No heat transport;
- Dirichlet (1st kind) and Neumann (2nd kind) boundary conditions.

The point of exposure was positioned at the downstream border of the source area (see Fig.2.1). The calculated concentration values at different times were then used for the cumulative risk calculation as reported in the next section.

The input parameters used for the FEFLOW simulations are reported in Table 2.1.

**Risk calculation**

Risk was calculated using Eq. (I.2) for the Exposure-Duration model and the ASTM-RBCA approach. In the latter one, exposure duration, *ED*, was set equal to 25 years, whereas in the former one, *ED* was set equal to the time required for source depletion, given by Eq. (2.12). When the numerical and Source-Depletion models were used, the risk was calculated by dividing the whole exposure period in a given number of exposure intervals. For each interval the average concentration at point of exposure and the corresponding incremental risk were calculated. Thus the total risk, $R_T$, was calculated as the sum of the incremental risk values associated to each exposure interval:

$$R_T = \sum_{i=1}^{n} R_i \tag{2.23}$$

Where $R_i$ is the risk calculated to a generic *i-th* time interval, calculated using Eq. (I.2) and with *ED* equal to the duration of the time interval itself:

$$R_i = SF \cdot \frac{\mathrm{CR} \cdot \mathrm{EF}}{\mathrm{BW} \cdot \mathrm{AT}} \cdot \sum C_{poe,i} \cdot \mathrm{ED}_i \tag{2.24}$$

## INPUT PARAMETERS

Application of both analytical and numerical models was carried out using the default values for all the input parameters provided in the ISPRA document (ISPRA, 2008). All properties related to the site and contamination source were taken from this reference as well as the soil physical properties (Table 2.1).

Benzene was considered as target pollutant with a representative concentration equal to 0,1 mg/L in groundwater, which correspond to a value 100 times higher than the current target value set by the Italian legislation (D.lgs 152/06). All exposure parameters were taken for industrial/commercial scenario.

**Table 2.1**. Input Parameters.

| Symbol | Parameter | Units | Sand | Loam | Clay |
|---|---|---|---|---|---|
| $i$ | Groundwater Gradient | m/m | 0.01 | 0.01 | 0.01 |
| $S_w$ | Length of source-zone area | m | 45 | 45 | 45 |
| $\rho_s$ | Bulk Density | g/cm$^3$ | 1.7 | 1.7 | 1.7 |
| $K_{sat}$ | Saturated Hydraulic Conductivity | cm/s | 8.3E-03 | 2.9E-04 | 5.7E-05 |
| $\theta_e$ | Soil Porosity | cm$^3$/cm$^3$ | 0.385 | 0.352 | 0.312 |
| $f_{oc}$ | Mass Fraction of Organic Carbon | g/g | 0.001 | 0.001 | 0.001 |
| $K_{oc}$ | Organic Carbon / Water partition coefficient | mL/g | 62 | 62 | 62 |
| $K_d$ | Soil / Water Partitioning Coefficient (*) | mL/g | 0.062 | 0.062 | 0.062 |
| $C_0$ | Initial Concentration | mg/L | 0.1 | 0.1 | 0.1 |

(*) *Soil / Water Partitioning Coefficient:* $K_d = K_{oc} \cdot f_{oc}$

## RESULTS AND DISCUSSIONS

The results reported in this section provide the values of source concentration and carcinogenic risk from contaminated groundwater ingestion, obtained by applying both the numerical and analytical models, described above.

**Concentration Profiles**

Fig.2.2 reports the time profile of benzene concentration at the source-area for three different soils (Sand, Loam and Clay) obtained applying the ASTM-RBCA, the Exposure-Duration model, the Source-Depletion model and the numerical model discussed above. The results of the latter model refer to the concentration calculated at a position corresponding to the outlet section of the contamination source, assuming its initial geometry. This allows a fair comparison with the result of the Source-Depletion model, which is based on a plug flow approximation. The Exposure-Duration model and the Source-Depletion model do not account for the longitudinal and transverse dispersion during contaminant's migration. For this reason the results obtained by the application of these models have been compared with the FEFLOW results assuming:

- Contaminant's migration with low dispersion ($a_x = a_y = a_z = 0.1$ m)
- Contaminant's migration with dispersion ($a_x = 10$ m; $a_y = a_z = 1$ m)

where $a_x$ is the longitudinal dispersivity and $a_y$, $a_z$ are the transverse and vertical dispersivities respectively.

As shown in Fig.2.2, the time required for source depletion increases from sandy to clay texture, for all approaches used. For instance, the *ED* calculated by the Exposure-Duration model increases from 1 year for sandy soil to 20 years for loamy soils and exceeds 25 years for clay soils.

Making reference to the case of sandy soils, reported in Fig.2.2, it can be noticed that, using the Exposure-Duration model, the time required for source depletion assuming constant source concentration, would result equal to approximately 1 year, that is much less than the 25 years default exposure duration. The result provided by the source depletion model is somehow in between, with a source depletion time of approximately 3 years, although in this approach the source concentration is not constant but decreases with time.

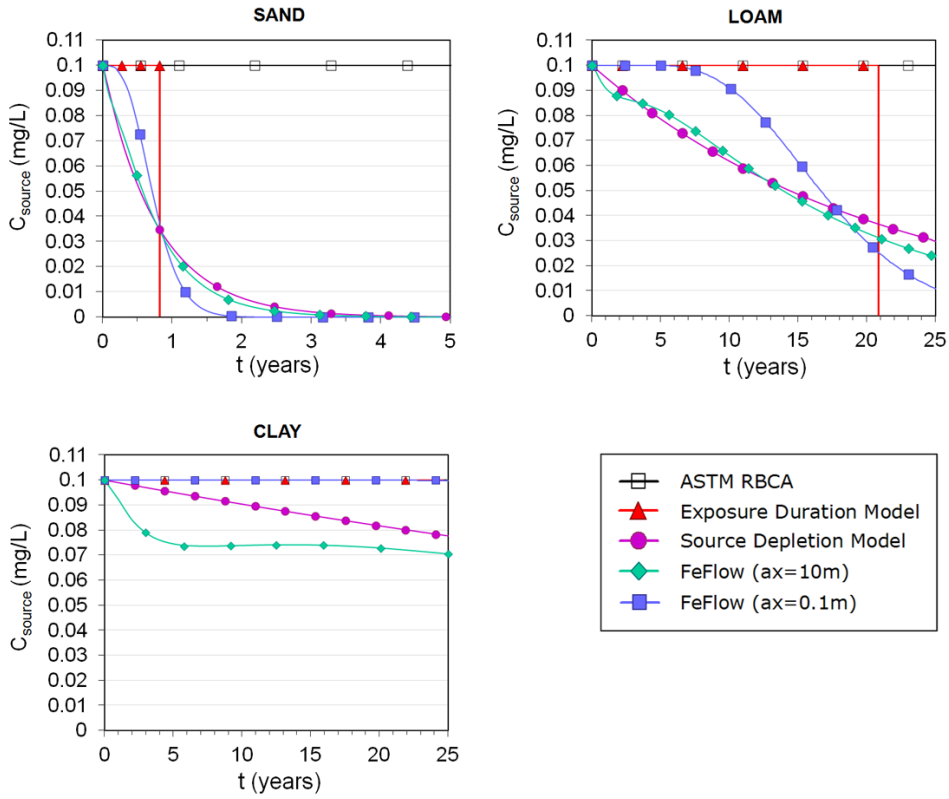


**Figure 2.2.** Benzene Source Concentration (Csource) vs. Time (t).

This result is in quite good agreement with the one provided by the numerical model. Similar results are obviously obtained for the other soil textures, although with different time scales. Nevertheless, given the different nature of the proposed models, i.e. steady state for the Exposure-Duration and ASTM-RBCA ones and transient for the numerical and Source-Depletion ones, a fair comparison can be done more correctly in terms of exposure and therefore of risk, and is reported in the next section.

**Risk calculation**

Risk values obtained for the three investigated soil textures, using the different modelling approaches are reported in Fig.2.3. The comparison shows that for permeable soil (e.g. Sand; see Fig.2.3a) the ASTM-RBCA approach provides more conservative carcinogenic Risk values ($R > 1x10^{-5}$), two orders of magnitude higher than those obtained applying the Exposure-Duration model ($R \approx 6x10^{-7}$). Looking at Fig.2.3a it can

be noticed that the results of the Exposure-Duration model are in this case similar to those provided by the Source-Depletion model and slightly more conservative than those given by the FEFLOW simulations.

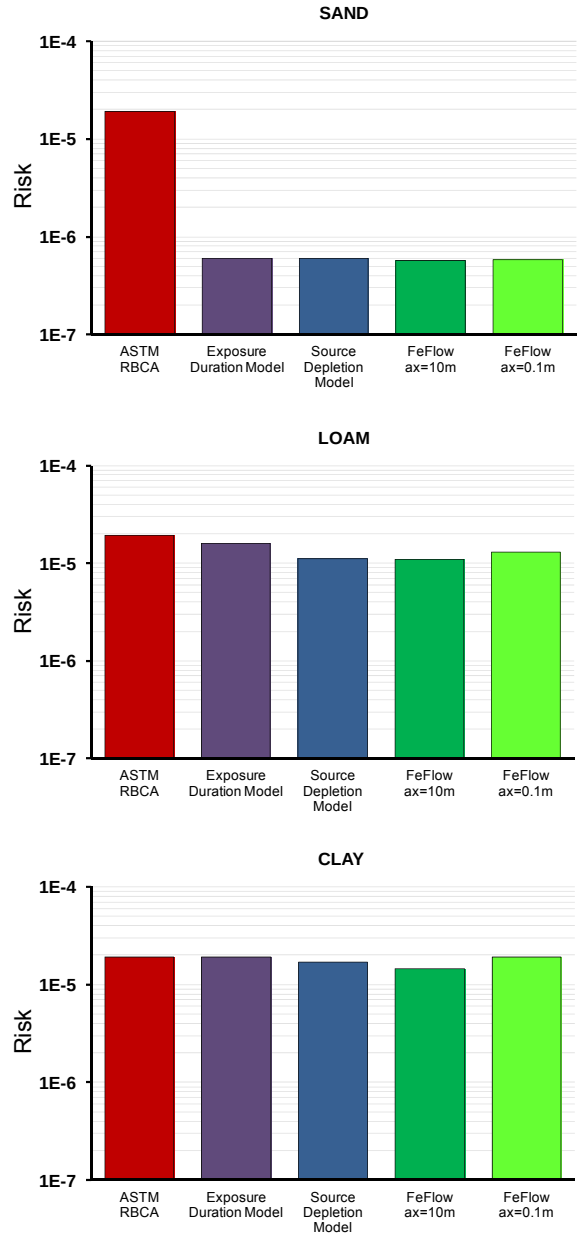


**Figure 2.3.** Carcinogenic Risk associated to ingestion of benzene-contaminated groundwater for Sand (a), Loam (b) and Clay (c).

The difference between the proposed model and the ASTM-RBCA one, is reduced when a loamy soil is considered (Fig.2.3b) whereas the two models provide identical results in the case of a clay soil (Fig.2.3c). These results are in agreement with the calculated depletion time (see Fig.2.2), which increases, as seen before, from a sandy to a clay soil. This means that, at least in the case of benzene, using the standard ASTM-RBCA approach would lead to an important overestimation of the calculated risk for sandy soils, a lower one for loamy ones and more realistic result for clay soils.

This suggests that the proposed models provide a more realistic picture of the risk condition with respect to the ASTM-RBCA approach, but still more conservative than the one given by a numerical model, although most of the intrinsic simplicity of the ASTM-RBCA approach is maintained, especially as far as the analytical model is concerned.

**Limits of validity of the Exposure-Duration model**

In view of the results shown above it can be stated that the proposed Exposure-Duration model (easier to apply than the Source-Depletion one), can be used to account for the depletion of the concentration source, although assuming no NAPL is present and respecting the feature of Tier 2 risk analysis models, i.e. using analytical equations.

As previously described, the exposure duration is given by Eq. (2.19); this means that if the depletion time is lower than the default exposure duration (25 years for industrial receptors), it will be equal to the effective exposure duration, $ED_{eff}$, given by Eq. (2.18). In this case, $ED_{eff}$ is a function of both the constituent properties, trough the partition coefficient, $K_d$, and the media characteristics, trough the hydrological parameters $K_s$, $i$, $\theta_e$ and $\rho_s$. This suggests that the exposure duration for a given soil type is limited by the source depletion time, depending on the value of the partition coefficient $K_d$ and that of the hydraulic gradient, $i$. In other words, for any soil type characterized by a given value of $K_s$, $\theta_e$ and $\rho_s$, there exists a maximum value of the partition coefficient $K_d$* below which the condition $ED_{eff} < ED$ holds true and therefore the Exposure-Duration model application can be suggested. Fig.2.4 reports these $K_d$* values for different soil types, as a function of hydraulic gradient. Looking at this figure, it can be noticed that the $K_d$* value at constant hydraulic gradient, $i$, decreases going from coarse soils to more fine grained ones. For known media properties, Fig.2.4 can be used to evaluate if the

partition coefficient of a given constituent falls above or below the relevant $K_d$* value, and thus if the proposed model deserves to be applied for a more correct and realistic evaluation of the exposure duration.

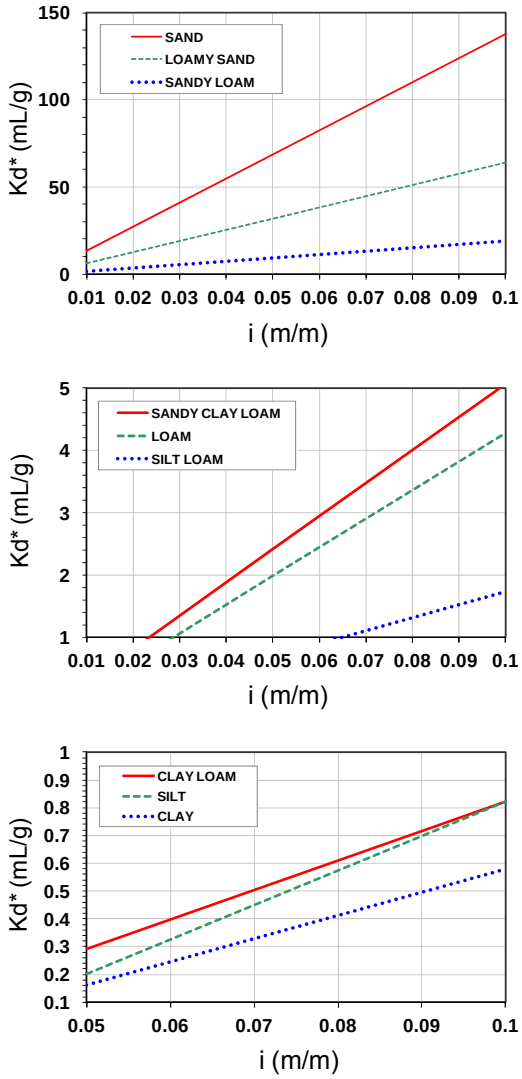


**Figure 2.4.** Limit Soil-Water Partition Coefficient (Kd*) vs. Groundwater Gradient (i).

Such a comparison is made more clear looking at Fig.2.5, where the effective exposure duration is reported for different soil textures and hydraulic gradient values, as a function of the contaminant partition coefficient $K_d$. Let us consider the case of benzene

characterized by a $K_d$ value of 0.062 mL/g (assuming a mass fraction of organic carbon of 0.001 g/g). For a groundwater flow with i=0.01, Fig.2.5a shows that the effective exposure duration, $ED_{eff}$, is of few years for sandy to sandy loam soils, 14 years for a Sandy clay loam, 21 years for a Loamy soil and the full default exposure duration of 25 years just for finer grained soils.

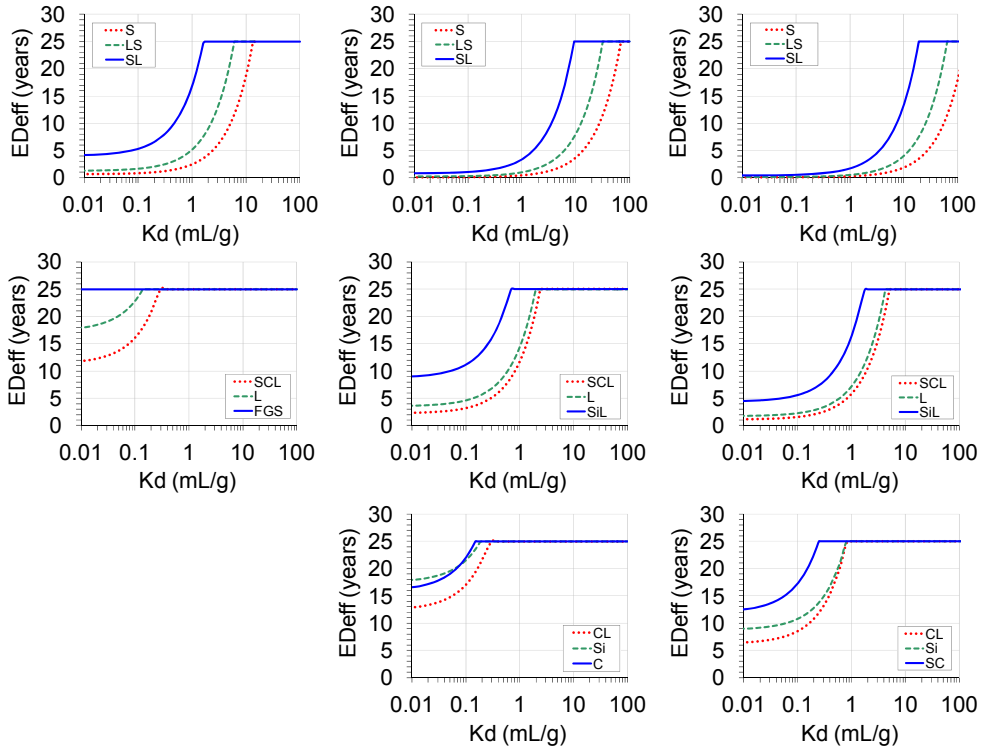


**Figure 2.5.** Average exposure duration ($ED_{eff}$) vs. soil/water partition coefficient (Kd). (a) Groundwater gradient (i = 0.01 m/m). (b) Groundwater gradient (i = 0.05 m/m). (c) Groundwater gradient (i = 0.1 m/m). S = Sand, LS = Loamy Sand, SL = Sandy Loam, SCL = Sandy Clay Loam, L = Loam, SiL = Silty Loam, CL = Clay Loam, Si =Silt, C = Clay, FGS = Finer grained soils, SC = Sandy Clay. Finer grained soils include silt loam, clay loam, silt, clay.

Increasing the hydraulic gradient to 0.05 and 0.1 (Fig.2.5b and 2.5c, respectively), $ED_{eff}$, for all soil types will be even lower, once again below the default ED. In all these cases, the Exposure-Duration model is useful to get a more physically sound description of the effective exposure time. Application of this model would be useful for all contaminants that are characterized by a partition coefficient value $K_d$, lower than the corresponding $K_d$*, which depends on the hydro-geological site-specific characteristics.

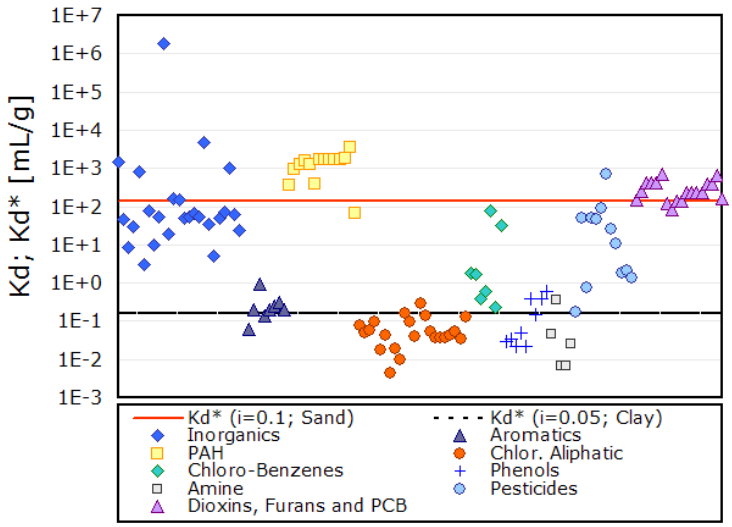


**Figure 2.6**. Limit Soil-Water Partition Coefficient ($K_d$*) vs. Soil- Water Partition Coefficient ($K_d$).

Fig.2.6 compares the $K_d$ data of the main contaminants, with the $K_d$* values for two limiting hydro-geological conditions, corresponding on the one hand to a sandy soil with $i$ = 0.1 and on the other hand to a clay soil with $i$ = 0.05. It is worth noting that for a sandy soil the $K_d$* is higher than the partition coefficients of most contaminants, suggesting that neglecting the use of the Exposure-Duration model would lead, to an overestimation of the actual exposure duration and therefore of the human health risk. On the other hand, in the case of the clay soil, the importance of the proposed model would be limited to just few contaminants classes, such as the chlorinated aliphatics, phenols and amines, characterized by higher mobility in groundwater system.

# SECTION 3

# LEACHING OF DISSOLVED PLUMES TO GROUNDWATER

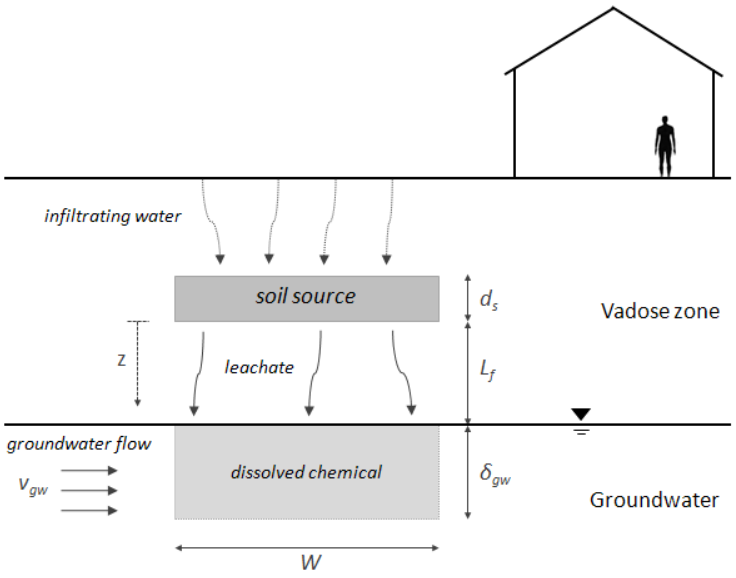


This chapter is partially taken from:

*Baciocchi R., Verginelli I. (2010). Attenuazione Naturale Intrinseca governata dall'Analisi di Rischio. Report for Eni Refining & Marketing (In Italian).*

*Verginelli I., Baciocchi R. Role of natural attenuation in modeling the leaching of contaminants in the risk analysis framework. Submitted to the Journal of Environmental Management.*

## BACKGROUND

Contamination of soils by petroleum products due to leaking underground storage tanks, accidental spills or improper surface applications is a widespread environmental problem (Karapanagioti et al. 2003). When the volume of spilled product is small, the hydrocarbon may be retained in an immobile condition in the unsaturated zone by capillary forces (Andre et al. 2009). In this case, source zones generating a dissolved-phase, may lead to a long term risk to groundwater since plume in the vadose zone can gradually leach by infiltrating water. Whereas a significant volume spill of Nonaqueous Phase Liquids (DNAPL or LNAPL) may take hours to days to reach a water table, a dissolved plume leached from a shallow source may require years to decades (Rivett et al. 2011). In this time framework if natural attenuation processes are significant, leached plumes may never reach groundwater, or else be substantially delayed with reduced concentrations (Rivett et al. 2011). As a matter of fact, in the last decades several studies have demonstrated the occurrence of natural attenuation in the unsaturated zone (Lundegard and Johnson 2006; Johnson et al. 2006; Kastanek et al. 1999; Hers et al. 2000; Roggemans et al. 2000). Hence, accounting for these processes is a crucial issue in order to properly assess the risk for groundwater contamination from point sources (Troldborg et al. 2009). However, in most screening tools for risk assessment, the description of transport through the unsaturated zone is very simplified. For instance, the leachate ASTM model (ASTM, 2000) accounts just for dissolution of contaminants into infiltrating water and dilution within the underlying groundwater, whereas no attenuation pathways are considered. The simplicity of this approach has led to a wide application of this model for the calculation of risk-based remediation standards. In fact, the risk assessment procedure is usually performed using simple analytical fate and transport models (i.e. RBCA Tier 2 application), that represent a reasonable compromise between the need for a detailed site assessment and the advantage of handling a rather simple and easy-to-use management tool. In addition, the site-specific data required for the application of these simple models are quite limited and are generally associated to the geometric descriptions of the source and to the identification of the physical properties of the environmental media through which migration is occurring. Therefore, only in very specific situations, where a more detailed description

of the contaminant transport through numerical models is required, risk assessment is performed following the Tier 3 approach.

Despite this approach has clear advantages, the experience gained over the years has highlighted that the leachate ASTM model can lead in some cases to an overestimation of the concentrations expected in the underlying aquifer.

In this view, in order to evaluate the expected significance of the different attenuation pathways, in this chapter an analytical model accounting for the transport and attenuation by multiple mechanisms in the unsaturated zone and in the source, was used. Namely, this model accounts for the key processes affecting the contaminants leaching scenario such as advection due to infiltrating water, dispersion and diffusion, sorption, first-order degradation in the water phase and source depletion due to biodegradation and dissolution. These features allow to highlight the dependence and the expected relevance of natural attenuation and depletion timeframes on soil conditions, site geometry and compounds properties. To this end, after a brief description of the model, several simulations related to typical contamination scenarios are reported and discussed in order to highlight in which cases the ASTM model is expected to lead to an overestimation of the risk for the downstream receptor.

# MODELING

## Fate and Transport models

Fate and transport models in the risk assessment procedure can be applied in a forward-calculation mode where constituent concentration at point of exposure ($C_{poe}$) is predicted based on source area concentration ($C_{source}$):

$$C_{poe} = C_{source} \cdot FT \tag{3.1}$$

where $FT$ is the transport factor, that accounts for the attenuation of the compound along the migration pathway.

Analytical models can also be applied in a back-calculation mode to determine the source-area constituent concentration corresponding to an acceptable concentration at the point of interest (ASTM, 2000).

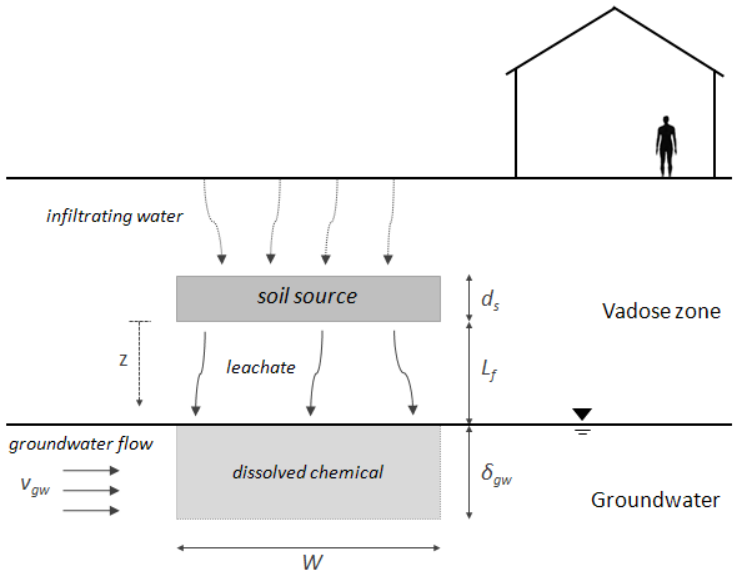


**Figure 1.** Conceptual model. The symbol z represents the spatial variable and is positive with increasing depth. The origin of z is placed at the bottom of the soil source.

The transport factor focused in this chapter is the Leaching Factor, $LF$, representing the ratio between total soil concentration and groundwater. $LF$ accounts for the

contaminant's attenuation during the transport from the source, located in the vadose zone, to the groundwater table.

The conceptual model of the leaching process of chemicals to ground water is reported in Fig.1.

**ASTM model**

The leachate model proposed by the ASTM standard is based on the following assumptions: (i) constant chemical concentration in soil, (ii) linear equilibrium partitioning between the different phases, (iii) steady-state leaching from the vadose zone to ground water resulting from the constant leaching rate and (iv) well-mixed dispersion of the leachate within the groundwater "mixing zone". Under these conditions the leaching factor, *LF*, is calculated as follows:

$$LF_{ASTM} = \frac{1}{K_{sw} \cdot LDF} \tag{3.2}$$

$K_{sw}$ is the soil - water partition coefficient:

$$K_{sw} = \frac{\theta_w + H \cdot \theta_a + \rho_s \cdot K_d}{\rho_s} \tag{3.3}$$

Where $\theta_w$ is the water-filled porosity of the soil, $H$ the dimensionless Henry's law constant, $\theta_a$ the air-filled porosity, $\rho_s$ the bulk soil density and $K_d$ the soil sorbed - water partition coefficient.

*LDF* is the Leachate Dilution Factor, which accounts for the dilution of the concentration occurring when the contaminant is transferred from the leachate to groundwater:

$$LDF = 1 + \frac{v_{gw} \cdot \delta_{gw}}{I_{ef} \cdot W} \tag{3.4}$$

Where $\delta_{gw}$ is the groundwater mixing zone height, $v_{gw}$ the groundwater Darcy velocity, W the width of source-zone area longitudinal to the groundwater flow and $I_{ef}$ the water infiltration rate.

Hence the ASTM model accounts just for the soil-water partitioning and the dilution occurring in groundwater, whereas no contaminant attenuation (e.g. biodegradation) or source depletion are considered. In the next section a model accounting for the different attenuation processes is reported.

**Natural Attenuation model**

***Attenuation during transport***

The steady state 1-D transport and reaction of leached contaminants in the vadose zone can be described by the usual diffusion-advection differential equation with reaction term:

$$D\frac{d^2C_w}{dz^2} - v_{leach}\cdot\frac{dC_w}{dz} - \lambda\cdot\theta_w\cdot C_w = 0 \tag{3.5}$$

where $C_w$ is the solute concentration in the water phase, $\lambda$ the first-order degradation rate and $D$ the dispersion-diffusion coefficient:

$$D = \alpha_z\cdot v_{leach} + D^{eff} \tag{3.6}$$

With $\alpha_z$ representing the contaminant dispersivity, $L_f$ the water table depth and $D^{eff}$ the effective porous medium diffusion coefficient:

$$D^{eff} = D_w\cdot\frac{\theta_w^{10/3}}{\theta_e^{2}} \tag{3.7}$$

Where $D_w$ is the diffusion coefficient in water, $\theta_w$ the water-filled porosity of the soil and $\theta_e$ the effective soil porosity.

The time required for infiltrating water to reach the overlying water table ($t_w$) can be calculated by applying the Green & Ampt (1911) equation:

$$t_w = R\cdot\frac{\theta_a}{K_{sat}}\cdot\left[L_f - \left(H_w - h_{cr}\right)\cdot\ln\left(\frac{H_w + L_f - h_{cr}}{H_w - h_{cr}}\right)\right] \tag{3.8}$$

where $\theta_a$ is the air-filled porosity of the soil, $K_{sat}$ the hydraulic conductivity of the wetted zone, $H_w$ the ponding depth of water at the surface, $h_{cr}$ the wetting front suction head and $L_f$ the water table depth.

Hence the time required for the contaminant of concern to reach the water table ($t_{leach}$) can be estimated as a function of the retardation coefficient specific of the contaminant, $R$:

$$t_{leach} = R \cdot t_w \tag{3.9}$$

Assuming a linear equilibrium partitioning, the retardation coefficient can be determined as follows:

$$R = 1 + \frac{\rho_s \cdot K_{sw}}{\theta_e} \tag{3.10}$$

Where $\theta_e$ is the effective soil porosity, $\rho_s$ the soil bulk density and $K_{sw}$ the soil-water partition coefficient.

**Analytical solution.** An analytical solution of Eq. (3.5) was obtained by assuming the following boundary conditions: $C = C_0$ at $z = 0$ and $D\, d^2C/dz^2 = 0$ at $z = L_f$. Under these assumptions, the attenuation factor occurring during leaching, $\alpha_{leach}$ ($C_{Lf}/C_0$), can be calculated as follows:

$$\alpha_{leach} = \frac{\sigma \cdot \exp(k \cdot L_f)}{k \cdot \sinh(\sigma \cdot L_f) + \sigma \cdot \cosh(\sigma \cdot L_f)} \tag{3.11}$$

With:

$$k = \frac{L_f}{2 \cdot D \cdot t_{leach}} \tag{3.12}$$

$$\sigma = \sqrt{k^2 + \frac{\lambda \cdot \theta_w}{D}} \tag{3.13}$$

Where $\lambda$ is the first-order degradation rate and $D$ the dispersion-diffusion coefficient described in Eq. (3.6).

**Depleting Source**

The change of the mass source ($m_s$) over time ($t$), due to infiltrating water and biodegradation, can be described by the following mass balance:

$$-\frac{dm_s}{dt} = \mu_{\inf} + \mu_{bio} \tag{3.14}$$

Where $\mu_{inf}$ and $\mu_{bio}$ are the mass lost per unit time by leaching (Eq. 3.15) and by biodegradation (Eq. 3.16) respectively, which can be calculated as follows:

$$\mu_{\inf} = \frac{I_{ef}}{R} A \cdot C_w(t) \tag{3.15}$$

$$\mu_{bio} = \lambda_{source} \cdot \theta_w \cdot A \cdot d_s \cdot C_w(t) \tag{3.16}$$

$C_w$ is the source concentration in the water phase, $\lambda_{source}$ is the first-order kinetic rate constant, $A$ the source area, $d_s$ the source thickness and $I_{ef}$ the water infiltration rate.

The mass source, $m_s$, can be expressed in terms of the total source concentration $C_{tot}$:

$$m_s = \rho_s \cdot A \cdot d_s \cdot C_{tot}(t) \tag{3.17}$$

The total concentration $C_{tot}$, assuming linear equilibrium partitioning, is given by the sum of the concentrations in the different phases of the soil:

$$C_{tot} = \frac{1}{\rho_s}\left(\theta_w + H \cdot \theta_a + \rho_s \cdot K_d\right) \cdot C_w + C_{free} \tag{3.18}$$

$C_{free}$ is the concentration of the contaminant as free phase and is present only when the total concentration, $C_{tot}$, exceeds the saturation concentration $C_{sat}$:

$$C_{sat} = K_{sw} \cdot S \tag{3.19}$$

With $S$ representing the solubility of the contaminant and $K_{sw}$ the soil-water partition coefficient reported in Eq. (3.3).

Hence the source depletion can be described by substituting Eqs. (3.15) - (3.17) in Eq. (3.14):

$$-\rho_s \cdot A \cdot d_s \cdot \int_{C_0}^{C(t)} \frac{1}{\left( \frac{I_{eff}}{R} \cdot A + \lambda_{source} \cdot \theta_w \cdot A \cdot d_s \right)} \cdot \frac{dC_{tot}}{\frac{C_{tot}}{K_{sw}}} = \int_0^t dt \tag{3.20}$$

Eq. (3.20) was solved by dividing the problem into different domains corresponding to the condition of initial source concentration above or below the saturation limit, $C_{sat}$:

$$C_{tot}(t) = \begin{cases} C_{tot}(0) - C_{sat} \cdot \mu \cdot t & \text{for } C_{tot}(0) > C_{sat} \\ C_{tot}(0) \cdot \exp[-\mu \cdot (t - t^*)] & \text{for } C_{tot}(0) \le C_{sat} \end{cases} \tag{3.21}$$

With:

$$\mu = \frac{I_{eff}}{R \cdot d_s \cdot \rho_s \cdot K_{sw}} + \frac{\lambda_{source} \cdot \theta_w}{\rho_s \cdot K_{sw}} \tag{3.22}$$

It is worth noting that Eq. (3.21) is valid above the saturation concentration as long as the total concentration is lower than the residual concentration ($C_{res}$) which represent the upper limit above which the free phase (i.e. mobile NAPL) is expected to leach directly without the infiltrating water. In fact, as described by ASTM (2000), free phase may be present in unsaturated soil, but immobile due to capillary, viscous, and gravity forces acting on the bulk free phase.

$t^*$ reported in Eq. (3.21) is the time at which the initial source concentration reaches the saturation conditions (i.e. $C_{tot}(t) = C_{sat}$):

$$t^* = \frac{C_{tot}(0) - C_{sat}}{C_{sat} \cdot \mu} \tag{3.23}$$

Namely when the initial source concentration is higher than the saturation concentration ($C_{sat}$), assuming that the dissolution of the free product is faster or comparable to the attenuation processes which lead to a decrease of the concentration in the water phase, the source depletion can be described as a linear decrease of the concentration in the free phase, i.e. the concentrations of the other phases are assumed constant and equal to the saturated conditions. On the contrary, when the source concentration reaches the saturation conditions (i.e. $C_{free} = 0$) the depletion law becomes exponential, since

infiltrating water and biodegradation processes reduce the concentration in water phase and consequently, assuming a linear equilibrium partitioning, also in the sorbed and vapor phase.

Thus the change of the solute concentration over time $C_w(t)$, in the case of initial source concentration below the saturation limit, $C_{sat}$ (i.e. $t^* < 0$), will be equal to:

$$C_w(t) = C_w(0) \cdot \exp(-\mu \cdot t) \qquad \text{if } t^* \le 0 \tag{3.24}$$

In the case of $t^* > 0$ (i.e. $C_{tot} > C_{sat}$) the change of the solute concentration over time $C_w(t)$, can be calculated as follows:

$$C_w(t) = \begin{cases} S & \text{if } t \le t^* \\ S \cdot \exp[-\mu(t - t^*)] & \text{if } t > t^* \end{cases} \tag{3.25}$$

Hence the modified leaching factor, $LF_{bio}$, may be calculated by combining Eq. (3.2) with Eq. (3.11) and Eqs. (3.24) – (3.25) as follows:

$$LF_{bio}(t) = \frac{\alpha_{leach} \cdot \alpha_{dep}(t)}{K_{sw} \cdot LDF} \tag{3.26}$$

Where:

$$\alpha_{DEP}(t) = \begin{cases} \exp[-\mu \cdot t] & \text{for } t^* \le 0 \\ \exp[-\mu \cdot (t - t^*)] & \text{for } t > t^* \\ 1 & \text{for } t \le t^* \end{cases} \tag{3.27}$$

**Risk calculation**

The overall risk was can be calculated by dividing the whole exposure period (e.g. 25 years) in a given number of exposure intervals. For each interval the average concentration at point of exposure ($C_{poe}$) can be calculated using Eq. (3.1) and Eq. (3.26). Thus the total risk, $R_T$, can be calculated as the sum of the incremental risk values associated to each exposure interval:

$$R_T = \sum_{i=1}^{n} R_i \tag{3.28}$$

Where $R_i$ is the risk calculated to a generic *i-th* time interval, with *ED* equal to the duration of the time interval itself:

$$R_i = SF \cdot \frac{\mathrm{CR} \cdot \mathrm{EF}}{\mathrm{BW} \cdot \mathrm{AT}} \cdot \sum C_{poe,i} \cdot \mathrm{ED}_i \tag{3.29}$$

Where *SF* is the slope factor, *CR* is the ingestion rate, *EF* the Exposure Frequency, *ED* the Exposure Duration, *BW* the Body Weight, and *AT* the Averaging Time.
The same equation can be used for the calculation of the hazard index (*HI*) substituting the slope factor, *SF*, with the reference dose, *RfD*:

$$HI_i = \frac{1}{RfD} \cdot \frac{\mathrm{CR} \cdot \mathrm{EF}}{\mathrm{BW} \cdot \mathrm{AT}} \cdot \sum C_{poe,i} \cdot \mathrm{ED}_i \tag{3.30}$$

## RESULTS AND DISCUSSION

The model described above, was solved analytically and used to assess under which site conditions natural attenuation is expected to play a significant role. To this end, solutions have been calculated, using representative parameter ranges and values (Table 3.1 and Table 3.2).

**Table 3.1**. Model Input Parameters (unless otherwise noted in figures).

| Parameter | Symbol | Unit | Value | |
|---|---|---|---|---|
| | | | SAND | CLAY |
| Water table depth | $L_f$ | m | 0.5; 1; 2; 10 | |
| Source Thickness | $d_s$ | m | 1; 5 | |
| Length of source-zone area | $W$ | m | 45 | |
| Dispersivity factor (*) | $\alpha$ | cm | 0.33 x $L_f^{0.62}$ | |
| Ponding depth | $H_w$ | m | 0.3 | |
| Soil Bulk density | $\rho_s$ | g/cm$^3$ | 1.7 | |
| Water-filled porosity | $\theta_w$ | - | 0.2 | |
| Groundwater Gradient | $i$ | m/m | 0.01 | |
| Organic Fraction | $f_{oc}$ | - | 0.001 | 0.01 |
| Effective Infiltration | $I_{ef}$ | cm/year | 10 | 1 |
| Effective soil porosity | $\theta_e$ | - | 0.38 | 0.31 |
| Suction head | $h_{cr}$ | cm | -4 | -111.7 |
| Hydraulic conductivity | $K_{sat}$ | m/s | 8.3E-05 | 5.6E-07 |

*(*) Vanderborght and Vereecken, 2007.*

Namely these elaborations are aimed to evaluate the different leaching behavior as a function of the site-specific characteristics and chemical properties of the contaminants. In this view, in order to evaluate the relevance of the natural attenuation depending on the chemical properties, the model described in this chapter is applied to BTEX and PAHs which are characterized by completely different behaviors. In fact, as known, BTEX are quite soluble and characterized by relatively high biodegradation constant rates. Evidence for vadose zone biodegradation of BTEX has been seen at several field studies reporting typical average median values of biodegradation constant rates in the order of 0.01 and 10 $d^{-1}$ (e.g. see Davis et al. 2009, DeVaull 1997, Hers et al. 2000, Hoener et al. 2006). On the contrary, PAHs are largely sorbed to the soil and are slowly

biodegradable. Typical biodegradation rate constants values available in literature for these compounds are in the range of 0.0001 to 0.01 $d^{-1}$ (e.g. see Brauner et al. 2002, Blum et al. 2009, Thiele-Bruhn and Brümmer 2005, Bockelmann et al. 2001).

**Table 3.2**. Chemical properties for BTEX and some PAHs (ISS-ISPESL, 2009).

| **Compounds** | **Class** | **S** | **H** | **$K_{oc}$** | **$D_w$** | **$K_{sw}$ SAND foc = 0.001** | **$K_{sw}$ CLAY foc = 0.01** |
|---|---|---|---|---|---|---|---|
| | | *mg/L* | *-* | *L/kg* | *$cm^2/s$* | *L/kg* | *L/kg* |
| Benzene | BTEX | 1.75E+3 | 2.28E-1 | 6.20E+1 | 9.80E-6 | 1.45E-1 | 8.00E-1 |
| Ethylbenzene | BTEX | 1.69E+2 | 3.23E-1 | 2.04E+2 | 7.80E-6 | 3.04E-1 | 2.22E+0 |
| Stirene | BTEX | 3.10E+2 | 1.13E-1 | 9.12E+2 | 8.00E-6 | 9.73E-1 | 9.30E+0 |
| Toluene | BTEX | 5.26E+2 | 2.72E-1 | 1.40E+2 | 8.60E-6 | 2.31E-1 | 1.58E+0 |
| Xilene | BTEX | 1.85E+2 | 3.14E-1 | 1.96E+2 | 7.80E-6 | 2.95E-1 | 2.14E+0 |
| Benzo(a)anthracene | PAHs | 9.40E-3 | 1.37E-4 | 3.58E+5 | 9.00E-6 | 3.58E+2 | 3.58E+3 |
| Benzo(a)pyrene | PAHs | 1.62E-3 | 4.63E-5 | 9.69E+5 | 9.00E-6 | 9.69E+2 | 9.69E+3 |
| Benzo(b)fluorantene | PAHs | 1.50E-3 | 4.55E-3 | 1.23E+6 | 5.56E-6 | 1.23E+3 | 1.23E+4 |
| Benzo(g,h,i)perylene | PAHs | 7.00E-4 | 3.00E-5 | 1.60E+6 | 5.65E-5 | 1.60E+3 | 1.60E+4 |
| Benzo(k)fluorantene | PAHs | 8.00E-4 | 3.45E-5 | 1.23E+6 | 5.56E-6 | 1.23E+3 | 1.23E+4 |
| Crysene | PAHs | 1.60E-3 | 3.88E-3 | 3.98E+5 | 6.21E-6 | 3.98E+2 | 3.98E+3 |
| Dibenzopyrenes | PAHs | 2.49E-3 | 3.08E-6 | 1.66E+6 | 5.18E-6 | 1.66E+3 | 1.66E+4 |
| Indenopyrene | PAHs | 2.20E-5 | 6.56E-5 | 3.47E+6 | 5.66E-6 | 3.47E+3 | 3.47E+4 |
| Pyrene | PAHs | 1.35E-1 | 4.51E-4 | 6.80E+4 | 7.20E-6 | 6.80E+1 | 6.80E+2 |

In addition, in order to highlight the processes controlling the vadose zone transport and the attenuation of plumes leached from source zone, the results hereby presented, separately discuss the influence of natural attenuation occurring during the transport and in the source zone.

**Attenuation during leaching**

Fig.3.2 reports the leachate attenuation factor ($\alpha_{leach}$), calculated with the model described in this chapter, as a function of the time required for the contaminant to reach the water table. The simulations were performed assuming different water depths and different biodegradation constant rates. The obtained results, reported in the figure, show that the increase of the time required for the contaminant to reach the water table leads to a corresponding significant decrease of the calculated attenuation factor. Namely, for leaching time higher than 10 days, the attenuation due to biodegradation

and dispersion is expected to lead to a relevant attenuation of the solute concentration up to several order of magnitude. This is more evident for deeper groundwater (e.g. $L_f$ = 10 m, Fig. 3.2d) and for high biodegradation rate constants (see e.g. $\lambda$ = 1 $d^{-1}$). On the contrary, for time frames below 1 day the attenuation factor during the transport is negligible even in the case of very high biodegradation constant rates (i.e. $\lambda$ = 1 $d^{-1}$).

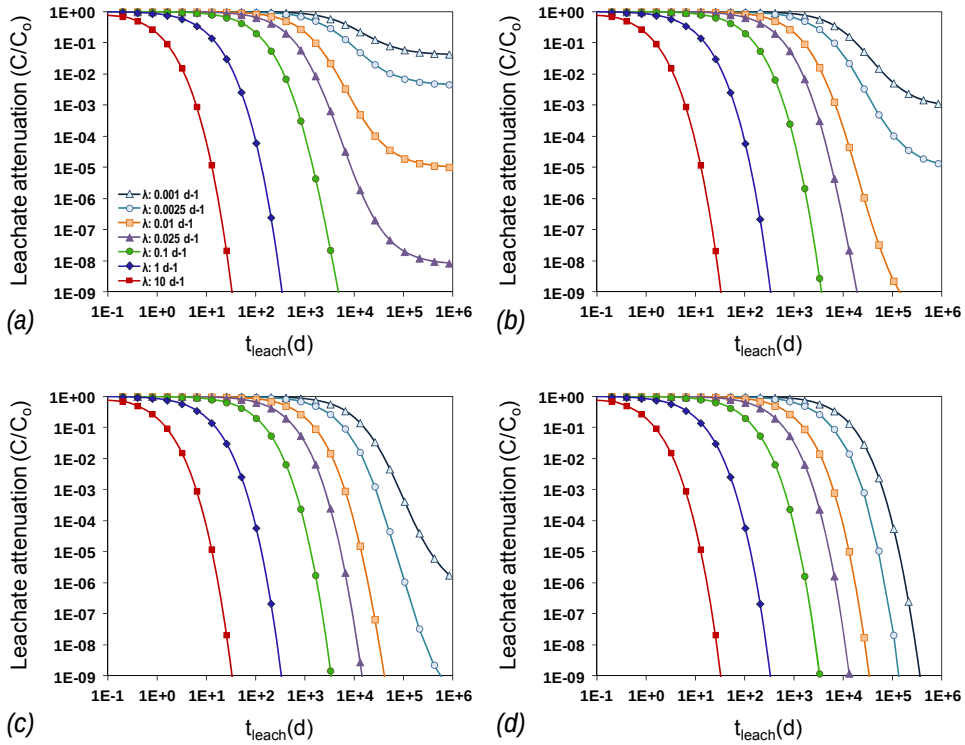


**Figure 3.2.** Leachate attenuation factor ($\alpha_{leach}$) calculated as a function of the time required for the contaminant to reach the underlying aquifer ($t_{leach}$). The results are reported assuming different biodegradation constant rates and aquifer depths: (a) $L_f$ = 0.5 m; (b) $L_f$ = 1 m; (c) $L_f$ = 2 m, (d) $L_f$ = 10 m.

To assess more specifically this behavior, Fig. 3.3 reports the time required for BTEX and some PAHs to reach the water table calculated with Eq. (3.8) assuming the same scenarios reported in Fig. 3.2. This figure shows that BTEX are generally characterized by leaching times in the range of 0.1 - 10 days whereas the PAHs, for the same scenario, are expected to reach the water table after 10 - 100 years (i.e. $10^4$ - $10^5$ days). In fact as discussed above, the time required to reach the water tables depends on the site specific conditions (e.g. soil texture) but especially on the contaminant properties. In fact,

soluble contaminants move quickly in the subsurface with infiltration rates approaching the infiltration water. On the contrary, heavier contaminants are largely sorbed to the soil with traveling time retarded up to thousands times with respect to infiltrating water.

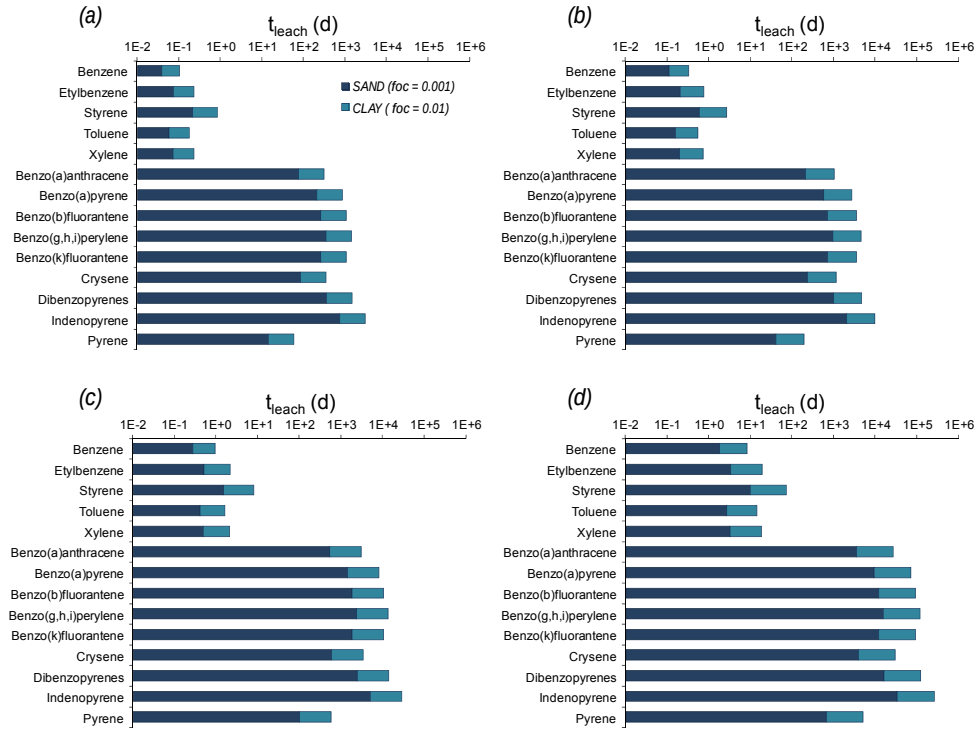


**Figure 3.3.** Time required to reach the water table ($t_{leach}$) calculated with the Green-Ampt equation (Eq. 3.8) for different aquifer depths: (a) $L_f$ = 0.5 m; (b) $L_f$ = 1 m; (c) $L_f$ = 2 m, (d) $L_f$ = 10 m.

Hence, by evaluating these results with the ones reported in Fig.3.2, it can be noticed that even assuming relatively slow biodegradation rates (e.g. $\lambda \leq 0.01$ $d^{-1}$), PAHs are expected to be significantly attenuated during the leaching process (e.g. Fig.3.2c shows that for $\lambda = 0.001$ $d^{-1}$ the attenuation factor for a leaching time of $10^5$ days is equal to $\alpha_{leach} = 10^{-3}$). Fig.3.2 also shows that for BTEX the different simulations approach each other, as long as relatively low biodegradation rate constants are considered (below $\lambda$ = 0.1 $d^{-1}$ for leaching time of 1 days). On the contrary, a slight attenuation is observed for higher biodegradation rate constant values and deep aquifers (e.g. see Fig.3.2d for a leaching time of 10 days and for $\lambda > 1$ $d^{-1}$).

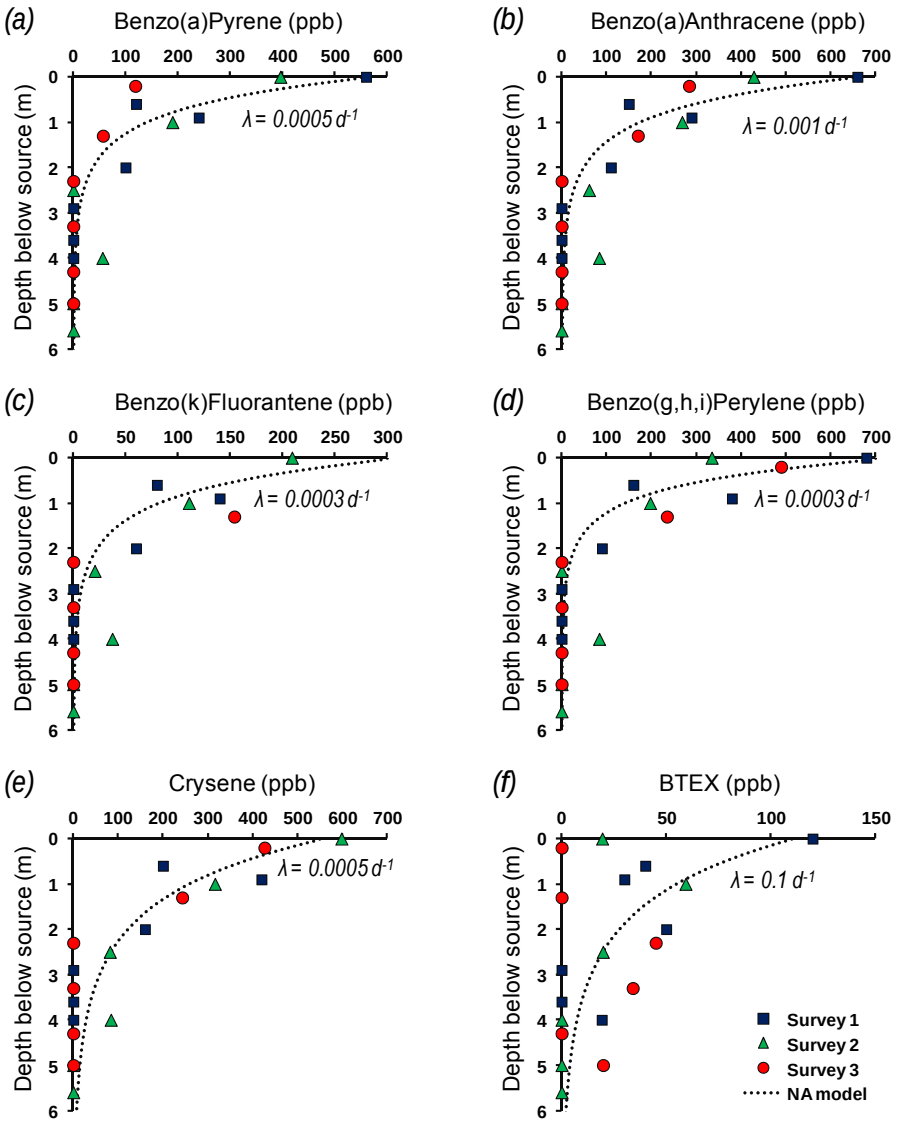


**Figure 3.4**. Concentration profiles of some PAHs and for BTEX measured in 3 surveys. For reference the profiles obtained with the model described in this chapter (NA model) are also reported. Soil: Silt Loam, $f_{oc}$: 0.001.

Fig.3.4 reports the concentration profiles in the vadose zone obtained during an investigation of a contaminated site located in a petrochemical complex of north Italy. Specifically, the figure shows the concentrations of some PAHs and BTEX measured in three surveys at different depths. For reference the profiles obtained with the model

described in this chapter are also reported. With reference to this figure it can be noticed that, especially for the PAHs, concentrations are significantly reduced with increasing depth, indicative of a non-negligible attenuation during transport. In addition the figure shows that the concentration profiles, simulated with the model, fits quite well trends observed in the field, confirming that neglecting the attenuation in the unsaturated zone can leach to an overestimation of the effective concentration in the subsurface. Finally it is worth noting that the first-order degradation rates used in the model to best fit the field data are achieved assuming values that are in line with those reported in the literature (Davis et al. 2009, DeVaull 1997, Brauner et al. 2002, Blum et al. 2009, Bockelmann et al. 2001). Namely, as discussed before, typical average median values of biodegradation constant rates for BTEX are in the order of 0.01 and 10 $d^{-1}$ whereas for PAHs are in the range of 0.0001 to 0.01 $d^{-1}$.

**Attenuation in the source**

Fig.3.5 reports the source attenuation factor ($\alpha_{dep}$) calculated with the developed model as a function of time. The results were obtained assuming different soil- water partition coefficients ($K_{sw}$) and different contamination scenarios assuming that the initial source concentration is lower than the saturation concentration, $C_{sat}$ (i.e. $C_{free}$ = 0). With reference to these figures it can be noticed, that the contaminant source attenuation is relevant only for soluble compounds characterized by partition coefficient below 10 L/kg. This suggest that the BTEX, that are characterized by $K_{sw}$ in the range of 0.1 – 10 L/kg (see Table 3.2), could be significant reduced over time (e.g. 10 – 100 years) and thus the ASTM model which assumes a constant time source concentration for the entire period of exposure can lead to a significant overestimation of the effective impact on the groundwater. On the contrary heavier compounds such as PAHs (characterized by $K_{sw}$ ranging from $10^3$ – $10^5$ L/kg) are very persistent and the source depletion mechanism could be neglected. Fig.3.5 also shows that the source attenuation rate, strongly depends on the site-specific conditions influencing the contaminant depletion such as the infiltration rate ($I_{ef}$), the occurrence of biodegradation in the source ($\lambda_{source}$) and the thickness of the source ($d_s$).

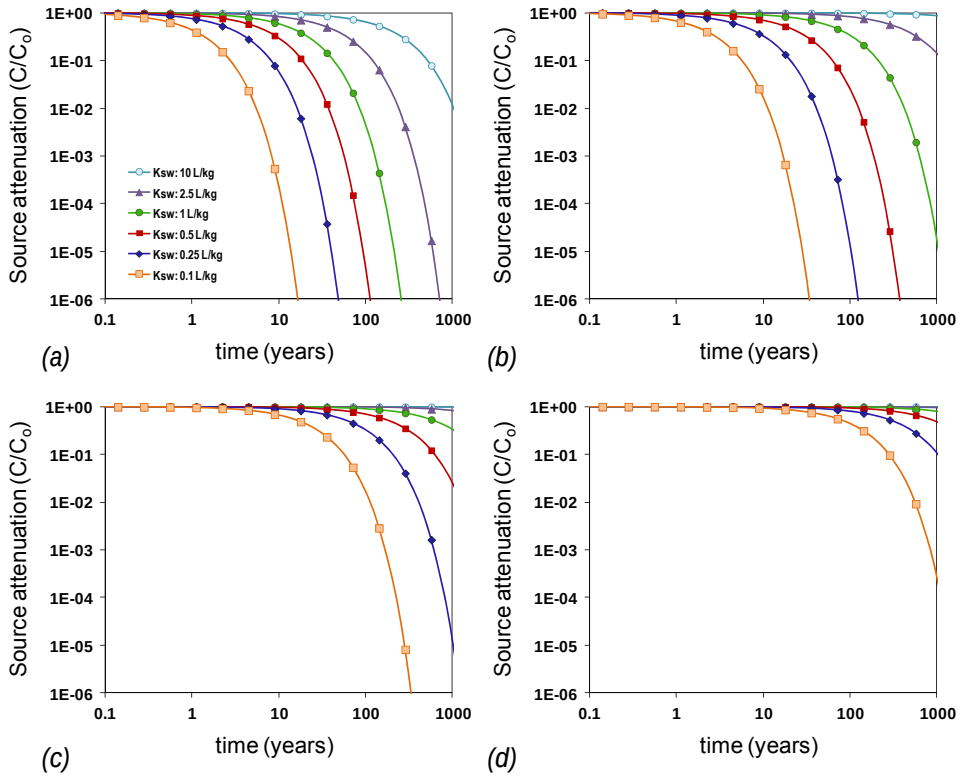


**Figure 3.5**. Source attenuation factor ($\alpha_{dep}$) calculated as a function of time for different soil-water partition coefficient values ($K_{sw}$) for different contaminant scenarios: (a) $\lambda_{source}$ = 0.001 $d^{-1}$, $I_{ef}$ =10 cm/year, $d_s$ = 1 m; (b) $\lambda_{source}$ = 0, $I_{ef}$ =10 cm/year, $d_s$ = 1 m; (c) $\lambda_{source}$ = 0, $I_{ef}$ =1 cm/year, $d_s$ = 1 m; (d) $\lambda_{source}$ = 0, $I_{ef}$ =1 cm/year, $d_s$ = 5 m. These results are obtained assuming a non-NAPL source.

In the case of initial source concentration higher than the saturation concentration, $C_{sat}$, Fig.3.5 can still be used but in this case the time for depletion should also account for the time $t^*$ required to reach the $C_{sat}$, below which the solute concentration in the source begins to decrease. Fig.3.6 reports the $t^*$ calculated with Eq. (3.23) for the same contaminant scenarios reported in Fig.3.5 for different partition coefficients. With reference to this figure it can be noticed that in the case of free phase in the subsurface (lower than the residual concentration $C_{res}$), the source attenuation results significant only for very soluble contaminants characterized by $K_{sw}$ lower than 1 L/kg. For instance, for the first scenario considered (Fig.3.6a and Fig.3.5a) and assuming an initial source concentration $C_{0,tot}$ ten times higher than the saturation concentration and a

contaminant with $K_{sw}$ = 0.1 L/kg, an attenuation in the source will be observed not after 0.1 years, as reported in Fig.3.5, but after more or less 20 years (i.e. $t+t^*$).

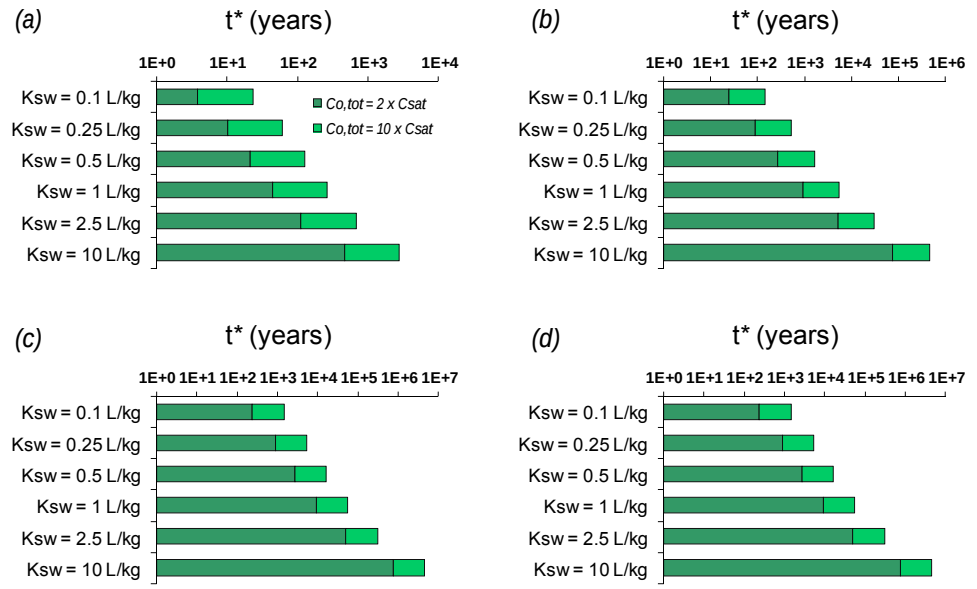


**Figure 3.6**. Calculated time required to reach the saturation concentration (t*) as a function of different soil-water partition coefficient values ($K_{sw}$) for the scenarios reported in Fig. 3.5: (a) $\lambda_{source}$ = 0.001 $d^{-1}$, $I_{ef}$ =10 cm/year, $d_s$ = 1 m; (b) $\lambda_{source}$ = 0, $I_{ef}$ =10 cm/year, $d_s$ = 1 m; (c) $\lambda_{source}$ = 0, $I_{ef}$ =1 cm/year, $d_s$ = 1 m; (d) $\lambda_{source}$ = 0, $I_{ef}$ =1 cm/year, $d_s$ = 5 m.

### Risk calculation

In this section the risk values obtained for different contaminant scenarios by applying the different modelling approaches described in this chapter are reported in Fig.3.7. Namely the carcinogenic risk associated to ingestion of benzene-contaminated and benzo(a)pyrene-contaminated groundwater was calculated using Eq. (3.29), assuming a solute source concentration of 1 and 0.001 mg/L, respectively. The comparison shows that the ASTM-RBCA approach provides more conservative carcinogenic risk values up to two orders of magnitude higher than those obtained applying the model accounting for the different natural attenuation processes. The magnitude of this overestimation depends strongly on the contaminant scenario and on the characteristics of the contaminant. In fact, for the more soluble contaminants, such as benzene, for which the attenuation mainly occurs in the source, this overestimation is more important for sandy

soils or reduced contamination thicknesses (see e.g. S3 and S4 in Fig.3.7). On the contrary for heavier compounds such as PAHs, the ASTM model tends to overestimate the overall risk for clay soils or deep groundwater, i.e. for scenarios leading to residence times of contaminants in the subsurface high enough to make the attenuation occurring during transport significant (see e.g. S1 and S2 in Fig.3.7).

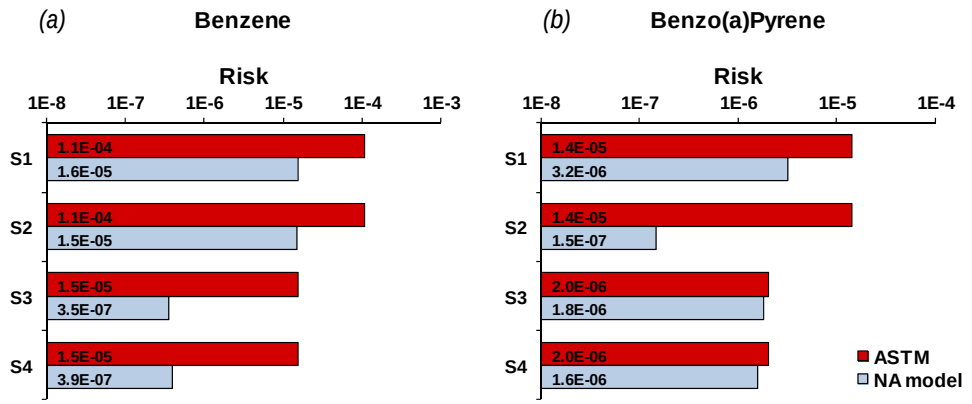


**Figure 3.7**. Carcinogenic Risk associated to ingestion of contaminated groundwater for benzene (a) and benzo(a)pyrene for different contaminant scenarios: (S1) Clay, foc = 0.01, d = 1 m, $L_f$ = 2m; (S2) Clay, foc = 0.01, d = 5 m, $L_f$ = 5m; (S3) Sand, foc = 0.001, d = 1 m, $L_f$ = 10 m; (S4) Sand, foc = 0.001, d = 5 m, $L_f$ = 25 m. The slope factor, SF, used for the calculation are 0.055 and 7.3 $(mg/kg/d)^{-1}$ for benzene and benzo(a)pyrene, respectively.

# SECTION 4

# DEVELOPMENT OF A NEW TOOL FOR THE RISK ASSESSMENT PROCEDURE

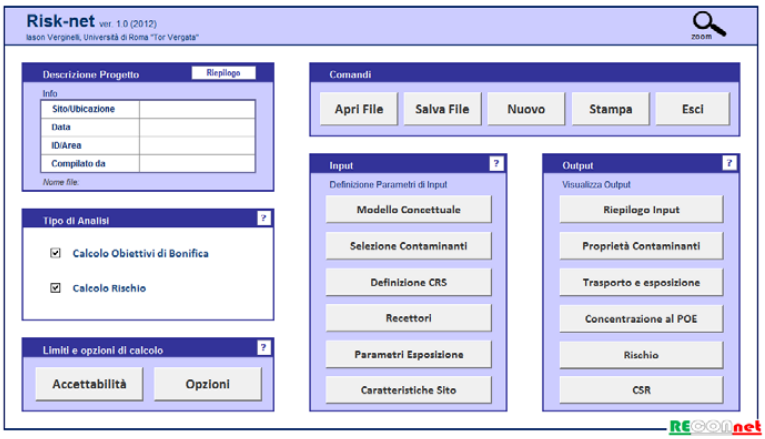


*This chapter is partially taken from:*

*Verginelli I. (2012). Risk-net – User guide. Report for the Reconnet network.*

## BACKGROUND

In Italy clean-up strategies currently focus on a risk-based approach for the definition of remediation goals. Several technical standards for the application of human health environmental risk analysis at contaminated sites are available at US and EU level since early ’90s.

One of the most widely adopted procedure for the application of risk assessment to contaminated sites, is the ASTM standard (E1739-95, E2081-00) which implements the Risk-Based Corrective Action (RBCA) at chemical release sites.

In Italy the methodological criteria developed by ISPRA (2008) is the reference document for the application of the human health risk-assessment. This document is based on the partial application of the ASTM-RBCA (2000) procedure. This approach focuses on the protection of human health and the environment and promotes cost-efficient remedies to address risks, thus allowing often limited resources to be targeted to sites posing the highest levels of risk. A key issue of the RBCA framework is the development of site-specific environmental cleanup criteria following a tiered risk evaluation approach. Namely in RBCA Tier 1, aimed to the definition of the contamination screening values, only on-site receptors are considered. Transport of contaminants is described through simple analytical models and conservative default values are used for all hydro-geological, geometrical and exposure data, without requiring any site characterization. In Tier 2, aimed to evaluate site-specific target levels, off-site receptors are included in the conceptual model, all input data should possibly be site-specific, whereas models used to describe contaminants’ transport are still analytical. Usually, the risk analysis procedure is performed using the Tier 2 conditions, that represent a reasonable compromise between the need for a detailed site assessment and the advantage of handling a rather simple and easy-to-use management tool. Therefore, only in very specific situations, where a more detailed description of the contaminant transport through numerical models is required, risk analysis is performed following the Tier 3 approach.

For the calculation of the Tier 1 and Tier 2 RBCA several software packages are available. The most commonly used in Italy, which have been validated in the ISPRA guidelines (2008), are: RBCA Tool Kit, BP-RISC and Giuditta.

However, as highlighted in the ISPRA document (2008), these softwares do not allow the full implementation of the risk analysis procedure defined in these guidelines and by the Italian law.

Thus in this work a new software (called Risk-net), designed to complete all calculations required for the ISPRA (2008) planning process, was developed.

Risk-net was developed by the Department of Civil Engineering of the University of Rome "Tor Vergata" and validated by the Reconnet network. The software is now available for free on the website of the Reconnet network: www.reconnet.net.

This chapter provides a general description of the Risk-net design, followed by a description of the main features and detailed information on modeling and calculation procedures.

## DESCRIPTION OF THE DEVELOPED SOFTWARE

The Risk-net software has been developed within the Reconnet network by the Department of Civil Engineering of the University of Rome "Tor Vergata", with the aim of providing a tool based on the ISPRA National guidelines for risk analysis application, developed following the ASTM-RBCA standard approach, but accounting for the regulatory framework set by the Italian National legislation on contaminated sites.

The software allows to apply the risk assessment procedure both in forward and backward mode, thus evaluating the risk or the clean-up objective for a contaminated site, respectively.

Namely for each exposure pathway activated by the user, Risk-net calculates, through the Fate and Transport (F&T) models described in the ISPRA guidelines (2008), the maximum steady state concentrations expected at the point of exposure. Afterward, on the basis of exposure parameters defined by the user, the daily dose assumed by each receptor considered is calculated. These doses combined with the corresponding toxicological parameters are used for the calculation of risk and remediation targets (CSR) for each contaminant and active route. Finally the effects related to the presence of multiple routes of exposure and multi-component contamination is calculated.

The key features of Risk-net include:

- *Risk-Based Cleanup Level Calculations: Risk-net c*ompletes all calculations required for Tier 1 and Tier 2 RBCA evaluations, including: risk-based exposure limits and attenuation factor derived from simple fate and transport models.
- *Fate and Transport Models:* Validated analytical models for air, groundwater and soil exposure pathways, including all models used in the ISPRA (2008) standard.
- *Chemical and Toxicological Database:* Integrated toxicological and chemical parameter library preloaded (ISS-ISPESL Database). The database is customizable by the user, including import features for management of external database.
- *User-Friendly Interface:* Point-and-click graphical user interface with on-line help, unit conversion and Load/Save capability.

### Main Screen

The main screen is automatically opened at startup (Fig.4.1). Most of the input and output screens are accessed from and return to this screen. On this screen the user enters project information, selects the type of analysis and calculations to be performed, and progressively steps through the evaluation process by navigating to the appropriate input and output screens.

In addition, the user may create, load and save user input data files.

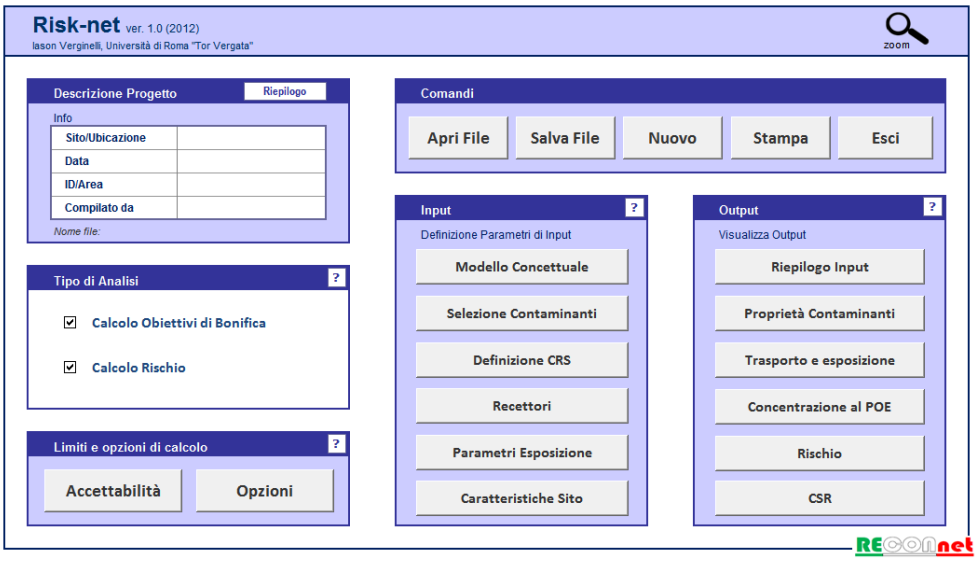


**Figure 4.1.** Main Screen of Risk-net.

### Input

**Exposure Pathways.** In this section the user must define the exposure scenario by selecting contaminated media(s), fate and transport pathways (if any), and associated exposure routes (see Fig.4.2). Namely the user needs to identify those pathways that are likely to be complete, based on knowledge of the locations of impacted soil or groundwater relative to the location and habits of people that might be exposed to the chemicals of concern.

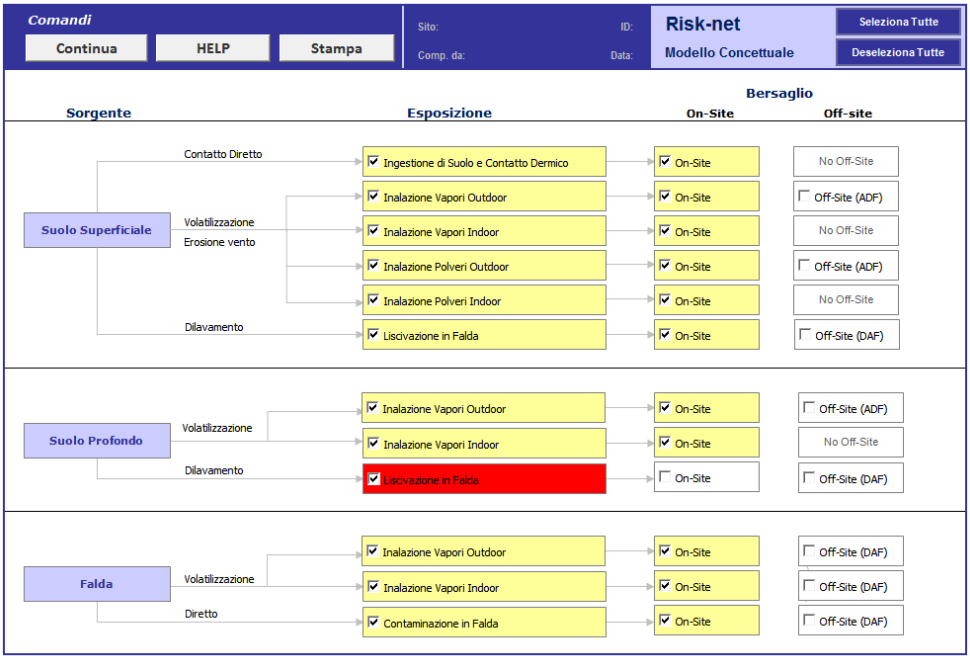


**Figure 4.2.** Exposure Pathways.

In Risk-net the following exposure pathways can be activated:

*Surface Soil*

- Dermal contact
- Soil ingestion
- Outdoor vapor inhalation
- Indoor vapor inhalation
- Outdoor particulate inhalation
- Indoor particulate inhalation
- Leaching to groundwater

*Subsurface Soil*

- Outdoor vapor inhalation
- Indoor vapor inhalation
- Leaching to groundwater

Groundwater

- Outdoor vapor inhalation

- Indoor vapor inhalation
- Affected groundwater

Moreover the user should specify if the exposure occurs on-site or off-site. In this context the term “on-site” refers to a receptor located at the source zone, whereas “off-site” refers to a receptor at any point away from the source zone, even if on the same property.

**Receptors.** After defining potential source media, transport models and exposure pathways, the user must select the types of soil use and the receptors (Fig.4.3).

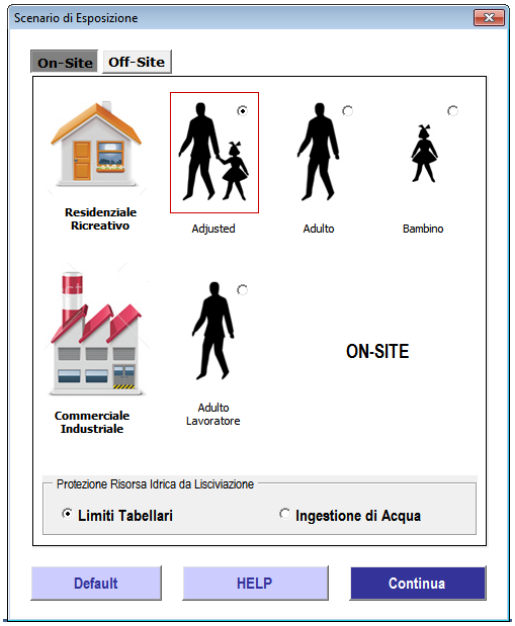


**Figure 4.3**. Receptors selection.

Namely the types of soil use and receptors are differentiated into:

Residential or Recreational use

- *Child*: Children (default age 6 and under), with a low body weight and small skin surface area.
- *Adult*: Adult with a full grown body weight and skin surface area.

- *Adjusted (Child + Adult)*: For the residential exposure scenario, the "age adjustment" option calculates an average exposure values among the child and adult values in order to adjust for varying body weights, exposure durations, skin areas, etc., for an exposure duration assumed to span periods of childhood and adulthood. Age adjustment is applied for carcinogenic contaminants only, where carcinogenic exposures are assumed to be chronic over the lifetime of the receptor.

Commercial or Industrial use

- *Adult*: Models an adult working at a full-time job.

**Chemicals of concern.** In this step (Fig.4.4) users identify chemicals that are of concern for the analysis. The Risk-net software includes a Chemical Toxicity database preloaded with the Database of ISS-ISPESL (2009).

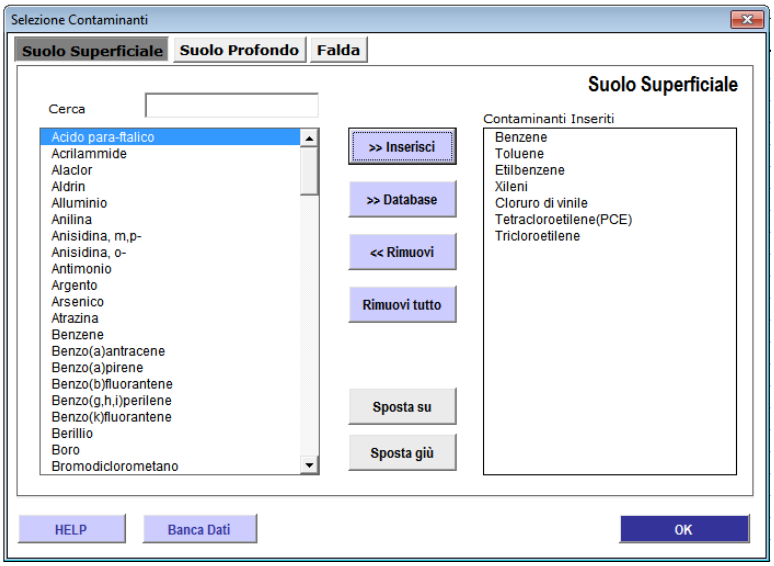


**Figure 4.4**. Selection of the chemicals of concern.

The chemicals of concern may be chosen from this database or new chemicals may be added or modified to the system database and then chosen as a chemical of concern (Fig.4.5).

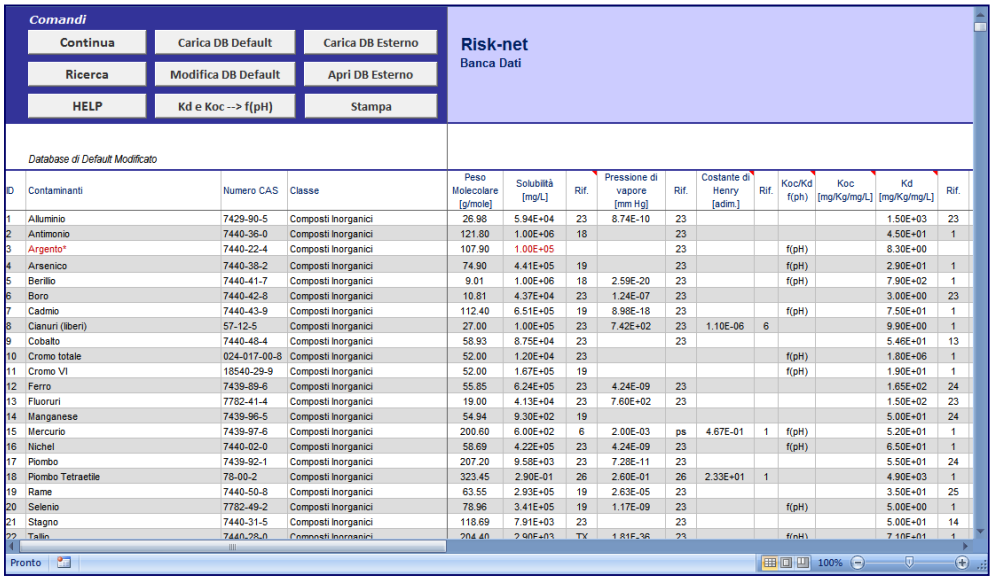


| ID | Contaminanti | Numero CAS | Classe | Peso Molecolare [g/mole] | Solubilità [mg/L] | Rif. | Pressione di vapore [mm Hg] | Rif. | Costante di Henry [adim.] | Rif. | Koc/Kd f(ph) | Koc [mg/Kg/mg/L] | Kd [mg/Kg/mg/L] | Rif. |
|---|---|---|---|---|---|---|---|---|---|---|---|---|---|---|
| 1 | Alluminio | 7429-90-5 | Composti Inorganici | 26.98 | 5.94E+04 | 23 | 8.74E-10 | 23 | | | | | 1.50E+03 | 23 |
| 2 | Antimonio | 7440-36-0 | Composti Inorganici | 121.80 | 1.00E+06 | 18 | | 23 | | | | | 4.50E+01 | 1 |
| 3 | Argento* | 7440-22-4 | Composti Inorganici | 107.90 | 1.00E+05 | | | 23 | | | f(pH) | | 8.30E+00 | |
| 4 | Arsenico | 7440-38-2 | Composti Inorganici | 74.90 | 4.41E+05 | 19 | | 23 | | | f(pH) | | 2.90E+01 | 1 |
| 5 | Berillio | 7440-41-7 | Composti Inorganici | 9.01 | 1.00E+06 | 18 | 2.59E-20 | 23 | | | f(pH) | | 7.90E+02 | 1 |
| 6 | Boro | 7440-42-8 | Composti Inorganici | 10.81 | 4.37E+04 | 23 | 1.24E-07 | 23 | | | | | 3.00E+00 | 23 |
| 7 | Cadmio | 7440-43-9 | Composti Inorganici | 112.40 | 6.51E+05 | 19 | 8.98E-18 | 23 | | | f(pH) | | 7.50E+01 | 1 |
| 8 | Cianuri (liberi) | 57-12-5 | Composti Inorganici | 27.00 | 1.00E+05 | 23 | 7.42E+02 | 23 | 1.10E-06 | 6 | | | 9.90E+00 | 1 |
| 9 | Cobalto | 7440-48-4 | Composti Inorganici | 58.93 | 8.75E+04 | 23 | | 23 | | | | | 5.46E+01 | 13 |
| 10 | Cromo totale | 024-017-00-8 | Composti Inorganici | 52.00 | 1.20E+04 | 23 | | | | | f(pH) | | 1.80E+06 | 1 |
| 11 | Cromo VI | 18540-29-9 | Composti Inorganici | 52.00 | 1.67E+05 | 19 | | | | | f(pH) | | 1.90E+01 | 1 |
| 12 | Ferro | 7439-89-6 | Composti Inorganici | 55.85 | 6.24E+05 | 23 | 4.24E-09 | 23 | | | | | 1.65E+02 | 24 |
| 13 | Fluoruri | 7782-41-4 | Composti Inorganici | 19.00 | 4.13E+04 | 23 | 7.60E+02 | 23 | | | | | 1.50E+02 | 23 |
| 14 | Manganese | 7439-96-5 | Composti Inorganici | 54.94 | 9.30E+02 | 19 | | | | | | | 5.00E+01 | 24 |
| 15 | Mercurio | 7439-97-6 | Composti Inorganici | 200.60 | 6.00E+02 | 6 | 2.00E-03 | ps | 4.67E-01 | 1 | f(pH) | | 5.20E+01 | 1 |
| 16 | Nichel | 7440-02-0 | Composti Inorganici | 58.69 | 4.22E+05 | 23 | 4.24E-09 | 23 | | | f(pH) | | 6.50E+01 | 1 |
| 17 | Piombo | 7439-92-1 | Composti Inorganici | 207.20 | 9.58E+03 | 23 | 7.28E-11 | 23 | | | | | 5.50E+01 | 24 |
| 18 | Piombo Tetraetile | 78-00-2 | Composti Inorganici | 323.45 | 2.90E-01 | 26 | 2.60E-01 | 26 | 2.33E+01 | 1 | | | 4.90E+03 | 1 |
| 19 | Rame | 7440-50-8 | Composti Inorganici | 63.55 | 2.93E+05 | 19 | 2.63E-05 | 23 | | | | | 3.50E+01 | 25 |
| 20 | Selenio | 7782-49-2 | Composti Inorganici | 78.96 | 3.41E+05 | 19 | 1.17E-09 | 23 | | | f(pH) | | 5.00E+00 | 1 |
| 21 | Stagno | 7440-31-5 | Composti Inorganici | 118.69 | 7.91E+03 | 23 | | 23 | | | | | 5.00E+01 | 14 |
| 22 | Tallio | 7440-28-0 | Composti Inorganici | 204.40 | 2.90E+03 | TX | 1.81E-36 | 23 | | | f(pH) | | 7.10E+01 | 1 |

**Figure 4.5**. Database of the software.

The values modified by the user change color to red and the chemical name is indicated with an asterisk.

**Source Concentration.** If baseline risks are to be calculated, the user must provide representative concentrations of the chemicals of concern in the relevant source media. Namely the user can define for each chemicals of concern total concentration in soil (or in groundwater) or specify the soil gas concentration as the source term (Fig.4.6).

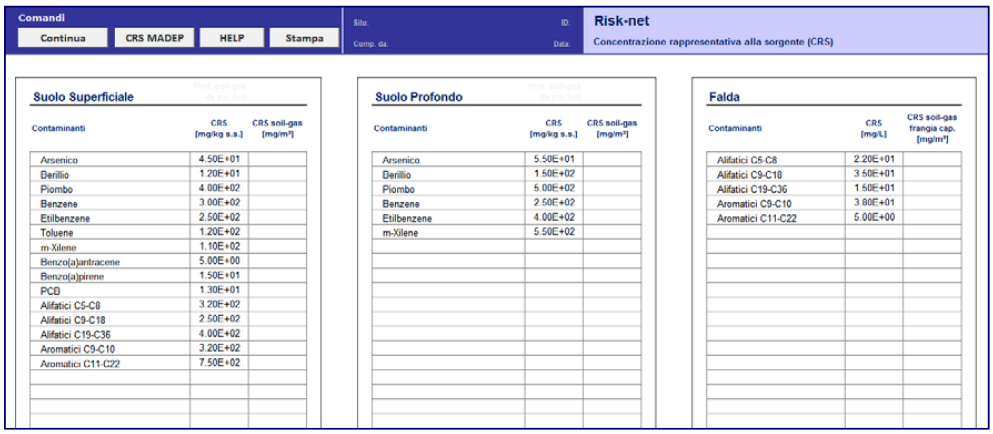


| Contaminanti | CRS [mg/kg s.s.] | CRS soil-gas [mg/m³] |
|---|---|---|
| Arsenico | 4.50E+01 | |
| Berillio | 1.20E+01 | |
| Piombo | 4.00E+02 | |
| Benzene | 3.00E+02 | |
| Etilbenzene | 2.50E+02 | |
| Toluene | 1.20E+02 | |
| m-Xilene | 1.10E+02 | |
| Benzo(a)antracene | 5.00E+00 | |
| Benzo(a)pirene | 1.50E+01 | |
| PCB | 1.30E+01 | |
| Alifatici C5-C8 | 3.20E+02 | |
| Alifatici C9-C18 | 2.50E+02 | |
| Alifatici C19-C36 | 4.00E+02 | |
| Aromatici C9-C10 | 3.20E+02 | |
| Aromatici C11-C22 | 7.50E+02 | |

| Contaminanti | CRS [mg/kg s.s.] | CRS soil-gas [mg/m³] |
|---|---|---|
| Arsenico | 5.50E+01 | |
| Berillio | 1.50E+02 | |
| Piombo | 5.00E+02 | |
| Benzene | 2.50E+02 | |
| Etilbenzene | 4.00E+02 | |
| m-Xilene | 5.50E+02 | |

| Contaminanti | CRS [mg/L] | CRS soil-gas frangia cap. [mg/m³] |
|---|---|---|
| Alifatici C5-C8 | 2.20E+01 | |
| Alifatici C9-C18 | 3.50E+01 | |
| Alifatici C19-C36 | 1.50E+01 | |
| Aromatici C9-C10 | 3.80E+01 | |
| Aromatici C11-C22 | 5.00E+00 | |

**Figure 4.6.** Representative Source concentration.

In addition, in the case of hydrocarbons contamination, the user can enter the concentration values for the different hydrocarbons fractions. Namely the user can choose between the Total Petroleum Hydrocarbon Criteria Working Group (TPHCWG) and the Massachusetts Department of Environmental Protection (MADEP) classification (Fig.4.7).

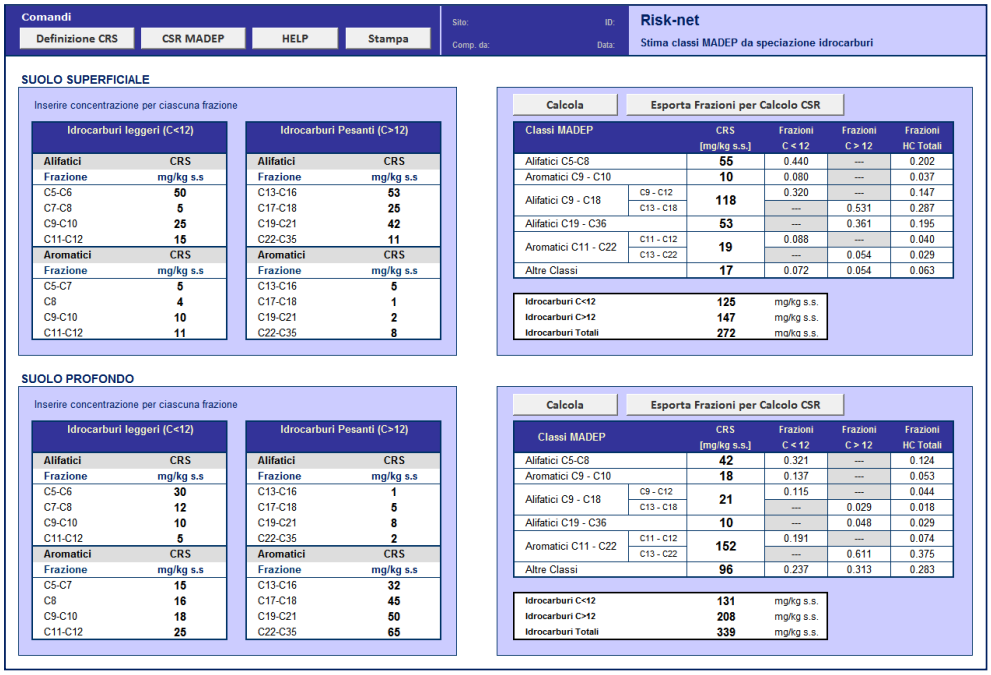


**Figure 4.7**. Hydrocarbons definition.

The software calculates the total concentration for C>12 and C<12 macro fractions.

**Exposure Parameters.** On this screen, the user must enter appropriate exposure factors for each complete pathway (Fig.4.8). Initially, this section contains default values corresponding to ISPRA guidelines (2008). There are different exposure factor columns representing the different types of receptors that can be modeled with the software. These receptor types allow the user to calculate baseline risks and cleanup levels based

on different physical (e.g., skin area, body weight, etc.) and exposure-related (e.g., soil ingestion rate, inhalation rate, etc.) parameters.

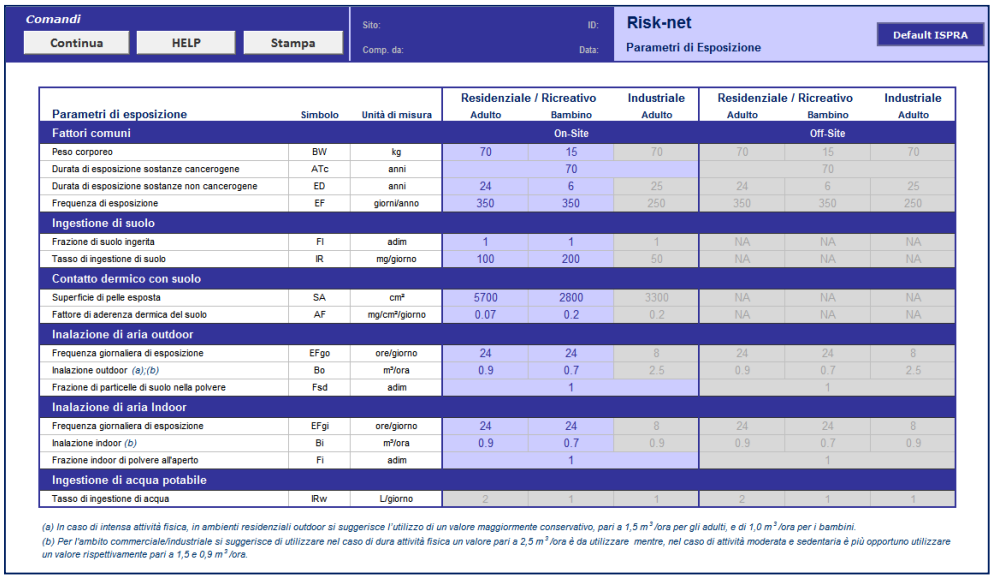

Comandi

Continua | HELP | Stampa

Sito: ID:

Comp. da: Data:

**Risk-net**

Parametri di Esposizione

Default ISPRA

| Parametri di esposizione | Simbolo | Unità di misura | Residenziale / Ricreativo Adulto | Residenziale / Ricreativo Bambino | Industriale Adulto | Residenziale / Ricreativo Adulto | Residenziale / Ricreativo Bambino | Industriale Adulto |
|---|---|---|---|---|---|---|---|---|
| **Fattori comuni** | | | | On-Site | | | Off-Site | |
| Peso corporeo | BW | kg | 70 | 15 | 70 | 70 | 15 | 70 |
| Durata di esposizione sostanze cancerogene | ATc | anni | | 70 | | | 70 | |
| Durata di esposizione sostanze non cancerogene | ED | anni | 24 | 6 | 25 | 24 | 6 | 25 |
| Frequenza di esposizione | EF | giorni/anno | 350 | 350 | 250 | 350 | 350 | 250 |
| **Ingestione di suolo** | | | | | | | | |
| Frazione di suolo ingerita | FI | adim | 1 | 1 | 1 | NA | NA | NA |
| Tasso di ingestione di suolo | IR | mg/giorno | 100 | 200 | 50 | NA | NA | NA |
| **Contatto dermico con suolo** | | | | | | | | |
| Superficie di pelle esposta | SA | $cm^2$ | 5700 | 2800 | 3300 | NA | NA | NA |
| Fattore di aderenza dermica del suolo | AF | $mg/cm^2/giorno$ | 0.07 | 0.2 | 0.2 | NA | NA | NA |
| **Inalazione di aria outdoor** | | | | | | | | |
| Frequenza giornaliera di esposizione | EFgo | ore/giorno | 24 | 24 | 8 | 24 | 24 | 8 |
| Inalazione outdoor *(a);(b)* | Bo | $m^3/ora$ | 0.9 | 0.7 | 2.5 | 0.9 | 0.7 | 2.5 |
| Frazione di particelle di suolo nella polvere | Fsd | adim | | 1 | | | 1 | |
| **Inalazione di aria Indoor** | | | | | | | | |
| Frequenza giornaliera di esposizione | EFgi | ore/giorno | 24 | 24 | 8 | 24 | 24 | 8 |
| Inalazione indoor *(b)* | Bi | $m^3/ora$ | 0.9 | 0.7 | 0.9 | 0.9 | 0.7 | 0.9 |
| Frazione indoor di polvere all'aperto | Fi | adim | | 1 | | | 1 | |
| **Ingestione di acqua potabile** | | | | | | | | |
| Tasso di ingestione di acqua | IRw | L/giorno | 2 | 1 | 1 | 2 | 1 | 1 |

*(a) In caso di intensa attività fisica, in ambienti residenziali outdoor si suggerisce l'utilizzo di un valore maggiormente conservativo, pari a 1,5 $m^3$/ora per gli adulti, e di 1,0 $m^3$/ora per i bambini.*

*(b) Per l'ambito commerciale/industriale si suggerisce di utilizzare nel caso di dura attività fisica un valore pari a 2,5 $m^3$/ora è da utilizzare mentre, nel caso di attività moderata e sedentaria è più opportuno utilizzare un valore rispettivamente pari a 1,5 e 0,9 $m^3$/ora.*

**Figure 4.8**. Definition of the exposure parameters.

**Site-Specific Parameters.** In this section the user provides the necessary site-specific parameters required for the application of the fate and transport models selected (Fig.4.9). Initially, this section contains default values corresponding to ISPRA guidelines (2008).

Namely the user must enter the following parameters:

- Vadose zone: source and soil geometry, soil properties, rainfall infiltration rate, fraction of organic carbon, ph, etc.
- Groundwater zone: source and groundwater geometry, physical characteristics, fraction of organic carbon and other transport properties.
- Outdoor air zone: source geometry, wind speed, dispersion in air, particulate emissions, etc.
- Indoor air zone: building geometry and properties, air exchange rate, indoor/outdoor differential pressure, etc.

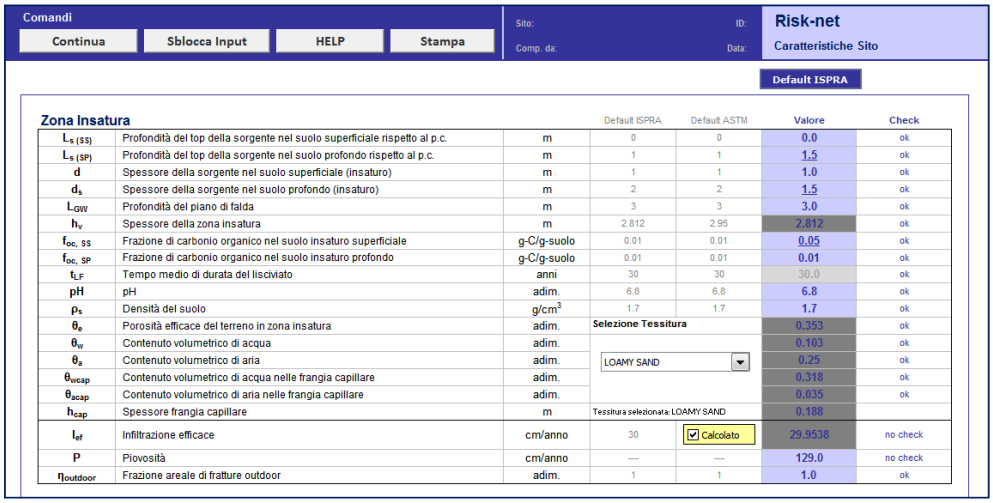


**Figure 4.9**. Definition of the Site-Specific Parameters.

## Output

***Input Parameters Summary.*** In this screen a summary of all input parameters and option calculation used in the software is reported. The values modified by the user are highlighted. In addition the software shows the parameters not required for the specific calculation (Fig.4.10).

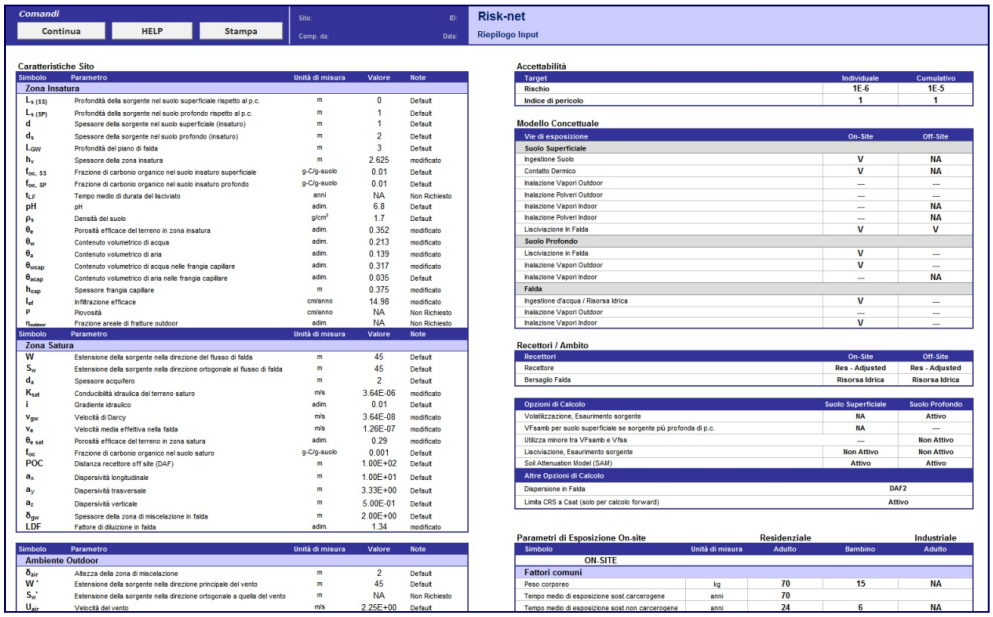


**Figure 4.10.** Input parameters summary.

***Exposure Pathway Flowchart.*** The Exposure pathway flowchart shows all selected source media, transport mechanisms, exposure media and receptors (Fig.4.11). This allows the user to visually verify the problem setup for the evaluation and, if necessary, revise the exposure pathway selections.

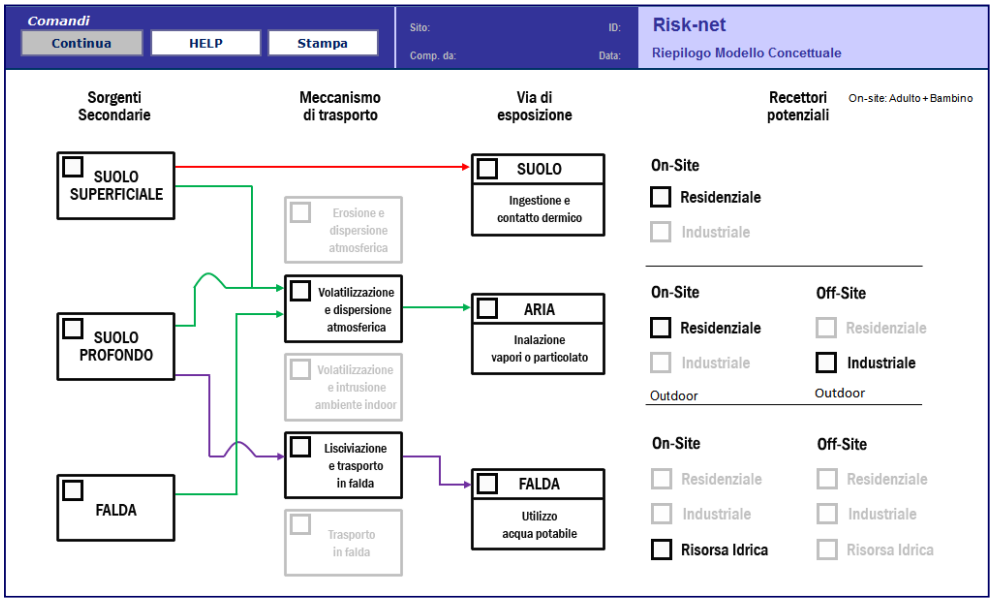


**Figure 4.11**. Exposure Pathway Flowchart.

***Chemical and toxicological data for the selected contaminants.*** This output screen (Fig.4.12) reports the chemical and toxicological data used for the selected contaminants. Chemicals with a user-customized entry are highlighted, and the specific entry that differs from the entry in the default chemical database is also highlighted.

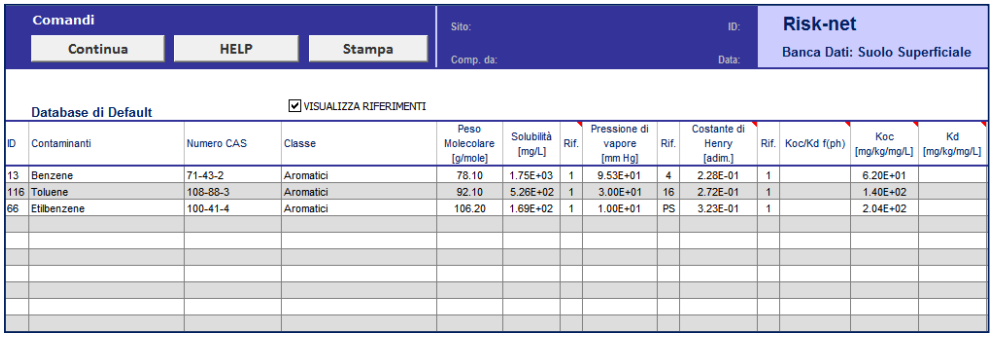


| ID | Contaminanti | Numero CAS | Classe | Peso Molecolare [g/mole] | Solubilità [mg/L] | Rif. | Pressione di vapore [mm Hg] | Rif. | Costante di Henry [adim.] | Rif. | Koc/Kd f(ph) | Koc [mg/kg/mg/L] | Kd [mg/kg/mg/L] |
|---|---|---|---|---|---|---|---|---|---|---|---|---|---|
| 13 | Benzene | 71-43-2 | Aromatici | 78.10 | 1.75E+03 | 1 | 9.53E+01 | 4 | 2.28E-01 | 1 | | 6.20E+01 | |
| 116 | Toluene | 108-88-3 | Aromatici | 92.10 | 5.26E+02 | 1 | 3.00E+01 | 16 | 2.72E-01 | 1 | | 1.40E+02 | |
| 66 | Etilbenzene | 100-41-4 | Aromatici | 106.20 | 1.69E+02 | 1 | 1.00E+01 | PS | 3.23E-01 | 1 | | 2.04E+02 | |

**Figure 4.12**. Chemical and toxicological data for the selected contaminants.

### *Intermediate Outputs*

***Fate & Transport models.*** This screen reports the fate and transport (F&T) factors calculated for the selected contaminants (Fig.4.13).

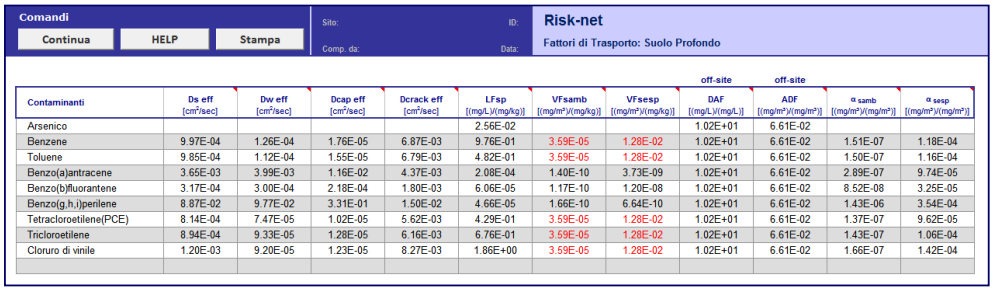


| Contaminanti | Ds eff [cm²/sec] | Dw eff [cm²/sec] | Dcap eff [cm²/sec] | Dcrack eff [cm²/sec] | LFsp [(mg/L)/(mg/kg)] | VFsamb [(mg/m³)/(mg/kg)] | VFsesp [(mg/m³)/(mg/kg)] | off-site DAF [(mg/L)/(mg/L)] | off-site ADF [(mg/m³)/(mg/m³)] | α samb [(mg/m³)/(mg/m³)] | α sesp [(mg/m³)/(mg/m³)] |
|---|---|---|---|---|---|---|---|---|---|---|---|
| Arsenico | | | | | 2.56E-02 | | | 1.02E+01 | 6.61E-02 | | |
| Benzene | 9.97E-04 | 1.26E-04 | 1.76E-05 | 6.87E-03 | 9.76E-01 | 3.59E-05 | 1.28E-02 | 1.02E+01 | 6.61E-02 | 1.51E-07 | 1.18E-04 |
| Toluene | 9.85E-04 | 1.12E-04 | 1.55E-05 | 6.79E-03 | 4.82E-01 | 3.59E-05 | 1.28E-02 | 1.02E+01 | 6.61E-02 | 1.50E-07 | 1.16E-04 |
| Benzo(a)antracene | 3.65E-03 | 3.99E-03 | 1.16E-02 | 4.37E-03 | 2.08E-04 | 1.40E-10 | 3.73E-09 | 1.02E+01 | 6.61E-02 | 2.89E-07 | 9.74E-05 |
| Benzo(b)fluorantene | 3.17E-04 | 3.00E-04 | 2.18E-04 | 1.80E-03 | 6.06E-05 | 1.17E-10 | 1.20E-08 | 1.02E+01 | 6.61E-02 | 8.52E-08 | 3.25E-05 |
| Benzo(g,h,i)perilene | 8.87E-02 | 9.77E-02 | 3.31E-01 | 1.50E-02 | 4.66E-05 | 1.66E-10 | 6.64E-10 | 1.02E+01 | 6.61E-02 | 1.43E-06 | 3.54E-04 |
| Tetracloroetilene(PCE) | 8.14E-04 | 7.47E-05 | 1.02E-05 | 5.62E-03 | 4.29E-01 | 3.59E-05 | 1.28E-02 | 1.02E+01 | 6.61E-02 | 1.37E-07 | 9.62E-05 |
| Tricloroetilene | 8.94E-04 | 9.33E-05 | 1.28E-05 | 6.16E-03 | 6.76E-01 | 3.59E-05 | 1.28E-02 | 1.02E+01 | 6.61E-02 | 1.43E-07 | 1.06E-04 |
| Cloruro di vinile | 1.20E-03 | 9.20E-05 | 1.23E-05 | 8.27E-03 | 1.86E+00 | 3.59E-05 | 1.28E-02 | 1.02E+01 | 6.61E-02 | 1.66E-07 | 1.42E-04 |

**Figure 4.13.** Fate & Transport models.

***Partition behavior of the selected contaminants.*** In this screen the user can assess the different partition behavior of the selected contaminants (Fig.4.14). This screen also reports the different concentrations at the point of exposure ($C_{poe}$) that are also calculated.

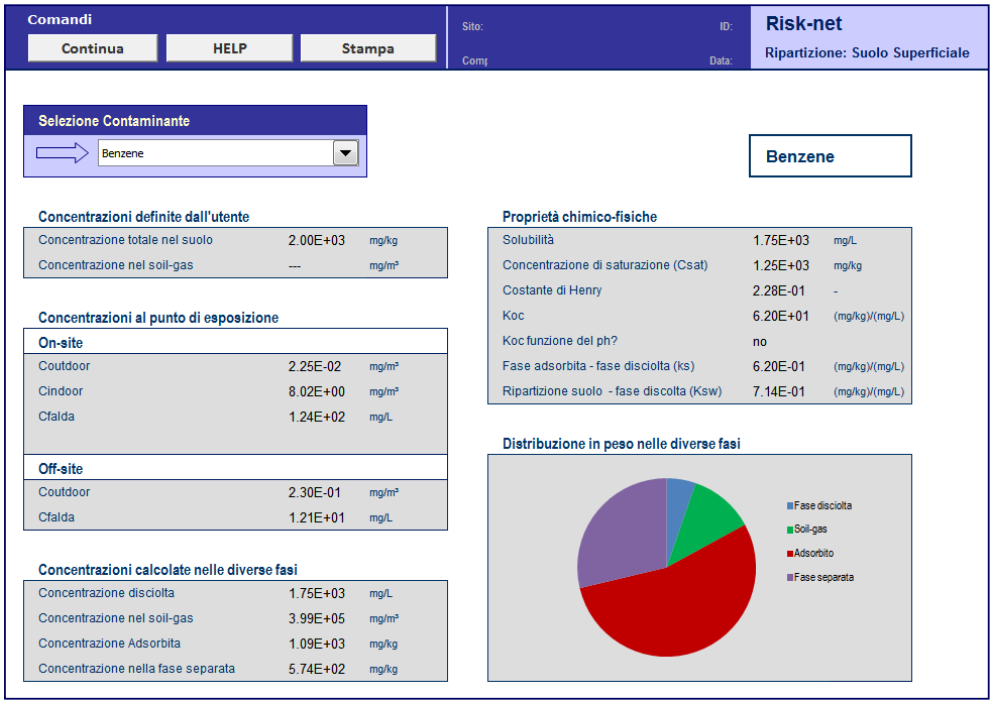


**Figure 4.14.** Partition behavior of the selected contaminants.

***Intake Rates***. This screen reports the intake rates calculated for the different exposure pathways for each receptor activated by the user (Fig.4.15).

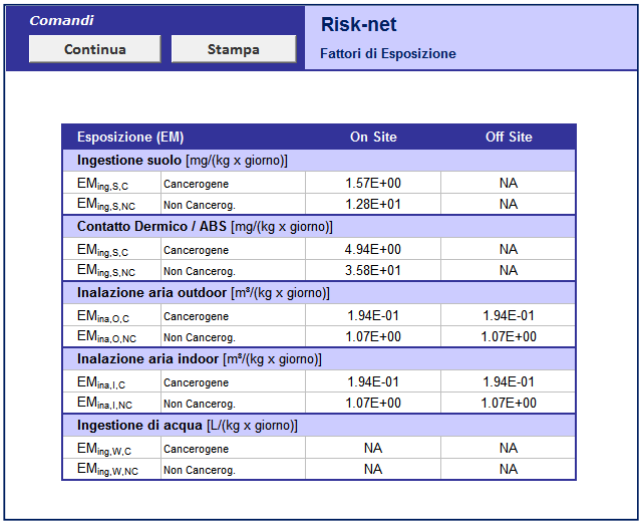


| Esposizione (EM) | | On Site | Off Site |
|---|---|---|---|
| **Ingestione suolo** [mg/(kg x giorno)] | | | |
| $EM_{ing,S,C}$ | Cancerogene | 1.57E+00 | NA |
| $EM_{ing,S,NC}$ | Non Cancerog. | 1.28E+01 | NA |
| **Contatto Dermico / ABS** [mg/(kg x giorno)] | | | |
| $EM_{ing,S,C}$ | Cancerogene | 4.94E+00 | NA |
| $EM_{ing,S,NC}$ | Non Cancerog. | 3.58E+01 | NA |
| **Inalazione aria outdoor** [m³/(kg x giorno)] | | | |
| $EM_{ina,O,C}$ | Cancerogene | 1.94E-01 | 1.94E-01 |
| $EM_{ina,O,NC}$ | Non Cancerog. | 1.07E+00 | 1.07E+00 |
| **Inalazione aria indoor** [m³/(kg x giorno)] | | | |
| $EM_{ina,I,C}$ | Cancerogene | 1.94E-01 | 1.94E-01 |
| $EM_{ina,I,NC}$ | Non Cancerog. | 1.07E+00 | 1.07E+00 |
| **Ingestione di acqua** [L/(kg x giorno)] | | | |
| $EM_{ing,W,C}$ | Cancerogene | NA | NA |
| $EM_{ing,W,NC}$ | Non Cancerog. | NA | NA |

**Figure 4.15.** Calculated Intake rates.

***Transient Domenico Analysis.*** In this screen the user can evaluate the transient groundwater modeling results for the different contaminants selected (Fig.4.16). This evaluation is not used for the risk and clean up levels calculation but can be useful for a risk management decision for example to assess when an exposure limit might be exceeded.

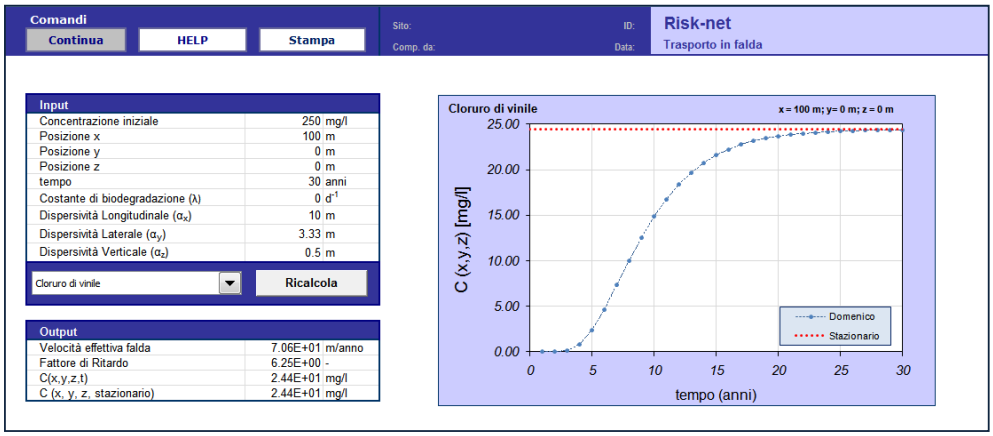


**Figure 4.16**. Transient Domenico Analysis.

***Green Ampt Analysis.*** In this screen the user can evaluate the leaching modeling results with the Green & Ampt (1911) equation for the different contaminants selected (Fig.4.17). This evaluation is not used for the risk and clean up levels calculation but can be useful for a risk management decision for example to assess the leaching velocity and the expected role of biodegradation in attenuating the contaminant selected.

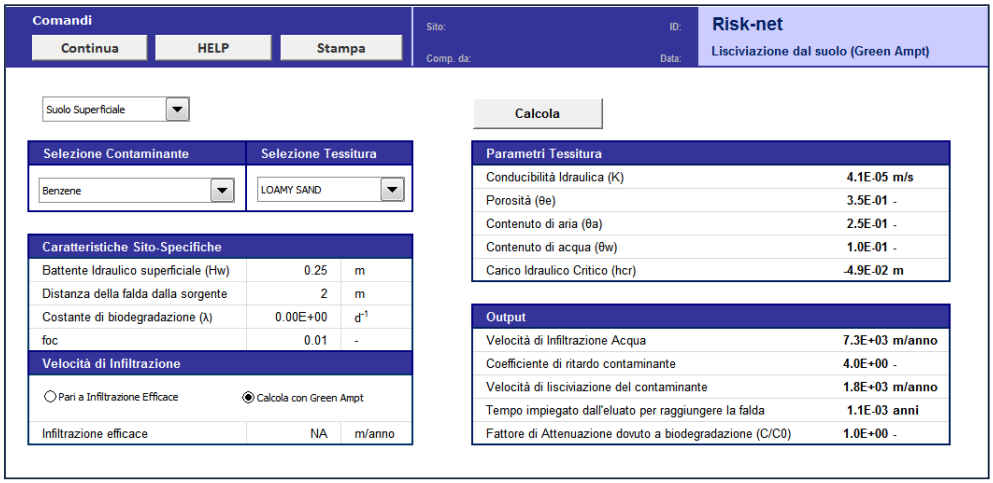


**Figure 4.17**. Green-Ampt Analysis.

**Baseline Risk.** For each media of interest (surface soils, subsurface soils and groundwater) the software reports the baseline risk calculations for each complete exposure pathway (outdoor air, indoor air, soil, etc) and the associated receptors (on-site or off-site). Namely the software calculate the human health risks associated with exposure to the contaminant on the basis of average daily intake rates and the corresponding toxicological parameters for carcinogenic and non-carcinogenic effects (Fig.4.18). In addition the software calculates the risk for the groundwater resource ($R_{gw}$) by comparing the groundwater concentrations calculated at the point of compliance (POC) with the values defined by the Italian law (*CSC*). For each complete pathway, the software provides both individual and additive constituent results for carcinogens (*R*) and non-carcinogens (*HI*).

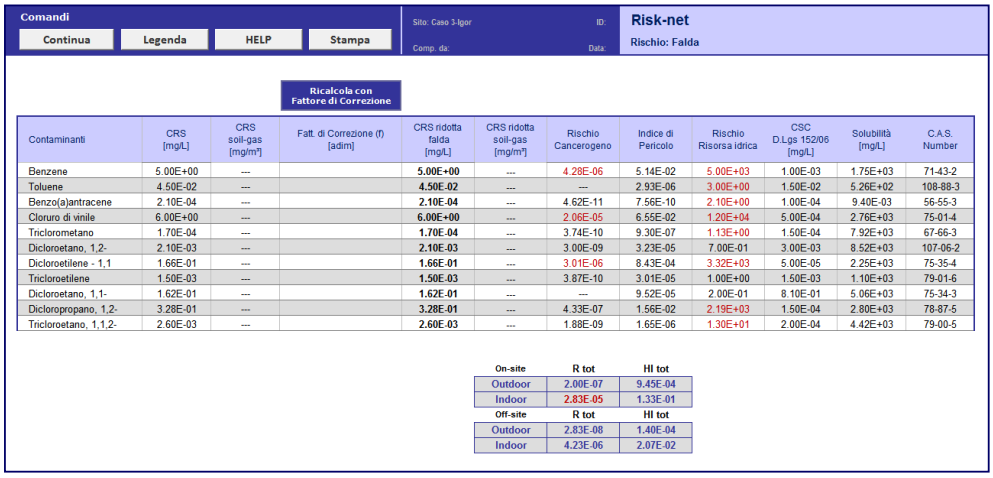


**Figure 4.18**. Risk calculation screen.

Besides the user can also visualize for each individual contaminant a summary of the different risks calculated and of the different fate and transport factors used for their derivation (Fig.4.19).

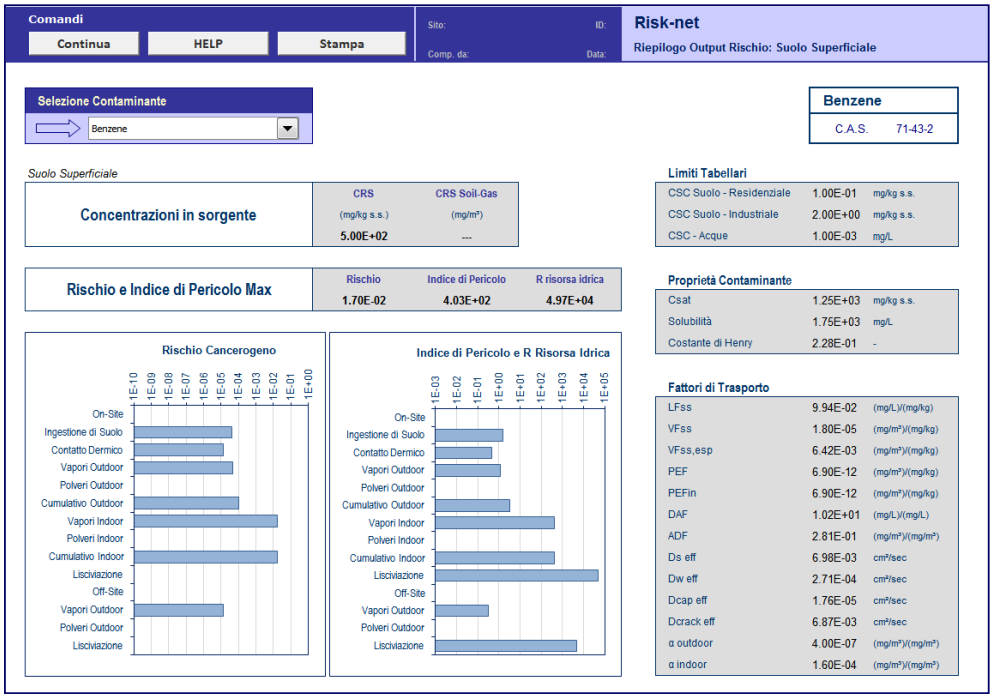


**Figure 4.19**. Risk calculation summary.

**Free-phase Liquid Migration.** In the case of source concentrations greater than the saturation concentration ($C_{sat}$) the software can be used to evaluate if the NAPL (nonaqueous phase liquid) detected in the soil is expected to be mobile. In fact as reported by the ASTM standard (2000) a NAPL may be present in soil, but immobile. The mobility of a NAPL is not governed by thermodynamic properties but by capillary, viscous and gravity forces acting on the bulk NAPL phase. To assess this aspect the software uses the screening model reported in the ASTM standard allowing to calculate for each contaminant (liquid at standard conditions of temperature and pressure) a screening concentration above which the NAPL is expected to become mobile (Fig.4.20).

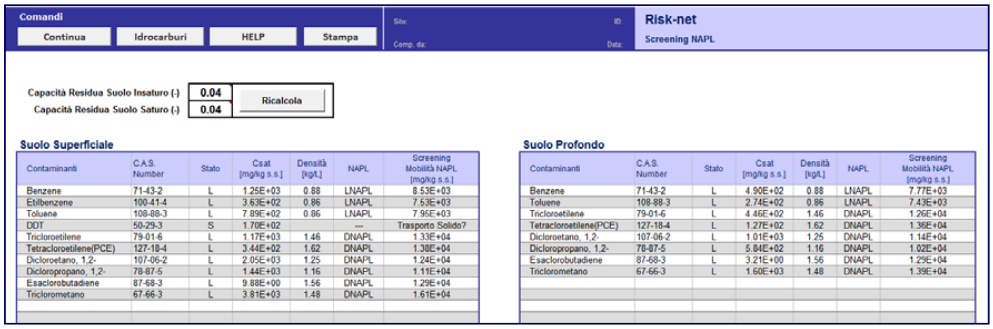


| Contaminanti | C.A.S. Number | Stato | Csat [mg/kg s.s.] | Densità [kg/L] | NAPL | Screening Mobilità NAPL [mg/kg s.s.] |
|---|---|---|---|---|---|---|
| Benzene | 71-43-2 | L | 1.25E+03 | 0.88 | LNAPL | 8.53E+03 |
| Etilbenzene | 100-41-4 | L | 3.63E+02 | 0.86 | LNAPL | 7.53E+03 |
| Toluene | 108-88-3 | L | 7.89E+02 | 0.86 | LNAPL | 7.95E+03 |
| DDT | 50-29-3 | S | 1.70E+02 | | --- | Trasporto Solido? |
| Tricloroetilene | 79-01-6 | L | 1.17E+03 | 1.46 | DNAPL | 1.33E+04 |
| Tetracloroetilene(PCE) | 127-18-4 | L | 3.44E+02 | 1.62 | DNAPL | 1.38E+04 |
| Dicloroetano, 1,2- | 107-06-2 | L | 2.05E+03 | 1.25 | DNAPL | 1.24E+04 |
| Diclopropano, 1,2- | 78-87-5 | L | 1.44E+03 | 1.16 | DNAPL | 1.11E+04 |
| Esaclorobutadiene | 87-68-3 | L | 9.88E+00 | 1.56 | DNAPL | 1.29E+04 |
| Triclorometano | 67-66-3 | L | 3.81E+03 | 1.48 | DNAPL | 1.61E+04 |

| Contaminanti | C.A.S. Number | Stato | Csat [mg/kg s.s.] | Densità [kg/L] | NAPL | Screening Mobilità NAPL [mg/kg s.s.] |
|---|---|---|---|---|---|---|
| Benzene | 71-43-2 | L | 4.90E+02 | 0.88 | LNAPL | 7.77E+03 |
| Toluene | 108-88-3 | L | 2.74E+02 | 0.86 | LNAPL | 7.43E+03 |
| Tricloroetilene | 79-01-6 | L | 4.46E+02 | 1.46 | DNAPL | 1.26E+04 |
| Tetracloroetilene(PCE) | 127-18-4 | L | 1.27E+02 | 1.62 | DNAPL | 1.36E+04 |
| Dicloroetano, 1,2- | 107-06-2 | L | 1.01E+03 | 1.25 | DNAPL | 1.14E+04 |
| Diclopropano, 1,2- | 78-87-5 | L | 5.84E+02 | 1.16 | DNAPL | 1.02E+04 |
| Esaclorobutadiene | 87-68-3 | L | 3.21E+00 | 1.56 | DNAPL | 1.29E+04 |
| Triclorometano | 67-66-3 | L | 1.60E+03 | 1.48 | DNAPL | 1.39E+04 |

**Figure 4.20**. Screening concentrations for NAPL.

**Clean up Levels.** For each media of interest (surface soils, subsurface soils and groundwater) the software reports the calculated cleanup levels for the different contaminants selected (Fig.4.21). Moreover, in order to compute cleanup levels based on cumulative risk effects, the software allows the user to adjust the individual constituent target levels calculated to meet the cumulative risk goals. Thus the clean-up levels calculated represent the maximum acceptable concentration in the affected source medium (soil or groundwater) that is protective of a human or groundwater receptor located at a relevant point of exposure (POE).

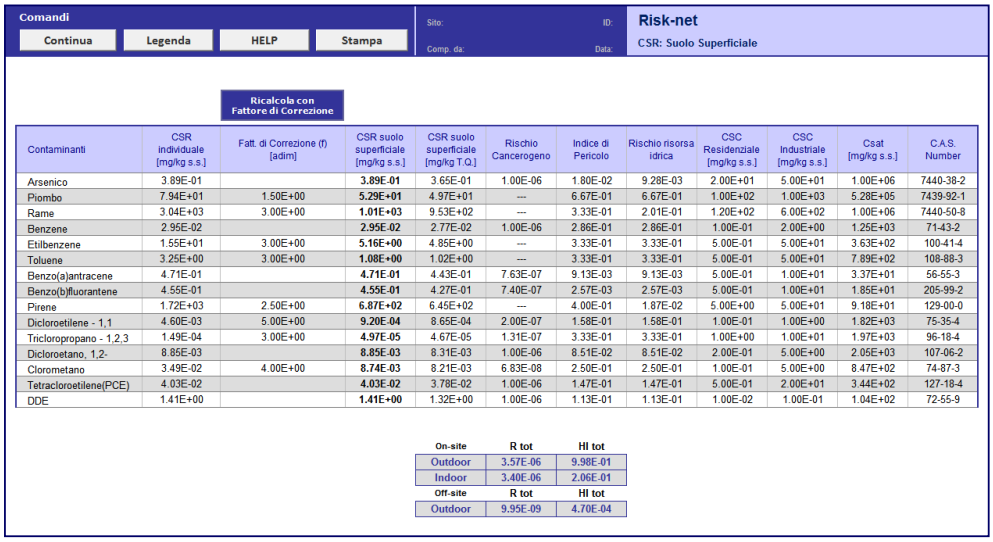

Comandi

Continua | Legenda | HELP | Stampa

Sito: ID: Comp. da: Data:

**Risk-net**

CSR: Suolo Superficiale

Ricalcola con Fattore di Correzione

| Contaminanti | CSR individuale [mg/kg s.s.] | Fatt. di Correzione (f) [adim] | CSR suolo superficiale [mg/kg s.s.] | CSR suolo superficiale [mg/kg T.Q.] | Rischio Cancerogeno | Indice di Pericolo | Rischio risorsa idrica | CSC Residenziale [mg/kg s.s.] | CSC Industriale [mg/kg s.s.] | Csat [mg/kg s.s.] | C.A.S. Number |
|---|---|---|---|---|---|---|---|---|---|---|---|
| Arsenico | 3.89E-01 | | **3.89E-01** | 3.65E-01 | 1.00E-06 | 1.80E-02 | 9.28E-03 | 2.00E+01 | 5.00E+01 | 1.00E+06 | 7440-38-2 |
| Piombo | 7.94E+01 | 1.50E+00 | **5.29E+01** | 4.97E+01 | --- | 6.67E-01 | 6.67E-01 | 1.00E+02 | 1.00E+03 | 5.28E+05 | 7439-92-1 |
| Rame | 3.04E+03 | 3.00E+00 | **1.01E+03** | 9.53E+02 | --- | 3.33E-01 | 2.01E-01 | 1.20E+02 | 6.00E+02 | 1.00E+06 | 7440-50-8 |
| Benzene | 2.95E-02 | | **2.95E-02** | 2.77E-02 | 1.00E-06 | 2.86E-01 | 2.86E-01 | 1.00E-01 | 2.00E+00 | 1.25E+03 | 71-43-2 |
| Etilbenzene | 1.55E+01 | 3.00E+00 | **5.16E+00** | 4.85E+00 | --- | 3.33E-01 | 3.33E-01 | 5.00E-01 | 5.00E+01 | 3.63E+02 | 100-41-4 |
| Toluene | 3.25E+00 | 3.00E+00 | **1.08E+00** | 1.02E+00 | --- | 3.33E-01 | 3.33E-01 | 5.00E-01 | 5.00E+01 | 7.89E+02 | 108-88-3 |
| Benzo(a)antracene | 4.71E-01 | | **4.71E-01** | 4.43E-01 | 7.63E-07 | 9.13E-03 | 9.13E-03 | 5.00E-01 | 1.00E+01 | 3.37E+01 | 56-55-3 |
| Benzo(b)fluorantene | 4.55E-01 | | **4.55E-01** | 4.27E-01 | 7.40E-07 | 2.57E-03 | 2.57E-03 | 5.00E-01 | 1.00E+01 | 1.85E+01 | 205-99-2 |
| Pirene | 1.72E+03 | 2.50E+00 | **6.87E+02** | 6.45E+02 | --- | 4.00E-01 | 1.87E-02 | 5.00E+00 | 5.00E+01 | 9.18E+01 | 129-00-0 |
| Dicloroetilene - 1,1 | 4.60E-03 | 5.00E+00 | **9.20E-04** | 8.65E-04 | 2.00E-07 | 1.58E-01 | 1.58E-01 | 1.00E-01 | 1.00E+00 | 1.82E+03 | 75-35-4 |
| Tricloropropano - 1,2,3 | 1.49E-04 | 3.00E+00 | **4.97E-05** | 4.67E-05 | 1.31E-07 | 3.33E-01 | 3.33E-01 | 1.00E+00 | 1.00E+01 | 1.97E+03 | 96-18-4 |
| Dicloroetano, 1,2- | 8.85E-03 | | **8.85E-03** | 8.31E-03 | 1.00E-06 | 8.51E-02 | 8.51E-02 | 2.00E-01 | 5.00E+00 | 2.05E+03 | 107-06-2 |
| Clorometano | 3.49E-02 | 4.00E+00 | **8.74E-03** | 8.21E-03 | 6.83E-08 | 2.50E-01 | 2.50E-01 | 1.00E-01 | 5.00E+00 | 8.47E+02 | 74-87-3 |
| Tetracloroetilene(PCE) | 4.03E-02 | | **4.03E-02** | 3.78E-02 | 1.00E-06 | 1.47E-01 | 1.47E-01 | 5.00E-01 | 2.00E+01 | 3.44E+02 | 127-18-4 |
| DDE | 1.41E+00 | | **1.41E+00** | 1.32E+00 | 1.00E-06 | 1.13E-01 | 1.13E-01 | 1.00E-02 | 1.00E-01 | 1.04E+02 | 72-55-9 |

| On-site | R tot | HI tot |
|---|---|---|
| Outdoor | 3.57E-06 | 9.98E-01 |
| Indoor | 3.40E-06 | 2.06E-01 |
| **Off-site** | **R tot** | **HI tot** |
| Outdoor | 9.95E-09 | 4.70E-04 |

**Figure 4.21**. Clean up levels screen.

In the case of hydrocarbons contamination, the software also calculates, according to the Italian law (D.Lgs 152/06 and D.Lgs 04/08), the clean up levels for the C>12 and C<12 macro fractions (Fig.4.22).

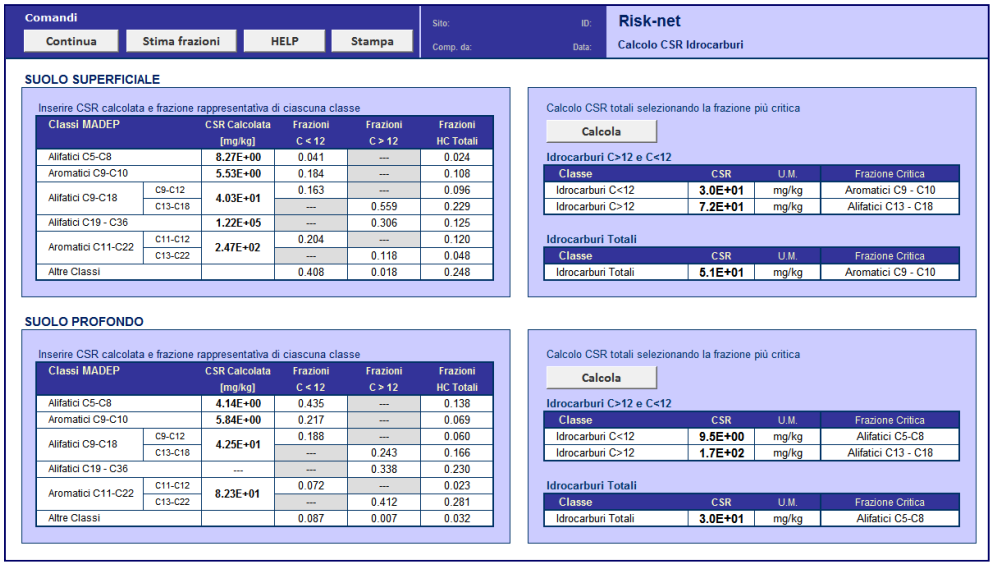

Comandi

Continua | Stima frazioni | HELP | Stampa

Sito: ID: Comp. da: Data:

**Risk-net**

Calcolo CSR Idrocarburi

**SUOLO SUPERFICIALE**

Inserire CSR calcolata e frazione rappresentativa di ciascuna classe

| Classi MADEP | | CSR Calcolata [mg/kg] | Frazioni C < 12 | Frazioni C > 12 | Frazioni HC Totali |
|---|---|---|---|---|---|
| Alifatici C5-C8 | | **8.27E+00** | 0.041 | --- | 0.024 |
| Aromatici C9-C10 | | **5.53E+00** | 0.184 | --- | 0.108 |
| Alifatici C9-C18 | C9-C12 | **4.03E+01** | 0.163 | --- | 0.096 |
| | C13-C18 | | --- | 0.559 | 0.229 |
| Alifatici C19 - C36 | | **1.22E+05** | --- | 0.306 | 0.125 |
| Aromatici C11-C22 | C11-C12 | **2.47E+02** | 0.204 | --- | 0.120 |
| | C13-C22 | | --- | 0.118 | 0.048 |
| Altre Classi | | | 0.408 | 0.018 | 0.248 |

Calcolo CSR totali selezionando la frazione più critica

Calcola

Idrocarburi C>12 e C<12

| Classe | CSR | U.M. | Frazione Critica |
|---|---|---|---|
| Idrocarburi C<12 | **3.0E+01** | mg/kg | Aromatici C9 - C10 |
| Idrocarburi C>12 | **7.2E+01** | mg/kg | Alifatici C13 - C18 |

Idrocarburi Totali

| Classe | CSR | U.M. | Frazione Critica |
|---|---|---|---|
| Idrocarburi Totali | **5.1E+01** | mg/kg | Aromatici C9 - C10 |

**SUOLO PROFONDO**

Inserire CSR calcolata e frazione rappresentativa di ciascuna classe

| Classi MADEP | | CSR Calcolata [mg/kg] | Frazioni C < 12 | Frazioni C > 12 | Frazioni HC Totali |
|---|---|---|---|---|---|
| Alifatici C5-C8 | | **4.14E+00** | 0.435 | --- | 0.138 |
| Aromatici C9-C10 | | **5.84E+00** | 0.217 | --- | 0.069 |
| Alifatici C9-C18 | C9-C12 | **4.25E+01** | 0.188 | --- | 0.060 |
| | C13-C18 | | --- | 0.243 | 0.166 |
| Alifatici C19 - C36 | | --- | --- | 0.338 | 0.230 |
| Aromatici C11-C22 | C11-C12 | **8.23E+01** | 0.072 | --- | 0.023 |
| | C13-C22 | | --- | 0.412 | 0.281 |
| Altre Classi | | | 0.087 | 0.007 | 0.032 |

Calcolo CSR totali selezionando la frazione più critica

Calcola

Idrocarburi C>12 e C<12

| Classe | CSR | U.M. | Frazione Critica |
|---|---|---|---|
| Idrocarburi C<12 | **9.5E+00** | mg/kg | Alifatici C5-C8 |
| Idrocarburi C>12 | **1.7E+02** | mg/kg | Alifatici C13 - C18 |

Idrocarburi Totali

| Classe | CSR | U.M. | Frazione Critica |
|---|---|---|---|
| Idrocarburi Totali | **3.0E+01** | mg/kg | Alifatici C5-C8 |

**Figure 4.22**. Clean up levels for hydrocarbons.

Afterwards the user can also visualize for each individual contaminant a summary of the clean up levels calculated and the different fate and transport factors used for their derivation (Fig.4.23).

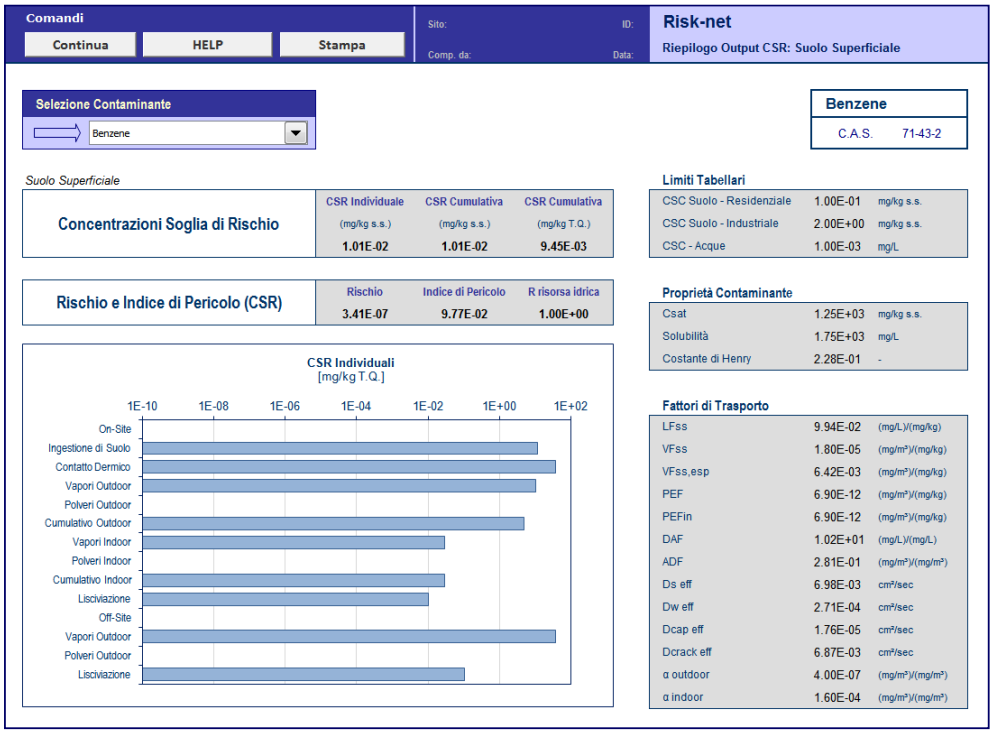


**Figure 4.23**. Clean up levels summary.

## MODELING PROCEDURES: RISK CALCULATION

**Individual Risk.** the estimation of risk for human health, correlated to exposure to a contaminant, is calculated in the software by applying the following equations:

$$R = E \cdot SF \qquad \text{Risk for carcinogenic contaminants} \tag{4.1}$$

$$HI = E / RfD \qquad \text{Hazard index for non carcinogenic contaminants} \tag{4.2}$$

Where $E$ is the daily chronic contaminant exposure rate, $SF$ the slope factor (i.e. the probability of incremental cancer case occurrence per unit dose) and $RfD$ the reference dose (i.e. the daily exposure rate that does not induce adverse effects on humans during the entire life).
The chronic daily contaminant assumption, $E$, is given by multiplying the concentration of the contaminant at the point of exposure, $C_{poe}$, with the effective exposure rate $EM$ (e.g. the daily ingested soil amount or inhaled air volume per unit body weight)

$$E = C_{poe} \cdot EM \tag{4.3}$$

The concentration at the point of exposure, $C_{poe}$, may be calculated by applying the following equation:

$$C_{poe} = FT \cdot CRS \tag{4.4}$$

where $CRS$ is the representative source concentration and $FT$ the fate and transport factor for the selected migration pathway.
Combining these equations the risk and the hazard index can be calculated as follows:

$$R = FT \cdot CRS \cdot EM \cdot SF \qquad \text{Risk for carcinogenic contaminants} \tag{4.5}$$

$$HI = \frac{FT \cdot CRS \cdot EM}{RfD} \qquad \text{Risk for non carcinogenic contaminants} \qquad (4.6)$$

This calculation is repeated for the different exposure and migration pathways active in the site using the appropriate exposure and fate & transport factors (for details, see the tables below).

The equations for the different F&T factors and intake rates are reported in the following paragraphs.

**Multiple exposure pathways**. The following figures (Fig.4.24 - 4.26) report the criteria used in the software for the calculation of the individual risk for each media of concern accounting for multiple exposure pathways.

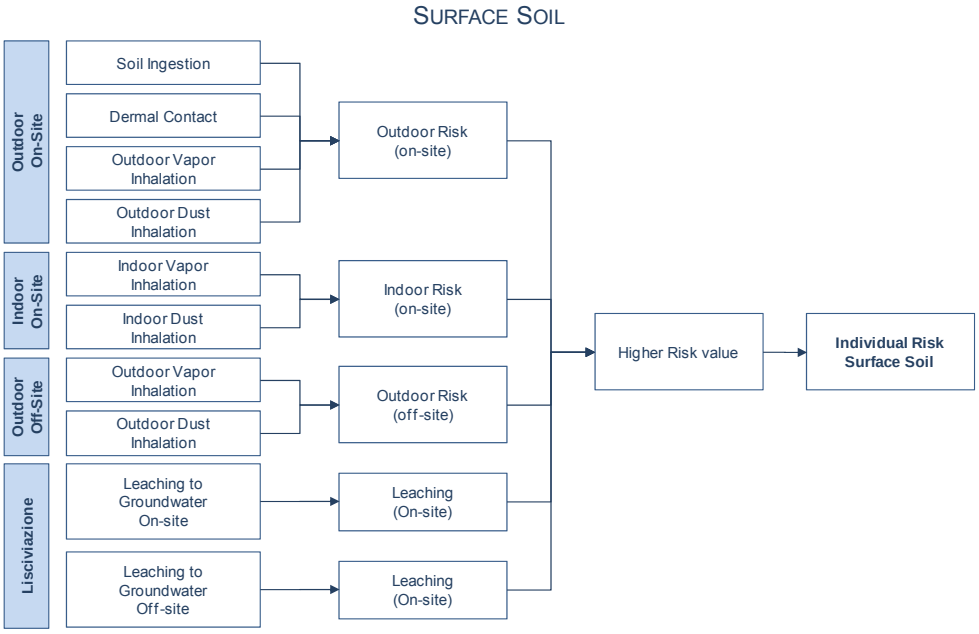


**Figure 4.24**. Risk – Surface soil. Multiple exposures.

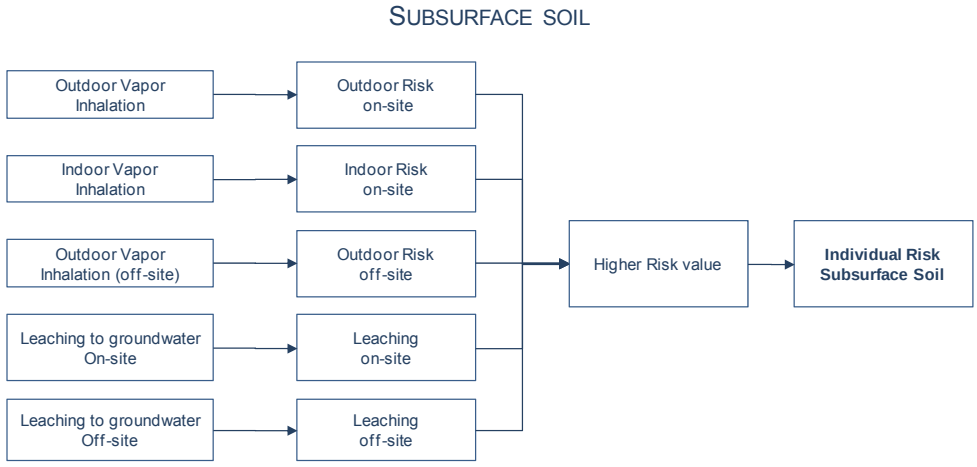


**Figure 4.25**. Risk – Subsurface soil. Multiple exposures.

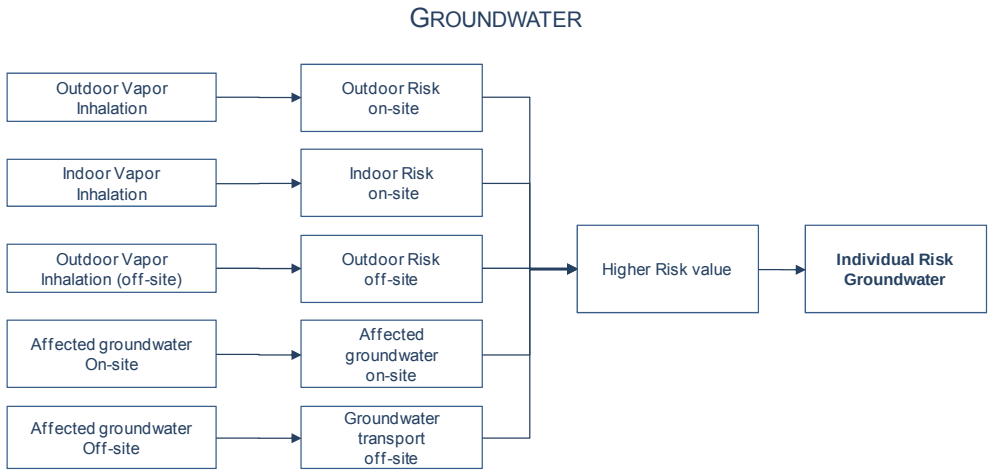


**Figure 4.26**. Risk – Groundwater. Multiple exposures.

**Cumulative Risk**. The cumulative risk is calculated as the sum of the incremental risk ($R_i$ and $HI_i$) values associated to each contaminant of concern as follows:

$$R_{tot} = \sum_{i=1}^{n} R_i \qquad \text{Cumulative risk for carcinogenic contaminants} \qquad (4.7)$$

$$HI_{tot} = \sum_{i=1}^{n} HI_i \qquad \text{Cumulative hazard index for non carcinogenic contaminants} \qquad (4.8)$$

**Risk for the groundwater resource.** The risk for the groundwater resource ($R_{GW}$) is calculated by comparing the value of concentration of the contaminant in the water table, at the point of compliance (POC) with the reference values defined by the Italian law (Threshold Concentrations Contamination, $CSC_{GW}$):

$$R_{GW} = \frac{C_{poe}}{CSC_{GW}} = \frac{FT \cdot CRS}{CSC_{GW}} \qquad (4.9)$$

**Table 4.1. Surface Soil: Risk and Hazard Index**

**Soil Ingestion (no off-site)**

$$R_{SS.IngS} = CRS \cdot SF_{Ing} \cdot EM_{IngS} \cdot 10^{-6}\ kg/mg$$

$$HI_{SS.IngS} = CRS \cdot \frac{EM_{IngS} \cdot 10^{-6}\ kg/mg}{RfD_{Ing}}$$

R = Carcinogenic Risk
HI = Hazard Index
CRS = Source Concentration
$SFI_{ng}$ = Slope factor - ingestion
RfD $I_{ng}$ = Reference dose - ingestion
$EMI_{ngs}$ = Soil Ingestion rate

**Dermal Contact (no off-site)**

$$R_{SS.ConD} = CRS \cdot SF_{Ing} \cdot EM_{ConD} \cdot 10^{-6}\ kg/mg$$

$$HI_{SS.ConD} = CRS \cdot \frac{EM_{ConD} \cdot 10^{-6}\ kg/mg}{RfD_{Ing}}$$

R = Carcinogenic Risk
HI = Hazard Index
CRS = Source Concentration
$SFI_{ng}$ = Slope factor for ingestion
RfD $I_{ng}$ = Reference dose - ingestion
$EM_{ConD}$ = Dermal contact rate

**Outdoor Vapor Inhalation**

$$R_{SS.InaO} = CRS \cdot SF_{Ina} \cdot EM_{InaO} \cdot VF_{ss} \cdot ADF$$

$$HI_{SS.InaO} = CRS \cdot \frac{EM_{InaO} \cdot VF_{ss} \cdot ADF}{RfD_{Ina}}$$

R = Carcinogenic Risk
HI = Hazard Index
CRS = Source Concentration
$SFI_{na}$ = Slope factor - inalazione
RfD $I_{na}$ = Reference dose - inhalation
$EM_{InaO}$ = Outdoor inhalation rate
$VF_{ss}$ = Outdoor volatilization factor
ADF = Atmospheric dispersion factor

**Outdoor Dust Inhalation**

$$R_{SS.InaOP} = CRS \cdot SF_{Ina} \cdot EM_{InaO} \cdot PEF \cdot ADF$$

$$HI_{SS.InaOP} = CRS \cdot \frac{EM_{InaO} \cdot PEF \cdot ADF}{RfD_{Ina}}$$

R = Carcinogenic Risk
HI = Hazard Index
CRS = Source Concentration
$SFI_{na}$ = Slope factor - inhalation
RfD $I_{na}$ = Reference dose - inhalation
$EM_{InaO}$ = Outdoor inhalation rate
PEF = Partculate emission factor
ADF = Atmospheric dispersion factor

**Outdoor risk**

$$R_{SS.outdoor} = R_{SS.IngS} + R_{SS.ConD} + R_{SS.InaO} + R_{SS.InaOP}$$

$$HI_{SS.outdoor} = HI_{SS.IngS} + HI_{SS.ConD} + HI_{SS.InaO} + HI_{SS.InaOP}$$

**Indoor Vapor Inhalation (no off-site)**

$$R_{SS.InaI} = CRS \cdot SF_{Ina} \cdot EM_{InaI} \cdot VF_{ssesp}$$

$$HI_{SS.InaI} = CRS \cdot \frac{EM_{InaI} \cdot VF_{ssesp}}{RfD_{Ina}}$$

R = Carcinogenic Risk
HI = Hazard Index
CRS = Source Concentration
$SFI_{na}$ = Slope factor - inhalation
RfD $I_{na}$ = Reference dose - inhalation
$EM_{InaI}$ = Indoor inhalation rate
$VF_{sesp}$ = Indoor volatilization factor

**Indoor Dust Inhalation (no off-site)**

$$R_{SS.InaIP} = CRS \cdot SF_{Ina} \cdot EM_{InaI} \cdot PEF_{in}$$

$$HI_{SS.InaIP} = CRS \cdot \frac{EM_{InaI} \cdot PEF_{in}}{RfD_{Ina}}$$

R = Carcinogenic Risk
HI = Hazard Index
CRS = Source Concentration
$SFI_{na}$ = Slope factor - inhalation
RfD $I_{na}$ = Reference dose - inhalation
$EM_{InaI}$ = Indoor inhalation rate
$PEF_{in}$ = Partculate indoor emission factor

**Table 4.1. Surface Soil: Risk and Hazard Index**

**Indoor risk**

$$R_{SS.Indoor} = R_{SS.InaI} + R_{SS.InaIP}$$

$$HI_{SS.Indoor} = HI_{SS.InaI} + HI_{SS.InaIP}$$

**Ingestion of water**

$$R_{SS.LF} = CRS \cdot \frac{SF_{Ing} \cdot EM_{IngW} \cdot LF_{ss}}{DAF}$$

$$HI_{SS.LF} = CRS \cdot \frac{EM_{IngW} \cdot LF_{ss}}{RfD_{Ing} \cdot DAF}$$

R = Carcinogenic Risk
HI = Hazard Index
CRS = Source Concentration
$SFI_{ng}$ = Slope factor - ingestion
RfD $I_{ng}$ = Reference dose - ingestion
$EMI_{ngW}$ = Water Ingestion rate
$LF_{ss}$ = Leaching factor
DAF = Groundwater dilution factor

**Risk and Hazard Index for surface soil**

$$R_{SS} = \max\left[R_{SS.outdoor}; R_{SS.Indoor}; R_{SS.LF}\right]$$

$$HI_{SS} = \max\left[HI_{SS.outdoor}; HI_{SS.Indoor}; HI_{SS.LF}\right]$$

For On-site Receptors ADF = 1; DAF = 1

**Table 4.2. Subsurface Soil: Risk and Hazard Index**

**Outdoor Vapor Inhalation**

$$R_{SP.InaO} = CRS \cdot SF_{Ina} \cdot VF_{samb} \cdot EM_{InaO} \cdot ADF$$

$$HI_{SP.InaO} = CRS \cdot \frac{VF_{samb} \cdot EM_{InaO} \cdot ADF}{RfD_{Ina}}$$

R = Carcinogenic Risk
HI = Hazard Index
CRS = Source Concentration
$SFI_{na}$ = Slope factor - inhalation
RfD $I_{na}$ = Reference dose - inhalation
$EM_{InaO}$ = Outdoor inhalation rate
$VF_{samb}$ = Outdoor volatilization factor
ADF = Atmospheric dispersion factor

**Indoor Vapor Inhalation (no off-site)**

$$R_{SP.InaI} = CRS \cdot SF_{Ina} \cdot VF_{sesp} \cdot EM_{InaI}$$

$$HI_{SP.InaI} = CRS \cdot \frac{VF_{sesp} \cdot EM_{InaI}}{RfD_{Ina}}$$

R = Carcinogenic Risk
HI = Hazard Index
CRS = Source Concentration
$SFI_{na}$ = Slope factor - inhalation
RfD $I_{na}$ = Reference dose - inhalation
$EM_{InaI}$ = Indoor inhalation rate
$VF_{sesp}$ = Indoor volatilization factor

**Ingestion of water**

$$R_{SP.LF} = CRS \cdot \frac{SF_{Ing} \cdot EM_{IngW} \cdot LF_{sp}}{DAF}$$

$$HI_{SP.LF} = CRS \cdot \frac{EM_{IngW} \cdot LF_{sp}}{RfD_{Ing} \cdot DAF}$$

R = Carcinogenic Risk
HI = Hazard Index
CRS = Source Concentration
$SFI_{ng}$ = Slope factor - ingestion
RfD $I_{ng}$ = Reference dose - ingestion
$EMI_{ngW}$ = Water Ingestion rate
$LF_{sp}$ = Leaching factor
DAF = Groundwater dilution factor

**Risk and Hazard Index for subsurface soil**

$$R_{SP} = \max\left[R_{SP.InaO}; R_{SP.InaI}; R_{SP.LF}\right]$$

$$HI_{SP} = \max\left[HI_{SP.InaO}; HI_{SP.InaI}; HI_{SP.LF}\right]$$

For On-site Receptors ADF = 1; DAF = 1

**Table 4.3. Groundwater: Risk and Hazard Index**

**Outdoor Vapor Inhalation**

$$R_{GW.InaO} = CRS \cdot \frac{SF_{Ina} \cdot VF_{wamb} \cdot EM_{InaO}}{DAF}$$

$$HI_{GW.InaO} = CRS \cdot \frac{VF_{wamb} \cdot EM_{InaO}}{RfD_{Ina} \cdot DAF}$$

R = Carcinogenic Risk
HI = Hazard Index
CRS = Source Concentration
$SFI_{na}$ = Slope factor - inhalation
$RfD\ I_{na}$ = Reference dose - inhalation
$EM_{InaO}$ = Outdoor inhalation rate
$VF_{wamb}$ = Outdoor volatilization factor
DAF = Groundwater dilution factor

**Indoor Vapor Inhalation**

$$R_{GW.InaI} = CRS \cdot \frac{SF_{Ina} \cdot VF_{wesp} \cdot EM_{InaI}}{DAF}$$

$$HI_{GW.InaI} = CRS \cdot \frac{VF_{wesp} \cdot EM_{InaI}}{RfD_{Ina} \cdot DAF}$$

R = Carcinogenic Risk
HI = Hazard Index
CRS = Source Concentration
$SFI_{na}$ = Slope factor - inhalation
$RfD\ I_{na}$ = Reference dose - inhalation
$EM_{InaI}$ = Indoor inhalation rate
$VF_{wesp}$ = Indoor volatilization factor
DAF = Groundwater dilution factor

**Ingestion of water**

$$R_{GW.D} = CRS \cdot \frac{SF_{Ing} \cdot EM_{IngW}}{DAF}$$

$$HI_{GW.D} = CRS \cdot \frac{EM_{IngW}}{RfD_{Ing} \cdot DAF}$$

R = Carcinogenic Risk
HI = Hazard Index
CRS = Source Concentration
$SFI_{ng}$ = Slope factor - ingestion
$RfD\ I_{ng}$ = Reference dose - ingestion
$EMI_{ngW}$ = Water Ingestion rate
DAF = Groundwater dilution factor

**Risk and Hazard Index for groundwater**

$$R_{GW} = \max\left[R_{GW.InaO}; R_{GW.InaI}; R_{GW.D}\right]$$

$$HI_{GW} = \max\left[HI_{GW.InaO}; HI_{GW.InaI}; HI_{GW.D}\right]$$

For On-site Receptors DAF = 1

**Table 4.4. Risk for the groundwater resource**

**Surface Soil – Leaching to Groundwater**

$$R_{SS.LF} = \frac{CRS \cdot LF_{ss}}{DAF \cdot CSC_{Falda} \cdot 10^{-3}\ mg/\mu g}$$

CRS = Source Concentration
$CSC_{falda}$ = Treshold concentration value
$LF_{ss}$ = Leaching factor
DAF = Groundwater dilution factor

**Subsurface Soil – Leaching to Groundwater**

$$R_{SP.LF} = \frac{CRS \cdot LF_{sp}}{DAF \cdot CSC_{Falda} \cdot 10^{-3}\ mg/\mu g}$$

CRS = Source Concentration
$CSC_{falda}$ = Treshold concentration value
$LF_{sp}$ = Leaching factor
DAF = Groundwater dilution factor

**Affected groundwater**

$$R_{GW.D} = \frac{CRS}{DAF \cdot CSC_{Falda} \cdot 10^{-3}\ mg/\mu g}$$

CRS = Source Concentration
$CSC_{falda}$ = Treshold concentration value
DAF = Groundwater dilution factor

For On-site Receptors DAF = 1

## MODELING PROCEDURES: CLEAN-UP LEVELS CALCULATION

The calculation of the remediation targets (Threshold Risk Concentrations, *CSR*) is performed by the application of the risk analysis procedure in backward mode. The clean-up levels calculated represent the maximum acceptable concentration in the affected source medium (soil or groundwater) that is protective of a human or groundwater receptor located at a relevant point of exposure.

**Individual Clean-up Levels (CSR).** The calculation of the clean-up levels (*CSR*) is performed using the same equations applied to calculate the risk (Eqs. 4.5-4.6), properly reversed and expressed in terms of the source concentration:

$$CSR = \frac{C_{poe}}{FT} = \frac{E}{EM \cdot FT} = \frac{TR}{SF \cdot EM \cdot FT} \qquad \text{for carcinogenic contaminants} \qquad (4.10)$$

$$CSR = \frac{Cpoe}{FT} = \frac{E}{EM \cdot FT} = \frac{THI \cdot RfD}{EM \cdot FT} \qquad \text{for non carcinogenic contaminants} \qquad (4.11)$$

Where:
*TR*: Target Risk for the single constituent (e.g. TR = $10^{-6}$)
*THI*: Target Hazard Index for the single constituent (THI = 1)
*E*: daily chronic contaminant exposure rate
*SF*: Slope Factor
*RfD*: Reference Dose
$C_{poe}$: Concentration at the point of exposure
*EM*: Intake rate
*FT*: Fate & Transport factor

This calculation is repeated for the different exposure and migration pathways active in the site using the appropriate exposure factors and transport (for details, see the tables below). The equations for the different F&T factors and intake rates are reported in the next paragraphs.

**Multiple exposure pathways.** The equations described above provide an assessment of the *CSR* for the single exposure pathway. The Individual *CSR* (associated to the single contaminant) is derived by cumulating the effects of the different exposure scenarios (e.g. Outdoor exposure) and then choosing the most conservative value (i.e. the lower value) between the *CSR* calculated for the different scenarios. Namely, the combined effect of multiple exposure is estimated as the reciprocal of the sum of the reciprocals of the *CSR* calculated for each route of exposure. Let assume, for example, the case of *CSR* for the calculation of exposure in outdoor environments:

$$CSR_{outdoor} = \frac{1}{1/CSR_{ing} + 1/CSR_{derm.cont} + 1/CSR_{dusts} + 1/CSR_{vapors}} \tag{4.12}$$

For other scenarios, see the tables below.

The following figures (Fig.4.27 - 4.29) report the criteria used in the software for the calculation of the individual clean-up levels for each media of concern accounting for multiple exposure pathways.

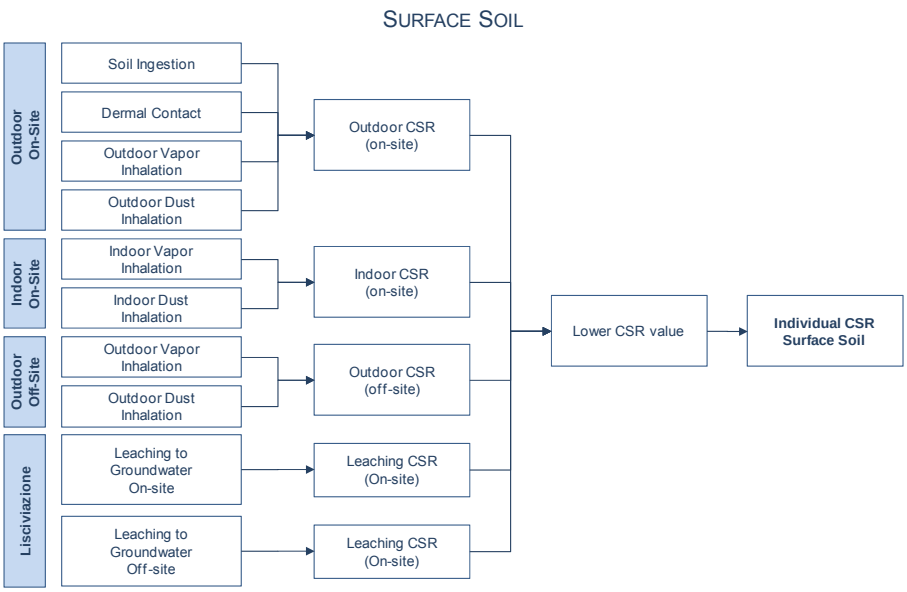


**Figure 4.27**. CSR – Surface soil. Multiple exposures.

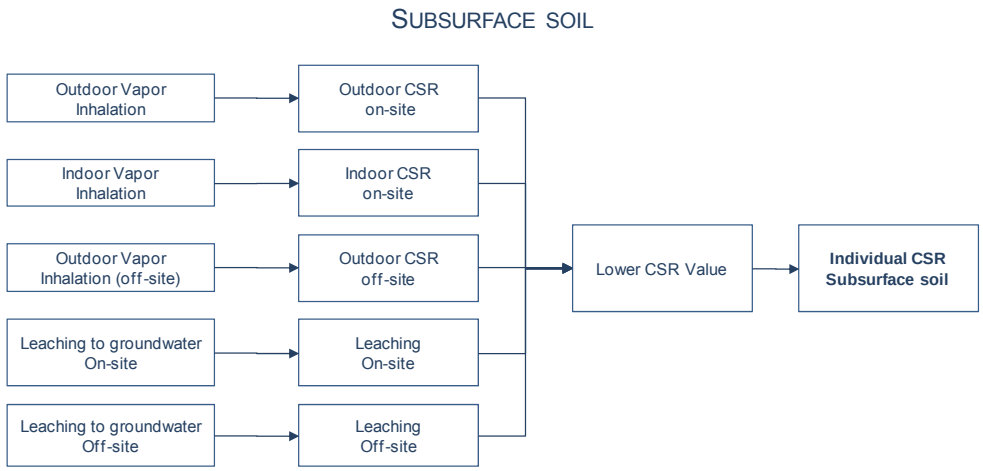


**Figure 4.28**. CSR – Subsurface soil. Multiple exposures.

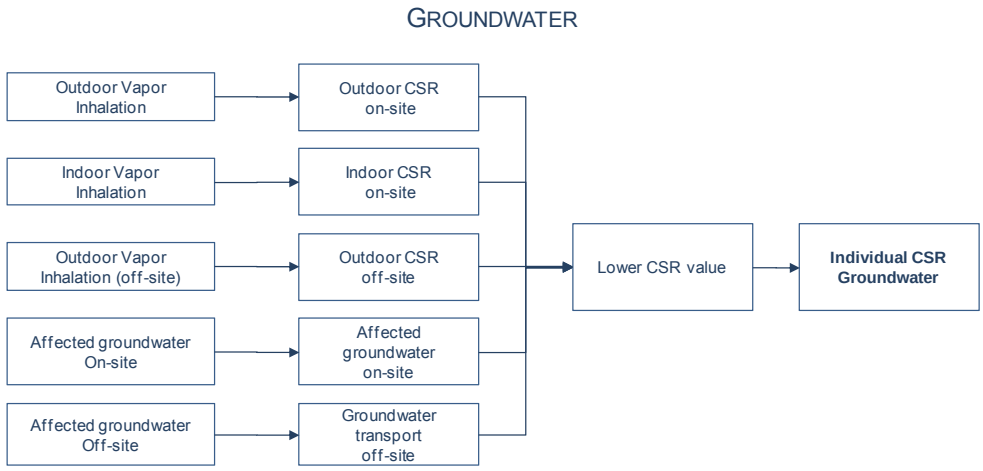


**Figure 4.29**. CSR – Groundwater. Multiple exposures.

**Cumulative CSR (Clean-up levels).** The *CSR* calculated above does not constitute yet the remediation targets since these concentrations only meet the condition of tolerable risk for exposure to a single contaminant. In fact, the individual *CSR* doesn't necessarily meet the requirement of cumulative target risk. Thus, to account for the effects of the cumulative risk, it's necessary to further reduce the individual *CSR* to

ensure the achievement of values of concentration such that the condition of acceptable cumulative risk is met:

$$\sum_{i}^{n} CSR_i^{cum} \cdot FT_i \cdot EM_i \cdot SF_i \leq TR \qquad \text{for carcinogenic contaminants} \tag{4.13}$$

$$\sum_{i}^{n} \frac{CSR_i^{cum} \cdot FT_i \cdot EM_i}{RfD_i} \leq THI \qquad \text{for non carcinogenic contaminants} \tag{4.14}$$

The *CSR* that meet both the individual and cumulative target limits represent the site-specific clean up levels for the contaminated matrix.

**Table 4.5. Surface Soil: CSR**

**Soil Ingestion (no off-site)**

$$CSR_{SS.Ing} = \min\begin{cases} CSR_{canc} = \dfrac{TR}{SF_{Ing} \cdot EM_{IngS} \cdot 10^{-6}\ kg/mg} \\ CSR_{non.canc} = \dfrac{THQ \cdot RfD_{Ing}}{EM_{IngS} \cdot 10^{-6}\ kg/mg} \end{cases}$$

$CSR_{canc}$ = CSR carcinogenic cont.
$CSR_{non\text{-}canc}$ = CSR non-carcinogenic
TR = Target Risk
THQ = Target Hazard Index
$SFI_{ng}$ = Slope factor - ingestion
RfD $I_{ng}$ = Reference dose - ingestion
$EMI_{ngs}$ = Soil Ingestion rate

**Dermal Contact (no off-site)**

$$CSR_{SS.ConD} = \min\begin{cases} CSR_{canc} = \dfrac{TR}{SF_{Ing} \cdot EM_{ConD} \cdot 10^{-6}\ kg/mg} \\ CSR_{non.canc} = \dfrac{THQ \cdot RfD_{Ing}}{EM_{ConD} \cdot 10^{-6}\ kg/mg} \end{cases}$$

$CSR_{canc}$ = CSR carcinogenic cont.
$CSR_{non\text{-}canc}$ = CSR non-carcinogenic
TR = Target Risk
THQ = Target Hazard Index
$SFI_{ng}$ = Slope factor - ingestion
RfD $I_{ng}$ = Reference dose - ingestion
$EM_{ConD}$ = Dermal contact rate

**Outdoor Vapors Inhalation**

$$CSR_{SS.InaO} = \min\begin{cases} CSR_{canc} = \dfrac{TR}{SF_{Ina} \cdot EM_{InaO} \cdot VF_{ss} \cdot ADF} \\ CSR_{non.canc} = \dfrac{THQ \cdot RfD_{Ina}}{EM_{InaO} \cdot VF_{ss} \cdot ADF} \end{cases}$$

$CSR_{canc}$ = CSR carcinogenic cont.
$CSR_{non\text{-}canc}$ = CSR non-carcinogenic
TR = Target Risk
THQ = Target Hazard Index
$SFI_{na}$ = Slope factor - inhalation
RfD $I_{na}$ = Reference dose – inhalation
$EM_{InaO}$ = Outdoor inhalation rate
$VF_{ss}$ = Outdoor Volatilization factor
ADF = Atmospheric dispersion factor

**Outdoor Dusts Inhalation**

$$CSR_{SS.InaOP} = \min\begin{cases} CSR_{canc} = \dfrac{TR}{SF_{Ina} \cdot EM_{InaO} \cdot PEF \cdot ADF} \\ CSR_{non.canc} = \dfrac{THQ \cdot RfD_{Ina}}{EM_{InaO} \cdot PEF \cdot ADF} \end{cases}$$

$CSR_{canc}$ = CSR carcinogenic cont.
$CSR_{non\text{-}canc}$ = CSR non-carcinogenic
TR = Target Risk
THQ = Target Hazard Index
$SFI_{na}$ = Slope factor - inhalation
RfD $I_{na}$ = Reference dose - inhalation
$EM_{InaO}$ = Outdoor inhalation rate
PEF = Particulate emission factor
ADF = Atmospheric dispersion factor

**Outdoor**

$$CSR_{SS.outdoor} = \begin{cases} \dfrac{1}{\dfrac{1}{CSR_{SS.IngS}} + \dfrac{1}{CSR_{SS.ConD}} + \dfrac{1}{CSR_{SS.InaO}} + \dfrac{1}{CSR_{SS.InaOP}}} & (\text{for } CSR_{InaO} \le C_{sat}) \\ \dfrac{TR - R_{\max,InaO}}{\dfrac{TR}{CSR_{SS.IngS}} + \dfrac{TR}{CSR_{SS.ConD}} + \dfrac{TR}{CSR_{SS.InaOP}}} & (\text{for } CSR_{InaO} > C_{sat}) \end{cases}$$

$$R_{\max,InaO} = \left(C_{sat} / CSR_{InaO}\right) \cdot TR \qquad (\text{for } CSR_{InaO} > C_{sat})$$

**Table 4.5. Surface Soil: CSR**

**Indoor Vapors Inhalation (no off-site)**

$$CSR_{SS.InaI} = \min \begin{cases} CSR_{canc} = \dfrac{TR}{SF_{Ina} \cdot EM_{InaI} \cdot VF_{ssesp}} \\ CSR_{non.canc} = \dfrac{THQ \cdot RfD_{Ina}}{EM_{InaI} \cdot VF_{ssesp}} \end{cases}$$

$CSR_{canc}$ = CSR carcinogenic cont.
$CSR_{non\cdot canc}$ = CSR non-carcinogenic
TR = Target Risk
THQ = Target Hazard Index
$SFI_{na}$ = Slope factor - inhalation
RfD $I_{na}$ = Reference dose - inhalation
$EM_{InaI}$ = Indoor inhalation rate
$VF_{sesp}$ = Indoor Volatilization factor

**Indoor Dusts Inhalation (no off-site)**

$$CSR_{SS.InaIP} = \min \begin{cases} CSR_{canc} = \dfrac{TR}{SF_{Ina} \cdot EM_{InaI} \cdot PEF_{in}} \\ CSR_{non.canc} = \dfrac{THQ \cdot RfD_{Ina}}{EM_{InaI} \cdot PEF_{in}} \end{cases}$$

$CSR_{canc}$ = CSR carcinogenic cont.
$CSR_{non\cdot canc}$ = CSR non-carcinogenic
TR = Target Risk
THQ = Target Hazard Index
$SFI_{na}$ = Slope factor - inhalation
RfD $I_{na}$ = Reference dose - inhalation
$EM_{InaI}$ = Indoor inhalation rate
$PEF_{in}$ = Particulate indoor emission factor

**Indoor**

$$CSR_{SS.Indoor} = \begin{cases} \dfrac{1}{\dfrac{1}{CSR_{SS.InaI}} + \dfrac{1}{CSR_{SS.InaIP}}} & (\text{for } CSR_{InaI} \le C_{sat}) \\ \dfrac{TR - R_{\max,InaI}}{\dfrac{TR}{CSR_{SS.InaIP}}} & (\text{for } CSR_{InaI} > C_{sat}) \end{cases}$$

Where

$$R_{\max,InaI} = \left(C_{sat} / CSR_{InaI}\right) \cdot TR \qquad (\text{for } CSR_{InaI} > C_{sat})$$

**Leaching to groundwater**

$$CSR_{SS.LF} = \min \begin{cases} CSR_{canc} = \dfrac{TR \cdot DAF}{SF_{Ing} \cdot EM_{IngW} \cdot LF_{ss}} \\ CSR_{non.canc} = \dfrac{THQ \cdot RfD_{Ing} \cdot DAF}{EM_{IngW} \cdot LF_{ss}} \end{cases}$$

$CSR_{canc}$ = CSR carcinogenic cont.
$CSR_{non\cdot canc}$ = CSR non-carcinogenic
TR = Target Risk
THQ = Target Hazard Index
$SFI_{ng}$ = Slope factor - ingestion
RfD $I_{ng}$ = Reference dose - ingestion
$EMI_{ngW}$ = Water ingestion rate
$LF_{ss}$ = Leaching Factor
DAF = Groundwater diluition factor

**CSR – Surface Soil**

$$CSR_{SS} = \min\left[CSR_{SS.outdoor}; CSR_{SS.Indoor}; CSR_{SS.LF}\right]$$

For On-site Receptors ADF = 1; DAF = 1

**Table 4.6. Subsurface Soil: CSR**

**Outdoor Vapors Inhalation**

$$CSR_{SP.InaO} = \min \begin{cases} CSR_{canc} = \dfrac{TR}{SF_{Ina} \cdot VF_{samb} \cdot EM_{InaO} \cdot ADF} \\ CSR_{non.canc} = \dfrac{THQ \cdot RfD_{Ina}}{VF_{samb} \cdot EM_{InaO} \cdot ADF} \end{cases}$$

$CSR_{canc}$ = CSR carcinogenic cont.
$CSR_{non\text{-}canc}$ = CSR non-carcinogenic cont.
TR = Target Risk
THQ = Target Hazard Index
$SFI_{na}$ = Slope factor - inhalation
RfD $I_{na}$ = Reference dose – inhalation
$EM_{InaO}$ = Outdoor inhalation rate
$VF_{samb}$ = Outdoor Volatilization factor
ADF = Atmospheric dispersion factor

**Indoor Vapors Inhalation (no off-site)**

$$CSR_{SP.InaI} = \min \begin{cases} CSR_{canc} = \dfrac{TR}{SF_{Ina} \cdot VF_{sesp} \cdot EM_{InaI}} \\ CSR_{non.canc} = \dfrac{THQ \cdot RfD_{Ina}}{VF_{sesp} \cdot EM_{InaI}} \end{cases}$$

$CSR_{canc}$ = CSR carcinogenic cont.
$CSR_{non\text{-}canc}$ = CSR non-carcinogenic cont.
TR = Target Risk
THQ = Target Hazard Index
$SFI_{na}$ = Slope factor - inhalation
RfD $I_{na}$ = Reference dose – inhalation
$EM_{InaI}$ = Indoor inhalation rate
$VF_{sesp}$ = Indoor Volatilization factor

**Leaching to groundwater**

$$CSR_{SP.LF} = \min \begin{cases} CSR_{canc} = \dfrac{TR \cdot DAF}{SF_{Ing} \cdot EM_{IngW} \cdot LF_{sp}} \\ CSR_{non.canc} = \dfrac{THQ \cdot RfD_{Ing} \cdot DAF}{EM_{IngW} \cdot LF_{sp}} \end{cases}$$

$CSR_{canc}$ = CSR carcinogenic cont.
$CSR_{non\text{-}canc}$ = CSR non-carcinogenic cont.
TR = Target Risk
THQ = Target Hazard Index
$SFI_{ng}$ = Slope factor - ingestion
RfD $I_{ng}$ = Reference dose - ingestion
$EMI_{ngW}$ = Water ingestion rate
$LF_{sp}$ = Leaching factor
DAF = Groundwater dilution factor

**CSR – Subsurface Soil**

$$CSR_{SP} = \min\left[CSR_{SP.InaO}; CSR_{SP.InaI}; CSR_{SP.LF}\right]$$

For On-site Receptors ADF = 1; DAF = 1

**Table 4.7. Groundwater: CSR**

**Outdoor Vapors Inhalation**

$$CSR_{GW.InaO} = \min \begin{cases} CSR_{canc} = \dfrac{TR \cdot DAF}{SF_{Ina} \cdot VF_{wamb} \cdot EM_{InaO}} \\ CSR_{non.canc} = \dfrac{THQ \cdot RfD_{Ina} \cdot DAF}{VF_{wamb} \cdot EM_{InaO}} \end{cases}$$

$CSR_{canc}$ = CSR carcinogenic cont.
$CSR_{non\cdot canc}$ = CSR non-carcinogenic cont.
TR = Target Risk
THQ = Target Hazard Index
$SFI_{na}$ = Slope factor - inhalation
RfD $I_{na}$ = Reference dose – inhalation
$EM_{InaO}$ = Outdoor inhalation rate
$VF_{wamb}$ = Outdoor Volatilization factor
DAF = Groundwater dilution factor

**Indoor Vapors Inhalation**

$$CSR_{GW.InaI} = \min \begin{cases} CSR_{canc} = \dfrac{TR \cdot DAF}{SF_{Ina} \cdot VF_{wesp} \cdot EM_{InaI}} \\ CSR_{non.canc} = \dfrac{THQ \cdot RfD_{Ina} \cdot DAF}{VF_{wesp} \cdot EM_{InaI}} \end{cases}$$

$CSR_{canc}$ = CSR carcinogenic cont.
$CSR_{non\cdot canc}$ = CSR non-carcinogenic cont.
TR = Target Risk
THQ = Target Hazard Index
$SFI_{na}$ = Slope factor - inhalation
RfD $I_{na}$ = Reference dose – inhalation
$EM_{InaI}$ = Indoor inhalation rate
$VF_{wesp}$ = Indoor Volatilization factor
DAF = Groundwater dilution factor

**Water Ingestion**

$$CSR_{GW.D} = \min \begin{cases} CSR_{canc} = \dfrac{TR \cdot DAF}{SF_{Ing} \cdot EM_{IngW}} \\ CSR_{non.canc} = \dfrac{THQ \cdot RfD_{Ing} \cdot DAF}{EM_{IngW}} \end{cases}$$

$CSR_{canc}$ = CSR carcinogenic cont.
$CSR_{non\cdot canc}$ = CSR non-carcinogenic cont.
TR = Target Risk
THQ = Target Hazard Index
$SFI_{ng}$ = Slope factor - ingestion
RfD $I_{ng}$ = Reference dose - ingestion
$EMI_{ngW}$ = Water ingestion rate
DAF = Groundwater dilution factor

**CSR - Groundwater**

$$CSR_{GW} = \min\left[CSR_{GW.InaO}; CSR_{GW.InaI}; CSR_{GW.D}\right]$$

For On-site Receptors DAF = 1

**Table 4.8. CSR Groundwater Resource**

**Surface Soil – Leaching to Groundwater**

$$CSR_{SS.LF} = \frac{CSC_{Falda} \cdot DAF}{LF_{ss}} \cdot 10^{-3}\ mg/\mu g$$

$CSC_{falda}$ = Treshold concentration value
$LF_{ss}$ = Leaching factor
DAF = Groundwater dilution factor

**Subsurface Soil – Leaching to Groundwater**

$$CSR_{SP.LF} = \frac{CSC_{Falda} \cdot DAF}{LF_{sp}} \cdot 10^{-3}\ mg/\mu g$$

$CSC_{falda}$ = Treshold concentration value
$LF_{sp}$ = Leaching factor
DAF = Groundwater dilution factor

**Affected Groundwater**

$$CSR_{GW.D} = DAF \cdot CSC_{Falda} \cdot 10^{-3}\ mg/\mu g$$

$CSC_{falda}$ = Treshold concentration value
DAF = Groundwater dilution factor

For On-site Receptors ADF = 1; DAF = 1

**Table 4.9. CSR: Petroleum Hydrocarbons**

**Hydrocarbons C< 12**

$$CSR_{C<12} = \min\left(CSR_{\text{MADEP1}} / frac_1^{C<12}; CSR_{\text{MADEP2}} / frac_2^{C<12}; .....; CSR_{\text{MADEPn}} / frac_n^{C<12}\right)$$

**Hydrocarbons C> 12**

$$CSR_{C>12} = \min\left(CSR_{\text{MADEP1}} / frac_1^{C>12}; CSR_{\text{MADEP2}} / frac_2^{C>12}; .....; CSR_{\text{MADEPn}} / frac_n^{C>12}\right)$$

**Total Hydrocarbons**

$$CSR_{HC} = \min\left(CSR_{\text{MADEP1}} / frac_1^{HC}; CSR_{\text{MADEP2}} / frac_2^{HC}; .....; CSR_{\text{MADEPn}} / frac_n^{HC}\right)$$

**Nomenclature**

$CSR_{\text{MADEPi}}$ = *calculated CSR for the i-th MADEP class*

$frac_i^{C<12}$ *and* $frac_i^{C>12}$ = *mass fraction of the i-th MADEP class for C>12 and C<12*

$frac_i^{HC}$ = *mass fraction of the i-th MADEP class for total hydrocarbons*

**Table 4.10. Screening for free phase migration (NAPL)**

**Vadose zone (ASTM E2081-00)**

$$RBSL_{NAPL} = \frac{\theta_w + H\left(\theta_a - \theta_o\right) + \rho_s \cdot K_s}{\rho_s} \cdot S + \frac{\theta_o \cdot \rho_o}{\rho_s} \cdot 10^6 \, \frac{mg}{kg}$$

**Saturated Zone (ASTM E2081-00)**

$$RBSL_{NAPL} = \frac{\left(\theta_{e,sat} - \theta_o\right) + \rho_s \cdot K_s}{\rho_s} \cdot S + \frac{\theta_o \cdot \rho_o}{\rho_s} \cdot 10^6 \, \frac{mg}{kg}$$

**Residual phase volume fraction, $\theta_o$ (-)**

$$\theta_o = \theta_{e,sat} \cdot S_{r,sat} \quad ; \quad \theta_o = \theta_e \cdot S_r$$

**Nomenclature**

$S_r$ = *Residual phase void fraction, vadose zone (-)*
$S_{r,sat}$ = *Residual phase void fraction, saturated zone (-)*
$\theta_w$ = *Volumetric water content (-)*
$\theta_a$ = *Volumetric air content (-)*
$\theta_e$ = *Effective porosity, unsaturated zone (-)*
$\theta_{e,sat}$ = *Effective porosity, saturated zone (-)*
$K_s$ = *Soil / water partition coefficient (kg/L)*
$H$ = *Henry constant (-)*
$\rho_s$ = *Dry soil bulk density (g/cm$^3$)*
$\rho_o$ = *Contaminant density (g/cm$^3$)*

## MODELING PROCEDURES: FATE & TRANSPORT FACTORS

The transport factors (*FT*) are involved in the indirect exposure assessment or where contaminants can reach targets only through migration and diffusion from the environmental compartment.

For the calculation of transport factors is essential to determine the physical characteristics of the environmental media affected (Vadose zone, groundwater, indoor and outdoor air) and the physico-chemical characteristics of contaminants in order to assess the distribution and dispersion of contaminants.

The transport factors considered in the software are:

From Surface Soil
- $VF_{ss}$: Outdoor volatilization factor
- $VF_{sesp}$: Indoor volatilization factor
- $PEF$: Outdoor particulate emission
- $PEF_{in}$: Indoor particulate emission
- $LF_{ss}$: Leaching factor

From Subsurface Soil
- $VF_{samb}$ Outdoor volatilization factor
- $VF_{sesp}$: Indoor volatilization factor
- $LF_{sp}$: Leaching factor

From Groundwater
- $VF_{wamb}$: Outdoor volatilization factor
- $VF_{wesp}$: Indoor volatilization factor
- $DAF$: Groundwater attenuation factor

Air Dispersion
- $ADF$: Air Dispersion Factor

The main assumptions on which are based the equations are:

- The concentration of pollutants in soil is uniformly distributed and constant throughout the entire exposure period;

- Soil is homogeneous and isotropic and incoherent;

- No biodegradation (with the exception of *DAF*) or other mechanisms of degradation / transformation of pollutants.

**Table 4.11. Surface Soil: Outdoor vapor volatilization**

$$VF_{ss}\left[\frac{mg/m^3_{air}}{mg/kg_{soil}}\right]=\min\begin{cases} VF_{ss}(1)=\dfrac{2\cdot W'\cdot\rho_s}{U_{air}\cdot\delta_{air}}\sqrt{\dfrac{D_s^{eff}\cdot H}{\pi\cdot\tau_{outdoor}\cdot(\theta_w+K_s\cdot\rho_s+H\cdot\theta_a)}}\cdot 10^3 \\ VF_{ss}(2)=\dfrac{W'\cdot\rho_s\cdot d}{U_{air}\cdot\delta_{air}\cdot\tau_{outdoor}}\cdot 10^3 \qquad \text{(optional)} \end{cases}$$

Optional check

$$VF_{ss}(1)=\begin{cases} \dfrac{2\cdot W'\cdot\rho_s}{U_{air}\cdot\delta_{air}}\sqrt{\dfrac{D_s^{eff}\cdot H}{\pi\cdot\tau_{outdoor}\cdot(\theta_w+K_s\cdot\rho_s+H\cdot\theta_a)}}\cdot 10^3 & \text{for } L_{s(SS)}=0 \\ \dfrac{H\cdot\rho_s}{(\theta_w+K_s\cdot\rho_s+H\cdot\theta_a)\cdot\left(1+\dfrac{U_{air}\cdot\delta_{air}\cdot L_{s(SS)}}{D_s^{eff}\cdot W'}\right)}\cdot 10^3 & \text{for } L_{s(SS)}>0 \end{cases}$$

**Nomenclature**
*d = Thickness of surface soil source (cm)*
*$L_{s\,(SS)}$ = Depth to surface soil source (cm)*
*$D_s^{eff}$ = Effective diffusivity in the vadose zone ($cm^2/s$)*
*W' = Width of source area parallel to wind direction (cm)*
*$\delta_{air}$ = Ambient air mixing zone height (cm)*
*$U_{air}$ = Wind speed(cm/s)*
*$\tau_{outdoor}$ = Averaging time for vapor flux (s)*
*$\theta_w$ = Volumetric water content in the vadose zone (-)*
*$\theta_a$ = Volumetric air content in the vadose zone (-)*
*$\theta_e$ = Effective porosity in the vadose zone (-)*
*H = Henry's law constant (-)*
*$\rho_s$ = Soil bulk density ($g/cm^3$)*

**Table 4.12. Surface Soil: Particulate emission**

Outdoor air

$$PEF\left[\frac{mg/m^3_{air}}{mg/kg_{soil}}\right]=\frac{P_e\cdot W'}{U_{air}\cdot\delta_{air}}\cdot 10^3$$

Indoor air

$$PEF_{in}\left[\frac{mg/m^3_{air}}{mg/kg_{soil}}\right]=PEF\cdot F_i$$

**Nomenclature**
*W' = Width of source area parallel to wind direction (cm)*
*$\delta_{air}$ = Ambient air mixing zone height (cm)*
*$U_{air}$ = Wind speed(cm/s)*
*$P_e$ = Particulate emission rate ($g/cm^2/s$)*
*Fi = Particulate Indoor fraction (-)*

**Table 4.13. Surface Soil: Indoor vapor volatilization**

$$VF_{ssesp}\left[\frac{mg/m^3_{air}}{mg/kg_{soil}}\right]=\min\begin{cases}VF_{ssesp}(1)\\ VF_{ssesp}(2)=\dfrac{\rho_s\cdot d}{L_b\cdot ER\cdot\tau_{indoor}}10^3 \quad \text{(optional)}\end{cases}$$

No differential outdoor/indoor pressure (Δp=0)

$$VF_{ssesp}(1)=\frac{\dfrac{H\cdot\rho_s}{(\theta_w+K_s\cdot\rho_s+H\cdot\theta_a)}\cdot\dfrac{D_s^{eff}}{\left(L_{s(SS)}-Z_{crack}\right)\cdot L_b\cdot ER}}{1+\dfrac{D_s^{eff}}{\left(L_{s(SS)}-Z_{crack}\right)\cdot L_b\cdot ER}+\dfrac{D_s^{eff}L_{crack}}{D_{crack}^{eff}\cdot\eta\cdot\left(L_{s(SS)}-Z_{crack}\right)}}\cdot 10^3$$

Differential outdoor/indoor pressure (Δp≠0)

$$VF_{ssesp}(1)=\frac{\dfrac{H\cdot\rho_s}{(\theta_w+K_s\cdot\rho_s+H\cdot\theta_a)}\cdot\dfrac{D_s^{eff}}{\left(L_{s(SS)}-Z_{crack}\right)\cdot L_b\cdot ER}\cdot e^{\xi}}{e^{\xi}+\dfrac{D_s^{eff}}{\left(L_{s(SS)}-Z_{crack}\right)\cdot L_b\cdot ER}+\dfrac{D_s^{eff}\cdot A_b}{Q_s\cdot\left(L_{s(SS)}-Z_{crack}\right)}\cdot\left(e^{\xi}-1\right)}\cdot 10^3$$

Convective Air Flow Through Foundation Cracks, $Q_s$ ($cm^3/s$)

$$Q_s=\frac{2\pi\cdot\Delta p\cdot k_v\cdot X_{crack}}{\mu_{air}\cdot\ln\left(\dfrac{2\cdot Z_{crack}\cdot X_{crack}}{A_b\cdot\eta}\right)} \qquad \xi=\frac{Q_s\cdot L_{crack}}{D_{crack}^{eff}\cdot A_b\cdot\eta}$$

**Nomenclature**

*$L_{crack}$ = Thickness foundations (cm)*
*$L_b$ = Enclosed space volume/infiltration area ratio (cm)*
*$Z_{crack}$ = Depth to base of enclosed space foundation (cm)*
*$d$ = Thickness of surface soil source (cm)*
*$L_{s\ (SS)}$ = Depth to surface soil source (cm)*
*$D_s^{eff}$ = Effective diffusivity in the vadose zone ($cm^2/s$)*
*$D_{crack}^{eff}$ = Effective diffusivity in the foundations ($cm^2/s$)*
*$\tau_{indoor}$ = Averaging time for vapor flux (s)*
*$ER$ = Enclosed-space air exchange rate (1/s)*
*$\eta$ = Areal fraction of cracks in foundations/walls (-)*
*$\theta_w$ = Volumetric water content in the vadose zone (-)*
*$\theta_a$ = Volumetric air content in the vadose zone (-)*
*$\theta_e$ = Effective porosity in the vadose zone (-)*
*$H$ = Henry's law constant (-)*
*$\rho_s$ = Soil bulk density ($g/cm^3$)*
*$X_{crack}$ = Enclosed space foundation perimeter (cm)*
*$\Delta p$ = Differential indoor/outdoor air pressure ($g/cm^2/s$)*
*$k_v$ = Soil vapor permeability ($cm^2$)*
*$A_b$ = Area of building foundation ($cm^2$)*
*$\mu_{air}$ = Vapor Viscosity (g/cm/s)*

**Table 4.14. Surface Soil: Leaching Factor**

$$LF\left[\frac{mg/L_{wat}}{mg/kg_{soil}}\right] = \min\begin{cases} LF(1) = \dfrac{K_{ws}\cdot SAM}{LDF} \\ LF(2) = \dfrac{d\cdot\rho_s}{I_{eff}\cdot\tau_{LF}} \quad \text{(optional)} \end{cases}$$

Soil Attenuation model, SAM (-)

$$SAM = \frac{d}{L_{gw} - L_{s(SS)}} \quad \text{(opzionale)}$$

Dilution Factor, LDF (-)

$$LDF = 1 + \frac{v_{gw}\cdot\delta_{gw}}{I_{eff}\cdot W}$$

Partition Coefficient (kg/L)

$$K_{ws} = \frac{\rho_s}{\theta_w + K_s\cdot\rho_s + H\cdot\theta_a} \qquad K_s = \begin{cases} K_d & \text{inorganics} \\ K_{oc}\cdot f_{oc} & \text{organics} \end{cases}$$

Groundwater mixing zone thickness, $\delta_{gw}$ *(cm)*

$$\delta_{gw} = (2\cdot 0.0056\cdot W^2)^{0,5} + d_a\cdot\left[1-\exp\left(-\frac{W\cdot I_{eff}}{v_{gw}\cdot d_a}\right)\right] \qquad \text{for } \delta_{gw} > d_a \;\rightarrow\; \delta_{gw} = d_a$$

Infiltration Rate (Optional)

$$I_{eff} = \beta\cdot P^2\cdot\eta_{outdoor}$$

*Sandy Soils (Sand, Loamy Sand and SandyLoam) β =0.0018; SIlty Soils (Sandy Clay Loam, Loam, Silt Loam and Silt) β =0.0009; Clay Soils (Clay Loam, Silty Clay Loam, Silty Clay, Sandy Clay and Clay) β =0.00018.*

**Nomenclature**

*$d$ = Thickness of surface soil source (cm)*
*$L_{gw}$ = Depth to groundwater. (cm)*
*$L_{s\,(SS)}$ = Depth to surface soil source (cm)*
*$v_{gw}$= Groundwater Darcy velocity (cm/s)*
*$K_{sat}$= Hydraulic Conductivity (cm/s)*
*$I_{eff}$ = Infiltration Rate (cm/s)*
*$\tau_{LF}$ = Averaging time for leachate flux (s)*
*$\theta_w$ = Volumetric water content in the vadose zone (-)*
*$\theta_a$ = Volumetric air content in the vadose zone (-)*
*$\theta_e$ = Effective porosity in the vadose zone (-)*
*$H$ = Henry's law constant (-)*
*$\rho_s$ = Soil bulk density (g/cm$^3$)*
*$f_{oc}$ = Organic Carbon Fraction (-)*
*$d_a$ = Groundwater Thickness (cm)*
*$W$ = Width of source area parallel to groundwater flow direction (cm)*
*$\alpha_z$ = Vertical Dispersivity (cm)*

**Table 4.15. Air Dispersion**

$$ADF\left[\frac{mg/m^3_{air,offsite}}{mg/m^3_{air,onsite}}\right]=\frac{Q}{2\pi\cdot U_{air}\cdot\sigma_y\cdot\sigma_z}\cdot\left[2\cdot\exp\left(-\frac{1}{2}\frac{\delta_{air}{}^2}{\sigma_z{}^2}\right)\right]$$

Where Q [$cm^3/s$]:

$$Q=U_{air}\cdot\delta_{air}\cdot S_w$$

**Nomenclature**

$S_w$ = *Width of source area orthogonal to wind direction* (cm)
$\delta_{air}$ = *Ambient air mixing zone height* (cm)
$U_{air}$ = *Wind Speed (cm/s)*
$\sigma_y$ = *Transverse air dispersion coefficient* (cm)
$\sigma_z$ = *Vertical air dispersion coefficient* (cm)

**Table 4.16. Subsurface Soil: Outdoor vapor volatilization**

$$VF_{samb}\left[\frac{mg/m^3_{air}}{mg/kg_{soil}}\right]=\min\begin{cases}VF_{samb}(1)=\dfrac{H\cdot\rho_s}{(\theta_w+K_s\cdot\rho_s+H\cdot\theta_a)\cdot\left(1+\dfrac{U_{air}\cdot\delta_{air}\cdot L_{s(SP)}}{D_s^{eff}\cdot W'}\right)}\cdot 10^3\\ VF_{samb}(2)=\dfrac{W'\cdot\rho_s\cdot d_s}{U_{air}\cdot\delta_{air}\cdot\tau_{outdoor}}\cdot 10^3 \quad \text{(optional)}\end{cases}$$

**Nomenclature**

$d_s$= *Thickness of subsurface soil source (cm)*
$L_{s\,(SP)}$ = *Depth to subsurface soil source (cm)*
$D_s^{eff}$ = *Effective diffusivity in the vadose zone* ($cm^2/s$)
$W'$ = *Width of source area parallel to wind direction (cm)*
$\delta_{air}$ = *Ambient air mixing zone height (cm)*
$U_{air}$ = *Wind speed(cm/s)*
$\tau_{outdoor}$ = *Averaging time for vapor flux (s)*
$\theta_w$ = *Volumetric water content in the vadose zone (-)*
$\theta_a$ = *Volumetric air content in the vadose zone (-)*
$\theta_e$ = *Effective porosity in the vadose zone (-)*
$H$ = *Henry's law constant (-)*
$\rho_s$ = *Soil bulk density* ($g/cm^3$)

**Table 4.17. Subsurface Soil: Indoor vapor volatilization**

$$VF_{sesp}\left[\frac{mg/m^3_{air}}{mg/kg_{soil}}\right]=\min\begin{cases}VF_{sesp}(1)\\ VF_{sesp}(2)=\dfrac{\rho_s\cdot d_s}{L_b\cdot ER\cdot\tau_{indoor}}10^3 \quad \text{(optional)}\end{cases}$$

No differential outdoor/indoor pressure (Δp=0)

$$VF_{sesp}(1)=\frac{\dfrac{H\cdot\rho_s}{(\theta_w+K_s\cdot\rho_s+H\cdot\theta_a)}\cdot\dfrac{D_s^{eff}}{\left(L_{s(SP)}-Z_{crack}\right)\cdot L_b\cdot ER}}{1+\dfrac{D_s^{eff}}{\left(L_{s(SP)}-Z_{crack}\right)\cdot L_b\cdot ER}+\dfrac{D_s^{eff}L_{crack}}{D_{crack}^{eff}\cdot\eta\cdot\left(L_{s(SP)}-Z_{crack}\right)}}\cdot 10^3$$

Differential outdoor/indoor pressure (Δp≠0)

$$VF_{sesp}(1)=\frac{\dfrac{H\cdot\rho_s}{(\theta_w+K_s\cdot\rho_s+H\cdot\theta_a)}\cdot\dfrac{D_s^{eff}}{\left(L_{s(SP)}-Z_{crack}\right)\cdot L_b\cdot ER}\cdot e^{\xi}}{e^{\xi}+\dfrac{D_s^{eff}}{\left(L_{s(SP)}-Z_{crack}\right)\cdot L_b\cdot ER}+\dfrac{D_s^{eff}\cdot A_b}{Q_s\cdot\left(L_{s(SP)}-Z_{crack}\right)}\cdot\left(e^{\xi}-1\right)}\cdot 10^3$$

Convective Air Flow Through Foundation Cracks, $Q_s$ ($cm^3/s$)

$$Q_s=\frac{2\pi\cdot\Delta p\cdot k_v\cdot X_{crack}}{\mu_{air}\cdot\ln\left(\dfrac{2\cdot Z_{crack}\cdot X_{crack}}{A_b\cdot\eta}\right)} \qquad \xi=\frac{Q_s\cdot L_{crack}}{D_{crack}^{eff}\cdot A_b\cdot\eta}$$

**Nomenclature**

*$L_{crack}$ = Thickness foundations (cm)*
*$L_b$ = Enclosed space volume/infiltration area ratio (cm)*
*$Z_{crack}$ = Depth to base of enclosed space foundation (cm)*
*$d_s$ = Thickness of subsurface soil source (cm)*
*$L_{s\ (SP)}$ = Depth to subsurface soil source (cm)*
*$D_s^{eff}$ = Effective diffusivity in the vadose zone ($cm^2/s$)*
*$D_{crack}^{eff}$ = Effective diffusivity in the foundations ($cm^2/s$)*
*$\tau_{indoor}$ = Averaging time for vapor flux (s)*
*ER = Enclosed-space air exchange rate (1/s)*
*$\eta$ = Areal fraction of cracks in foundations/walls (-)*
*$\theta_w$ = Volumetric water content in the vadose zone (-)*
*$\theta_a$ = Volumetric air content in the vadose zone (-)*
*$\theta_e$ = Effective porosity in the vadose zone (-)*
*H = Henry's law constant (-)*
*$\rho_s$ = Soil bulk density ($g/cm^3$)*
*$X_{crack}$ = Enclosed space foundation perimeter (cm)*
*$\Delta p$ = Differential indoor/outdoor air pressure ($g/cm^2/s$)*
*$k_v$ = Soil vapor permeability ($cm^2$)*
*$A_b$ = Area of building foundation ($cm^2$)*
*$\mu_{air}$ = Vapor Viscosity (g/cm/s)*

**Table 4.18. Subsurface Soil: Leaching Factor**

$$LF_{sp}\left[\frac{mg/L_{wat}}{mg/kg_{soil}}\right]=\min\begin{cases}LF_{sp}(1)=\dfrac{K_{ws}\cdot SAM}{LDF}\\ LF_{sp}(2)=\dfrac{d_s\cdot\rho_s}{I_{eff}\cdot\tau_{LF}}\end{cases}\qquad\text{(optional)}$$

Soil Attenuation model, SAM (-)

$$SAM=\frac{d_s}{L_{gw}-L_{s(SP)}}\qquad\text{(optional)}$$

Dilution Factor, LDF (-)

$$LDF=1+\frac{v_{gw}\cdot\delta_{gw}}{I_{eff}\cdot W}$$

Partition Coefficient (kg/L)

$$K_{ws}=\frac{\rho_s}{\theta_w+K_s\cdot\rho_s+H\cdot\theta_a}\qquad\qquad K_s=\begin{cases}K_d & \text{inorganics}\\ K_{oc}\cdot f_{oc} & \text{organics}\end{cases}$$

Groundwater mixing zone thickness, $\delta_{gw}$ *(cm)*

$$\delta_{gw}=(2\cdot 0.0056\cdot W^2)^{0,5}+d_a\cdot\left[1-\exp\left(-\frac{W\cdot I_{eff}}{v_{gw}\cdot d_a}\right)\right]\qquad\text{for }\delta_{gw}>d_a\ \rightarrow\ \delta_{gw}=d_a$$

Infiltration Rate

$$I_{eff}=\beta\cdot P^2\cdot\eta_{outdoor}$$

*Sandy Soils (Sand, Loamy Sand and SandyLoam) β =0.0018; SIlty Soils (Sandy Clay Loam, Loam, Silt Loam and Silt) β =0.0009; Clay Soils (Clay Loam, Silty Clay Loam, Silty Clay, Sandy Clay and Clay) β =0.00018.*

**Nomenclature**

*$d_s$ = Thickness of subsurface soil source (cm)*
*$L_{gw}$ = Depth to groundwater (cm)*
*$L_{s\,(SP)}$ = Depth to subsurface soil source (cm)*
*$v_{gw}$= Groundwater Darcy velocity (cm/s)*
*$K_{sat}$= Hydraulic Conductivity (cm/s)*
*$I_{eff}$ = Infiltration Rate (cm/s)*
*$\tau_{LF}$ = Averaging time for leachate flux (s)*
*$\theta_w$ = Volumetric water content in the vadose zone (-)*
*$\theta_a$ = Volumetric air content in the vadose zone (-)*
*$\theta_e$ = Effective porosity in the vadose zone (-)*
*H = Henry's law constant (-)*
*$\rho_s$ = Soil bulk density ($g/cm^3$)*
*$f_{oc}$ = Organic Carbon Fraction (-)*
*$d_a$ = Groundwater Thickness (cm)*
*W = Width of source area parallel to groundwater flow direction (cm)*
*$\alpha_z$ = Vertical Dispersivity (cm)*

**Table 4.19. Groundwater Attenuation Factor**

***DAF1 (-)***

$$\frac{1}{DAF1} = \exp\left[\frac{x}{2\cdot\alpha_x}\left(1-\sqrt{1+\frac{4\cdot\lambda\cdot\alpha_x\cdot R}{v_e}}\right)\right]\cdot\left[erf\left(\frac{S_w}{4\sqrt{\alpha_y\cdot x}}\right)\right]\cdot\left[erf\left(\frac{\delta_{gw}}{4\sqrt{\alpha_z\cdot x}}\right)\right]$$

***DAF2 (-)***

$$\frac{1}{DAF2} = \exp\left[\frac{x}{2\cdot\alpha_x}\left(1-\sqrt{1+\frac{4\cdot\lambda\cdot\alpha_x\cdot R}{v_e}}\right)\right]\cdot\left[erf\left(\frac{S_w}{4\sqrt{\alpha_y\cdot x}}\right)\right]\cdot\left[erf\left(\frac{\delta_{gw}}{2\sqrt{\alpha_z\cdot x}}\right)\right]$$

***DAF3(-)***

$$\frac{1}{DAF3} = \exp\left[\frac{x}{2\cdot\alpha_x}\left(1-\sqrt{1+\frac{4\cdot\lambda\cdot\alpha_x\cdot R}{v_e}}\right)\right]\cdot\left[erf\left(\frac{S_w}{4\sqrt{\alpha_y\cdot x}}\right)\right]$$

Effective groundwater velocity, $v_e$ (cm/s)

$$v_e = \frac{K_{sat}\cdot i}{\theta_{e,sat}}$$

Constituent retardation factor, R (-)

$$R = 1 + K_s\frac{\rho_s}{\theta_{e,sat}}$$

Longitudinal Dispersivity, $\alpha_x$ (cm)

$$\alpha_x = POC/10$$

Transversal Dispersivity, $\alpha_y$ (cm)

$$\alpha_y = \alpha_x/3$$

Vertical Dispersivity, $\alpha_z$ (cm)

$$\alpha_z = \alpha_x/20$$

***Nomenclature***

*$\lambda$ = First-order degradation rate (1/s)*
*$S_w$ = Width of source area orthogonal to groundwater flow (cm)*
*$\delta_{gw}$ = Groundwater mixing zone thickness (cm)*
*x = distance(cm)*
*$K_s$ = Soil-water sorption coefficient (mg/kg/mg/L)*
*$\theta_{e,sat}$ = Effective porosity, saturated zone (-)*
*$\rho_s$ = Soil bulk density (g/cm$^3$)*
*i = Hydraulic gradient (-)*
*$K_{sat}$ = Hydraulic conductivity(cm/s)*
*POC = Distance to groundwater recptor (cm)*

**Table 4.20. Groundwater: Indoor Vapors Volatilization**

No differential outdoor/indoor pressure (Δp=0)

$$VF_{wesp}\left[\frac{mg/m^3_{air}}{mg/L_{water}}\right]=\frac{H\cdot\dfrac{D_w^{eff}}{\left(L_{gw}-Z_{crack}\right)L_b\cdot ER}}{1+\dfrac{D_w^{eff}}{\left(L_{gw}-Z_{crack}\right)L_b\cdot ER}+\dfrac{D_w^{eff}\cdot L_{crack}}{D_{crack}^{eff}\left(L_{gw}-Z_{crack}\right)\eta}}\cdot 10^3$$

Differential outdoor/indoor pressure (Δp=0)

$$VF_{wesp}\left[\frac{mg/m^3_{air}}{mg/L_{water}}\right]=\frac{H\cdot\dfrac{D_w^{eff}}{\left(L_{gw}-Z_{crack}\right)L_b\cdot ER}\cdot e^{\xi}}{e^{\xi}+\dfrac{D_w^{eff}}{\left(L_{gw}-Z_{crack}\right)L_b\cdot ER}+\dfrac{D_w^{eff}\cdot A_b}{Q_s\cdot\left(L_{gw}-Z_{crack}\right)}\cdot(e^{\xi}-1)}\cdot 10^3$$

Convective Air Flow Through Foundation Cracks, $Q_s$ ($cm^3/s$)

$$Q_s=\frac{2\pi\cdot\Delta p\cdot k_v\cdot X_{crack}}{\mu_{air}\cdot\ln\left(\dfrac{2\cdot Z_{crack}\cdot X_{crack}}{A_b\cdot\eta}\right)}\qquad \xi=\frac{Q_s\cdot L_{crack}}{D_{crack}^{eff}\cdot A_b\cdot\eta}$$

**Nomenclature**

*$L_{crack}$ = Thickness foundations (cm)*
*$L_b$ = Enclosed space volume/infiltration area ratio (cm)*
*$Z_{crack}$ = Depth to base of enclosed space foundation (cm)*
*$L_{gw}$ = Depth to groundwater (cm)*
*$D_w^{eff}$ = Effective diffusivity from groundwater ($cm^2/s$)*
*$D_{crack}^{eff}$ = Effective diffusivity in the foundations ($cm^{2/}s$)*
*$\tau_{indoor}$ = Averaging time for vapor flux (s)*
*ER = Enclosed-space air exchange rate (1/s)*
*$\eta$ = Areal fraction of cracks in foundations/walls (-)*
*$\theta_w$ = Volumetric water content in the vadose zone (-)*
*$\theta_a$ = Volumetric air content in the vadose zone (-)*
*$\theta_e$ = Effective porosity in the vadose zone (-)*
*H = Henry's law constant (-)*
*$\rho_s$ = Soil bulk density ($g/cm^3$)*
*$X_{crack}$ = Enclosed space foundation perimeter (cm)*
*$\Delta p$ = Differential indoor/outdoor air pressure ($g/cm^2/s$)*
*$k_v$ = Soil vapor permeability ($cm^2$)*
*$A_b$ = Area of building foundation ($cm^2$)*
*$\mu_{air}$ = Vapor Viscosity (g/cm/s)*

**Table 4.21. Groundwater: Outdoor Vapors Volatilization**

$$VF_{wamb}\left[\frac{mg/m^3_{air}}{mg/L_{wat}}\right]=\frac{H}{1+\frac{U_{air}\cdot\delta_{air}\cdot L_{gw}}{D_w^{eff}\cdot W'}}\cdot 10^3$$

**Nomenclature**

*$L_{gw}$= Depth to Groundwater cm)*
*$D_w^{eff}$= Effective diffusivity from groundwater ($cm^2/s$)*
*W' = Width of source area parallel to wind direction (cm)*
*$\delta_{air}$ = Ambient air mixing zone height (cm)*
*$U_{air}$ = Wind speed(cm/s)*
*H = Henry's law constant (-)*

**Table 4.22. Diffusion Coefficient**

Diffusion Coefficient in the vadose zone

$$D_s^{eff}\left[\frac{cm^2}{s}\right]=\frac{D_a\cdot\theta_a^{3,33}}{\theta_e^{\,2}}+\frac{D_w\cdot\theta_w^{3,33}}{H\cdot\theta_e^{\,2}}$$

Diffusion Coefficient in the capillary fringe

$$D_{cap}^{eff}\left[\frac{cm^2}{s}\right]=\frac{D_a\cdot\theta_{acap}^{3,33}}{\theta_{e,cap}^{\,2}}+\frac{D_w\cdot\theta_{wcap}^{3,33}}{H\cdot\theta_{e,cap}^{\,2}}$$

Diffusion Coefficient in the foundations

$$D_{crack}^{eff}\left[\frac{cm^2}{s}\right]=\frac{D_a\cdot\theta_{acrack}^{3,33}}{\theta_{e,crack}^{\,2}}+\frac{D_w\cdot\theta_{wcrack}^{3,33}}{H\cdot\theta_{e,crack}^{\,2}}$$

Diffusion Coefficient from groundwater

$$D_w^{eff}\left[\frac{cm^2}{s}\right]=\frac{h_{cap}+h_v}{\frac{h_{cap}}{D_{cap}^{eff}}+\frac{h_v}{D_s^{eff}}}$$

***Nomenclature***

*$h_{cap}$ = Capillary fringe thickness (cm)*
*$h_v$ = Vadose zone thickness (cm)*
*$D_a$ = Diffusion coefficient in air ($cm^2/s$)*
*$D_w$ = Diffusion coefficient in water ($cm^2/s$)*
*$\theta_w$ = Volumetric water content in the vadose zone (-)*
*$\theta_a$ = Volumetric air content in the vadose zone (-)*
*$\theta_{wcap}$ = Volumetric water content in the capillary fringe (-)*
*$\theta_{acap}$ = Volumetric air content in the capillary fringe (-)*
*$\theta_{wcrack}$ = Volumetric water content in the foundations (-)*
*$\theta_{acrack}$ = Volumetric air content in the foundations (-)*
*$\theta_e$ = Effective Porosity in the vadose zone (-)*
*$\theta_{e,cap}$ = Effective Porosity in the capillary fringe (-)*
*$\theta_{e,crack}$ = Effective Porosity in the foundations (-)*
*H = Henry's law constant (-)*
*$\rho_s$ = Soil bulk density ($g/cm^3$)*

**Table 4.23. Saturation Concentration, $C_{sat}$**

Saturation Concentration

$$C_{sat}\left[mg/m^3\right]=\frac{\theta_w+H\cdot\theta_a+\rho_s\cdot K_s}{\rho_s}\cdot S$$

***Nomenclature***

*$\theta_w$ = Volumetric water content in the vadose zone (-)*
*$\theta_a$ = Volumetric air content in the vadose zone (-)*
*S = Solubility (mg/L)*
*H = Henry's law constant (-)*
*$\rho_s$ = Soil bulk density ($g/cm^3$)*

## MODELING PROCEDURES: INTAKE RATES

The exposure factors are used to describe the expected behavior for the different receptors within or near the site. Namely these models allow to calculate the average ingested or inhaled dose over the lifetime of the receptor.

The exposure pathways considered in the software are:

- Dermal contact with soil
- Ingestion of soil
- Inhalation of vapors in outdoor environments
- Inhalation of vapors in indoor environments
- Inhalation of particulate matter in outdoor environments
- Inhalation of particulate matter in indoor environments
- Inhalation of particulate matter in outdoor environments
- Inhalation of particulate matter in indoor environments
- Ingestion of water

The types of receptors considered are:

*Residential or Recreational Scenario*

- Child
- Adult
- Exposure Mediated (Adult + Child)

*Commercial or Industrial Scenario*

- Adult Worker

For the residential or recreation exposure scenarios, the software can calculate an average exposure value among the child and adult values in order to adjust for varying body weights, exposure durations, skin areas:

$$EM_{adj} = \begin{cases} EM_{child} + EM_{adult} & \text{carcinogenic contaminants} \\ EM_{child} & \text{non-carcinogenic contaminants} \end{cases} \quad (4.15)$$

Where $EM_{child}$ and $EM_{adult}$ are the intake rates calculated considering the parameters of exposure of a child and an adult, respectively.

**Table 4.24. Intake rates**

**Dermal Contact**

$$EM\left[\frac{mg}{kg\times day}\right]=\frac{SA\cdot AF\cdot ABS\cdot EF\cdot ED}{BW\cdot AT\cdot 365\ \frac{days}{year}}$$

BW = Body weight (kg)
EF = Exposure frequency (d/year)
ED = Exposure Duration (years)
AT = Averaging time (years) (*)
SA = Skin Surface Area ($cm^2$)
AF = Soil Dermal adherence factor (mg/($cm^2$ d)
ABS = Dermal adsorption factor (-)

**Soil ingestion**

$$EM\left[\frac{mg}{kg\times day}\right]=\frac{IR\cdot FI\cdot EF\cdot ED}{BW\cdot AT\cdot 365\ \frac{days}{year}}$$

BW = Body weight (kg)
EF = Exposure frequency (d/year)
ED = Exposure Duration (years)
AT = Averaging time (years) (*)
IR = Soil Ingestion rate (mg/ d)
FI = Soil ingestion fraction (-)

**Outdoor Vapors and Dust Inhalation**

$$EM\left[\frac{m^3}{kg\times day}\right]=\frac{B_o\cdot EF_{go}\cdot EF\cdot ED}{BW\cdot AT\cdot 365\ \frac{days}{year}}$$

BW = Body weight (kg)
EF = Exposure frequency (d/year)
ED = Exposure Duration (years)
AT = Averaging time (years) (*)
$EF_{go}$ = Daily Outdoor Exposure frequency (h/d)
$B_o$ = Outdoor Inhalation rate ($m^3$/h)

**Indoor Vapors and Dust Inhalation**

$$EM\left[\frac{m^3}{kg\times day}\right]=\frac{B_i\cdot EF_{gi}\cdot EF\cdot ED}{BW\cdot AT\cdot 365\ \frac{days}{year}}$$

BW = Body weight (kg)
EF = Exposure frequency (d/year)
ED = Exposure Duration (years)
AT = Averaging time (years) (*)
$EF_{gi}$ = Daily Indoor Exposure frequency (h/d)
$B_i$ = Indoor Inhalation rate ($m^3$/h)

**Water Ingestion (optional)**

$$EM\left[\frac{L}{kg\times day}\right]=\frac{IR_w\cdot EF\cdot ED}{BW\cdot AT\cdot 365\ \frac{days}{year}}$$

BW = Body weight (kg)
EF = Exposure frequency (d/year)
ED = Exposure Duration (years)
AT = Averaging time (years) (*)
$IR_w$ = Water Ingestion rate (L/d)

(*) For non-carcinogenic contaminants AT = ED

# CONCLUSIONS AND FINAL REMARKS

Risk assessment is a useful and widely applied tool for the management of contaminated sites, since it provides a rational and objective starting point for priority setting and decision making. Its application in most advanced countries has been prompted by the application of the Risk-Based Corrective Action (RBCA) framework, based on the corresponding ASTM standards.

Despite this, the experience and the increasing knowledge of the different natural processes taking place in the subsurface, gained over the years, have highlighted some critical issues of the RBCA application to contaminated sites. In particular, it is well known, that the ASTM fate and transport models result in many cases too simplified since they neglect several attenuation processes occurring in the subsurface that several experimental and field studies in the last decades have shown to be particularly relevant. These processes, acting without human intervention, can in fact lead to a significant reduction of the mass, toxicity, mobility, volume and concentrations of contaminants. The main focus of this Ph.D. thesis was to analyze these problems and provide, where possible, alternative solutions. Namely, the main topics addressed were the fate and transport models and the software used for the application of the Tier 2 RBCA planning process, which is the approach adopted in Italy for the definition of the site-specific clean up goals. To this aim different alternative modeling approaches accounting for the key natural attenuation processes occurring in the subsurface, while keeping the analytical form required for the RBCA Tier 2 application, were developed and applied to different contamination scenarios. In addition a new software, called Risk-net, designed to complete all calculations required for the ISPRA (2008) planning process, was developed.

The obtained results are briefly discussed below.

## VAPOR INTRUSION INTO INDOOR ENVIRONMENTS

Natural attenuation processes can be particularly effective in attenuating petroleum hydrocarbon vapors, either from groundwater or unsaturated soil sources. Nevertheless, most risk assessment procedures, such as the Johnson and Ettinger (1991) model, do not include vapor attenuation as a standard feature for developing clean-up levels. This assumption can lead to an overestimation of the overall human health risk, since vapor intrusion to indoor air is one of the most important exposure pathways at many contaminated sites impacted by volatile compounds.

To overcome this limitation, in this work, an analytical steady state vapor intrusion model including both anaerobic and oxygen-limited aerobic biodegradation was developed. The aerobic and anaerobic layer thickness are calculated by stoichiometrically coupling the reactive transport of vapors with oxygen transport and consumption. The model accounts for the different oxygen demand in the subsurface required to sustain the aerobic biodegradation of the compound(s) of concern and for the baseline soil oxygen respiration. In the case of anaerobic reaction under methanogenic conditions, the model accounts for the generation of methane which leads to a further oxygen demand, due to methane oxidation, in the aerobic zone. The model was solved analytically and applied, using representative parameter ranges and values, to identify under which site conditions the attenuation of hydrocarbons migrating into indoor environments is likely to be significant. Namely the simulations were performed assuming a soil contaminated by toluene only, by a BTEX mixture, by Fresh Gasoline and by Weathered Gasoline.

The obtained results suggest that for many scenarios, aerobic biodegradation is expected to be the main attenuation mechanism. This is due to the fact that the kinetic rates for aerobic biodegradation are generally much faster than anaerobic processes (up to 2 orders of magnitude). However, in cases where aerobic biodegradation results limited by the oxygen availability (e.g. for high source concentrations) anaerobic biodegradation may contribute significantly with increased attenuation up to one order of magnitude. The results have shown that anaerobic biodegradation can affect the attenuation of vapors in two ways: on the one hand by degrading the contaminants in the anaerobic zone and on the other hand by reducing the upward contaminant flux with

a consequent downward extension of the aerobic zone which leads to an enhancement of the aerobic biodegradation pathway. Generally, the second contribution appears to be the most important. This effect results more limited when anaerobic biodegradation occurs under methanogenic conditions. In this case the generation of methane leads to an increase in oxygen consumption, due to methane oxidation, with a consequent reduction of the layer thickness where aerobic biodegradation occurs.

The simulations have also shown that the attenuation due to biodegradation is strongly influenced by site-specific conditions. The main parameters investigated, which showed a strong influence on transport and consumption of vapors and oxygen in the subsurface, are the biodegradation constants, the source concentration, the cracks fraction of the building, the building area, the building pressure gradient, the source depth and the presence of more biodegradable substances in the subsoil.

## EXPOSURE DURATION TO CONTAMINATED GROUNDWATER

The present work was focused on the approach provided in the risk-assessment procedures for on-site receptors exposed to contaminated groundwater. In the ASTM-RBCA standard procedure, migration of contaminants is described through simple analytical models and the source contaminants concentration is supposed to be constant throughout the entire exposure period, i.e. 25-30 years. The latter assumption may often result over-protective of human health, leading to unrealistically low remediation goals. The aim of this work was to propose an alternative model taking in account the source depletion, while keeping the original simplicity and analytical form of the ASTM-RBCA approach. The results obtained by the application of this model were compared with those provided by the traditional ASTM-RBCA approach, by a model based on the source depletion algorithm of the RBCA ToolKit software and by a numerical model, allowing to assess its feasibility for inclusion in risk analysis procedures. The comparison with the output of the numerical model FEFLOW showed that the ASTM approach may lead, for some types of constituents and soils, to extremely conservative results in terms of risk. On the contrary, the developed Exposure-Duration model has provided more realistic results with respect to the ASTM-RBCA approach and is easier to apply and slightly more conservative than the RBCA ToolKit and the numerical one.

It is worth noting that the results discussed in this work were limited to on-site exposure to contaminated water by ingestion, but the approach proposed can be extended to other exposure pathways.

## LEACHING OF DISSOLVED PLUMES TO GROUNDWATER

Contamination of soils by petroleum products due to leaking underground storage tanks, accidental spills or improper surface applications is a widespread environmental problem. When the volume of spilled product is small, the hydrocarbon may be retained in an immobile condition in the unsaturated zone by capillary forces with the source zones generating a dissolved-phase, which may lead to a long term risk to groundwater due to gradually plume leach by infiltrating water. Whereas a significant volume spill of Nonaqueous Phase Liquids (DNAPL or LNAPL) may take hours to days to reach a water table, a dissolved plume leached from a shallow source may require years to decades. In this time framework if natural attenuation processes are significant, leached plumes may never reach groundwater, or else be substantially delayed with reduced concentrations (Rivett et al. 2011). To address this concept, this work was focused to assess the relevance of the different attenuation processes occurring during the transport in the unsaturated zone of dissolved organic compounds plumes leached from non-NAPL source zones. To this end, an analytical model accounting for source depletion and biodegradation, dispersion and diffusion during leaching was developed. In order to identify the general behavior rules depending on the site specific conditions and on the physical properties of the contaminants, the developed model was applied to several contamination scenarios. The obtained results suggest that BTEX are likely to be attenuated in the source due to their ready biodegradation (assuming biodegradation constant rates in the order of 0.01 - 1 $d^{-1}$) and mobility, whereas a minor relevance of the attenuation is expected to occur during transport, as these compounds generally migrate quite rapidly and consequently the time available for biodegradation to take place before reaching the aquifer is generally low. On the contrary, heavier compounds such as PAHs, that are more persistent in the vadose zone, can be attenuated during transport since the residence time in the subsurface can reach in some cases up to thousands of years. In this time framework, even with relatively slow biodegradation

(e.g. in the order of 0.0001 – 0.001 $d^{-1}$), attenuation can result significant. These results suggest that the ASTM model used in the risk assessment procedure, which neglects both these processes, can lead to an overall overestimation of the concentration reaching the groundwater and consequently of the risk calculated for the downstream receptor.

## RISK-NET

For the calculation of the RBCA procedure several software packages are available. The most commonly used in Italy, which have been validated in the ISPRA guidelines (2008), are the RBCA Tool Kit, the BP-RISC and Giuditta. However, as highlighted in the ISPRA document (2008), such softwares do not allow the full implementation of the risk analysis procedure defined in these guidelines according to the Italian law.

Thus in this work a new software (called Risk-net), designed to complete all calculations required for the ISPRA (2008) planning process, was developed. Risk-net was developed by the Department of Civil Engineering of the University of Rome "Tor Vergata" and validated by the Reconnet network. The software allows to apply the risk assessment procedure both in forward and backward mode, thus evaluating the risk or the clean-up objective for a contaminated site, respectively.

The program uses a simple and user-friendly graphical interface through which the user can simply define the different input parameters. To accelerate the compiling process, according to the conceptual model defined by the user, only the data actually used in the calculation are required. Some controls also allow to manage the presence of conceptual and numerical errors. The results are returned in terms of risk (for human health and groundwater resources) and remediation targets (Threshold Risk Concentrations, CSR). Intermediate outputs are also displayed allowing the user, to evaluate more critically the obtained results. The main features of Risk-net concern the possibility to use the program to perform analysis for the evaluation of the mobility of free product in the subsoil, the identification and visualization of contaminants distribution in the different phases of the soil (saturated and unsaturated), the presence of different receptors within (on-site) or near the site (off-site), the temporal and spatial evolution of the contamination in the aquifer and the calculation of clean-up levels for hydrocarbons

(Hydrocarbons C <12, Hydrocarbon C> 12 and Total Hydrocarbons) as a function of the different classes MADEP identified by the user.
The software can be downloaded for free from the website of the Reconnet network: www.reconnet.net.

## FINAL REMARKS

In conclusion, this study provided some new insight on the relevance of the different key natural attenuation processes usually taking place in the subsurface and highlighted for which contamination scenarios their inclusion as a standard feature for derivation of the site-specific clean up goals could provide a more realistic risk assessment. Namely, the obtained results showed that in many cases the standard ASTM-RBCA approach may lead, for some types of constituents and site-specific conditions, to extremely conservative results in terms of risk and consequently of site-specific clean-up goals. On the contrary, the different modeling approaches developed have provided more realistic and less conservative results with respect to the current ASTM procedure and thus may represent a simple but meaningful integration of the traditional RBCA approach, since they keep its original simplicity, but allow to overcome its limitations in correctly estimating risk for specific site conditions.
Finally, the developed software Risk-net, integrally based on the ISPRA guidelines for risk assessment and validated by the Reconnet network, may represent a useful tool for the suitable application of the risk-based approach to contaminated sites adopted in Italy. In this view, the different modeling approaches developed in this Ph.D. thesis, could be implemented in this software, allowing to develop an advanced integrated risk management approach.

# PUBLICATIONS, SUPPORTING DOCUMENTATION AND TOOLS

***Publications***

- Baciocchi R., Berardi S., Verginelli I. (2010). Human Health Risk Assessment: models for predicting the Effective Exposure Duration of On-Site Receptors Exposed to Contaminated Groundwater. Journal of Hazardous Materials 181(1–3), 226–233.

- Verginelli I., Grillo G., Massetti F., Sordini E. (2010). Limiti Tabellari e Analisi di Rischio nella Gestione dei Siti Contaminati. RS, Rifiuti Solidi 5, 327-338. CIPA Editore.

- Verginelli I., R. Baciocchi (2011). Modeling of vapor intrusion from hydrocarbon-contaminated sources accounting for aerobic and anaerobic biodegradation. Journal of Contaminant Hydrology 126 (3–4), 167–180.

- Baciocchi R., Berardi S., Forni A., Sconocchia A., Traversa A., Verginelli I., Villani I. (2012). Descrizione e validazione del nuovo software di Analisi di Rischio Risk-net. ECO, tecnologie per l'ambiente bonifiche e rifiuti, 18, 30-33. DEA Edizioni.

- Pantini S., Lombardi F., Verginelli I. (2012). Water-Balance Model For Predicting The Leachate Production In Landfills. Submitted to the International Journal of Environmental Science and Technology.

- Verginelli I., Baciocchi R. Role of natural attenuation in modeling the leaching of contaminants in the risk analysis framework. Submitted to the Journal of Environmental Management.

***Proceedings and workshops***

- Baciocchi R., Berardi S., D'Aprile L., Scozza E., Verginelli I. (2008). Validation of transport factors equations in Tier II risk analysis. Proceedings of the 10th FKZ/TNO conference on contaminated soils (ConSoil). Milan (Italy), June 2008.

- Baciocchi R., Berardi S., D'Aprile L., Scozza E., Verginelli I. (2008). Confronto fra modelli numerici e fattori di trasporto usati nell'Analisi di Rischio di livello 2. Proceedings of the International symposium of sanitary and environmental engineering (SIDISA 08). Florence (Italy), June 2008.

- Sordini E., Verginelli I. (2009). Criticità nella procedura di Analisi di Rischio. Research center of eni. Monterotondo (Italy), March 2009.

- Verginelli I., Baciocchi R., Grillo G., Sordini E. (2009). The applicability of natural attenuation to vapour intrusion risk assessment. Contaminated Site Management in Europe conference. Gent (Belgium), October 2009.

- Verginelli I., Baciocchi R., Grillo G., Massetti F., Sordini E. (2010). Modeling of vapor intrusion from contaminated soil and groundwater accounting for aerobic biodegradation. Proceedings of the 11th FKZ/TNO conference on contaminated soils (ConSoil). Salzburg (Austria), September 2010.

- Verginelli I., Berardi S. (2010). La procedura di analisi di rischio e software applicativi. "Settimana Ambiente 2010" conference. Milan (Italy), March 2010.

- Verginelli I. (2010). Modellizzazione della biodegradazione aerobica durante la migrazione di BTEX verso ambienti confinati. ISPRA Workshop "Valutazione del rischio da intrusione di vapori nei siti contaminati". Rome (Italy), July 2010.

- Baciocchi R. Cleriti G., Verginelli I., Innocenti I., Nardella A. (2010). Design criteria for In Situ Chemical Oxidation application. Proceedings of the X Symposium of environmental and sanitary engineering (SIBESA). Maceió (Brazil), March 2010.

- Verginelli I. (2011). Il software di Analisi di Rischio "Risk-net". Proceedings of the "Remediation Technologies conference" (REMTECH 2011). Ferrara (Italy), September 2011.

- Verginelli I., Baciocchi R. (2011). Analisi delle criticità della procedura di Analisi di Rischio mediante il software Risk-net. Proceedings of the "Remediation Technologies conference" (REMTECH). Ferrara (Italy), September 2011.

- Di Lonardo M.C., Lombardi F., Pantini S., Verginelli I., Sirini P., Ermolli F. (2011). Modeling the water-balance of sanitary landfills: a case study. Proceedings of the 13th International Waste Management and Landfill Symposium (Sardinia 2011). S. Margherita di Pula (Italy), October 2011.

- Di Lonardo M.C., Lombardi F., Pantini S., Verginelli I., Sirini P., Ermolli F. (2011). Applicazione ad un caso reale di un modello per la stima della produzione del percolato in discarica. Proceedings of the 13th International Waste Management and Landfill Symposium (Sardinia 2011). S. Margherita di Pula (Italy), October 2011.

- Verginelli I. (2011). Il nuovo software di Analisi di Rischio "Risk-net". Workshop "Analisi di Rischio", Unione Petrolifera. Rome (Italy), October 2011.

- Innocenti I., Massetti F., Porcelli F., Baciocchi R., Verginelli I., D'Aprile L. (2011). Results of a Pilot-Scale ISCO Treatment of a Former Refinery Site. Contaminated Site Management in Europe conference. Gent (Belgium), October 2011.

- Verginelli I. (2012). Il software di analisi di rischio Risk-net. Workshop "Il software di analisi di rischio sanitario-ambientale Risk-net (D.Lgs. 152/2006)" INAIL. Rome (Italy), January 2012.

- Verginelli I. (2012). Metodologie di valutazione del rischio chimico per i siti contaminati e per le discariche. "Settimana Ambiente 2012" conference. Milan (Italy), March 2012.

- Verginelli I., R. Baciocchi (2012). Modellazione della attenuazione naturale durante la migrazione di VOC verso gli ambienti confinati. Proceedings of the Workshop "Siti Contaminati. Esperienze negli interventi di risanamento" (SiCon 2012). Taormina (Italy), February 2012.

- Verginelli I., Baciocchi R. (2012). Caratteristiche e peculiarità del software Risk-net per l'applicazione dell'analisi di rischio ai siti contaminati. Proceedings of the Workshop "Siti Contaminati. Esperienze negli interventi di risanamento" (SiCon 2012). Taormina (Italy), February 2012.

- Pantini S., Lombardi F., Verginelli I. (2012). Water-Balance Model For Predicting The Leachate Production In Landfills. Accepted for oral presentation to ISWA 2012 conference. Florence (Italy).

***Tecnical Reports***

- Baciocchi R., Verginelli I. (2008). Stato dell'arte in tema di applicazione dell'Analisi di Rischio. Technical report produced for eni Refining & Marketing.

- Baciocchi R., Verginelli I. (2010). Attenuazione Naturale Intrinseca governata dall'Analisi di Rischio. Technical report produced for eni Refining & Marketing.

- Verginelli I. (2011). Risk-net, Manuale d'uso. Technical report for the RECONnet network (Rete Nazionale sulla gestione e la Bonifica dei Siti Contaminati).

- Berardi S., Forni A., Sconocchia A., Traversa A., Verginelli I., Villani I. (2012). Validazione del software Risk-net". Technical report for the RECONnet network (Rete Nazionale sulla gestione e la Bonifica dei Siti Contaminati).

- Baciocchi R., Pantini S., Verginelli I. (2012). Definizione di metodologie di analisi del rischio connesso alla gestione dei siti contaminati. Technical report produced for Istituto eni Donegani.

***Tools***

- Verginelli I. (2011). Risk-net. Software and user guide. Reconnet.

- Verginelli I., Forni A. (2012). Leach8. Tool for the application of the risk-assessment procedure to leachate landfill. Reconnet.

# LIST OF ABBREVIATIONS

| | |
|---|---|
| API | American Petroleum Institute |
| ASTM | American Society for Testing and Materials |
| BTEX | Benzene, Toluene, Ethylbenzene, Xylene |
| CRS | Representative Source Concentration |
| $C_{sat}$ | Soil Saturation Concentration |
| CSC | Threshold Risk-Based Concentration Value |
| CSR | Threshold Risk Concentrations |
| DNAPL | Dense Non-Aqueous Phase Liquid |
| EPA | Environmental Protection Agency |
| F&T | Fate & Transport models |
| GW | Groundwater |
| HC < 12 | Light Weight Hydrocarbon |
| HC > 12 | Heavy Weight Hydrocarbon |
| HI | Hazard Index |
| ISPRA | National Higher Institute for Environmental Research |
| J&E | Johnson & Ettinger model |
| LNAPL | Light Non-Aqueous Phase Liquid |
| NA | Natural Attenuation |
| NAPL | Non-Aqueous Phase Liquid |
| PAHs | Polycyclic Aromatic Compounds |
| POC | Point of compliance |
| POE | Point of exposure |
| R | Carcinogenic Risk |
| RBCA | Risk-Based Corrective Actions |
| Reconnet | Network on the management and remediation of contaminated sites |
| RfD | Reference Dose |
| SF | Slope Factor |
| SP | Subsurface Soil |
| SS | Surface Soil |
| VOC | Volatile Organic Compounds |

# NOMENCLATURE

## VAPOR INTRUSION (SECTION 1)

| *Symbol* | *Parameter* | *Units* |
|---|---|---|
| $A_b$ | Cross-sectional foundations area | $m^2$ |
| $C_0$ | Concentration at the bottom of the building | $g/m^3$ |
| $C_a$ | Concentration at the aerobic to anaerobic interface | $g/m^3$ |
| $C_{indoor}$ | Indoor concentration | $g/m^3$ |
| $C_{O2,0}$ | Oxygen concentration at the bottom of the building | $g/m^3$ |
| $C_{O2,amb}$ | Oxygen ambient concentration | $g/m^3$ |
| $C_{O2,tresh}$ | Minimum $O_2$ to sustain aerobic biodegradation | $g/m^3$ |
| $C_{sat}$ | Saturation concentration in the soil | mg/kg |
| $C_{source,sg}$ | Soil-gas source concentration | $g/m^3$ |
| $C_{source,tot}$ | Total soil concentration | mg/kg |
| $C_{source,w}$ | Solute concentration | mg/l |
| $D_{air}$ | Diffusion coefficient in air | $m^2/s$ |
| $D^{eff}$ | Effective diffusion coefficient | $m^2/s$ |
| $D_{wat}$ | Diffusion coefficient in water | $m^2/s$ |
| $ER$ | Volume air exchanges per unit time | $s^{-1}$ |
| $f_{oc}$ | Organic carbon fraction | $g_{oc}/ g_{soil}$ |
| $H$ | Dimensionless Henry's constant | - |
| $h_{cap}$ | Thickness of the capillary fringe | m |
| $i$ | Versor of the vertical advective flow | - |
| $k_a$ | Inverse of the diffusive-aerobic reaction length | $m^{-1}$ |
| $k_{an}$ | Inverse of the diffusive-anaerobic reaction length | $m^{-1}$ |
| $K_{oc}$ | Organic carbon partition coefficient | (mg/kg)/(mg/l) |
| $k_v$ | Soil permeability to vapor flow | $m^2$ |
| $k_{wind}$ | Wind position-dependent coefficient | - |
| $L$ | Depth of the source from the bottom of the building | m |
| $L_a$ | Thickness of the aerobic soil layer | m |

| | | |
|---|---|---|
| $L_{an}$ | Thickness of the anaerobic soil layer | m |
| $L_{crack}$ | Foundations thickness | m |
| $L_{mix}$ | Building volume to foundation area ratio | m |
| $L_{vad}$ | Vadose zone thickness | m |
| $P_{wind}$ | Dynamic air pressure associated with wind | Pa |
| $Q_{cross}$ | Cross sectional flow | $m^3/s$ |
| $Q_s$ | Convective flow rate from the soil into the building | $m^3/s$ |
| $Q_{s/b}$ | Vertical pressure-driven advection flow | $m^3/s$ |
| $S$ | Solubility | mg/l |
| $S_{mix}$ | Effective solubility in the case of a mixture | mg/l |
| $T_{indoor}$ | Indoor temperature | K |
| $T_{soil}$ | Soil temperature | K |
| $v_D$ | Darcy velocity | m/s |
| $v_{wind}$ | Wind speed | m/s |
| $x$ | Vertical axis (x=0 at the bottom of the building) | m |
| $X_{crack}$ | Foundations perimeter | m |
| $Z_{crack}$ | Foundations depth | m |
| $Z_{sub}$ | Depth of the sub-slab region | m |
| $\gamma$ | Stochiometric Mass Ratio O2/CiHi | $g\text{-}O_2/g\text{-}C_iH_i$ |
| $\Delta p$ | Pressure difference between the soil and the building | Pa |
| $\eta$ | Areal cracks fraction of the foundation area | - |
| $\theta_a$ | Vapour-filled soil porosity | - |
| $\theta_e$ | Soil porosity | - |
| $\theta_w$ | Water-filled soil porosity | - |
| $\lambda_a$ | Aerobic biodegradation first-order rate constant | $s^{-1}$ |
| $\lambda_{an}$ | Anaerobic biodegradation first-order rate constant | $s^{-1}$ |
| $\Lambda_{base}$ | Zero-order baseline soil oxygen respiration | $mg_{O2}/g_{oc}/h$ |
| $\mu$ | Vapor viscosity | Pa · s |
| $\rho$ | Outdoor air density | $g/m^3$ |
| $\rho_s$ | Soil bulk density | $g/m^3$ |
| $\varphi_{CH4}$ | Stochiometric Mass Ratio $CH_4/C_iH_i$ | $g\text{-}CH_4/g\text{-}C_iH_i$ |

## EXPOSURE DURATION (SECTION 2)

| *Symbol* | *Parameter* | *Units* |
|---|---|---|
| $C_0$ | Initial Concentration | mg/L |
| $C_{poe}$ | Concentration at point of exposure | mg/L |
| $C_w$ | Concentration In Liquid Phase | g/m$^3$ |
| $E$ | Daily chronic contaminant exposure rate | mg/(kg x d) |
| $ED$ | Exposure Duration | years |
| $ED_{eff}$ | Average Exposure Duration | years |
| $f_{oc}$ | Mass Fraction of Organic Carbon | g/g |
| $HQ$ | Hazard Quotient | --- |
| $i$ | Groundwater gradient | m/m |
| $K_d$ | Soil / Water Partition Coefficient | L/kg |
| $K_d$* | Limit Soil / Water Partition Coefficient | L/kg |
| $K_{oc}$ | Organic Carbon / Water partition coefficient | mL/g |
| $K_s$ | Saturated Hydraulic Conductivity | cm/s |
| $M_s$ | Mass in soil sorbed phase | kg |
| $M_{tot}$ | Total mass initially present | kg |
| $M_{transp}$ | Mass transported | kg |
| $M_w$ | Mass in dissolved phase | kg |
| $Q$ | Groundwater Flow | m$^3$/sec |
| $R$ | Lifetime Cancer Risk | --- |
| $RfD$ | Reference Dose | mg/(kg x d) |
| $S_d$ | Thickness of source-zone area | cm |
| $SF$ | Slope Factor | 1/[mg/(kg x d)] |
| $SSTL$ | Site Specific Target Level | mg/kg or mg/L |
| $S_w$ | Length of source-zone area parallel to groundwater flow | cm |
| $t$ | Time | years |
| $U_{gw}$ | Ground water Darcy velocity | cm/d |
| $V$ | Source Volume | m$^3$ |
| $W_{gw}$ | Width of source-zone area | cm |
| $\theta_e$ | Soil Porosity | cm$^3$/cm$^3$ |
| $\rho_s$ | Dry Soil Bulk Density | g/cm$^3$ |

## LEACHING TO GROUNDWATER (SECTION 3)

| Symbol | Parameter | Units |
|---|---|---|
| $A$ | Source area | $m^2$ |
| $C_{free}$ | Free phase concentration | mg/kg |
| $C_{poe}$ | Concentration at the point of exposure | mg/L |
| $C_{sat}$ | Saturation concentration in the soil | mg/kg |
| $C_{source}$ | Source concentration | mg/kg |
| $C_{tot}$ | Total source concentration | mg/kg |
| $C_w$ | Solute Concentration | mg/L |
| $d_s$ | Source thickness | m |
| $D_w$ | Diffusion coefficient in water | $m^2/s$ |
| $f_{oc}$ | Organic carbon fraction | $g_{oc}/ g_{soil}$ |
| $H$ | Dimensionless Henry's constant | - |
| $h_{cr}$ | Wetting front suction head | m |
| $H_w$ | Ponding depth | m |
| i | Groundwater Gradient | - |
| $I_{ef}$ | Effective infiltration | m/s |
| $K_d$ | Soil sorbed - water partition coefficient | (mg/kg)/(mg/L) |
| $K_{sat}$ | Hydraulic Conductivity | m/s |
| $K_{sw}$ | Total Soil - water partition coefficient | (mg/kg)/(mg/L) |
| $LDF$ | Leachate Dilution Factor | - |
| $L_f$ | Depth of the water table from the bottom of the source | m |
| $R$ | Retardation coefficient | - |
| $RfD$ | Reference Dose | mg/(kg x d) |
| $S$ | Solubility | mg/l |
| $SF$ | Slope Factor | $[mg/(kg \times d)]^{-1}$ |
| $v_{gw}$ | Darcy velocity | m/s |
| $v_{leach}$ | Leaching velocity | m/s |
| $W$ | Width of source area | m |
| $\alpha_z$ | Dispersivity | m |
| $\delta_{gw}$ | Mixing zone depth | m |
| $\theta_a$ | Vapour-filled soil porosity | - |
| $\theta_e$ | Soil porosity | - |
| $\theta_w$ | Water-filled soil porosity | - |
| $\lambda$ | Biodegradation first-order rate constant | $d^{-1}$ |
| $\lambda_{source}$ | Biodegradation first-order rate constant in the source | $d^{-1}$ |
| $\rho_s$ | Soil bulk density | $g/ m^3$ |

# REFERENCES

Abreu L.D., Ettinger R., McAlary T. (2009). Simulated soil vapor intrusion attenuation factors including biodegradation for petroleum hydrocarbons. Ground Water Monit. Rem. 29, 105-117.

Abreu L.D., Johnson P.C. (2005). Effect of vapor source: building separation and building construction on soil vapor intrusion as studied with a three-dimensional numerical model. Environ. Sci. Technol. 39, 4550–4561.

Abreu L.D., Johnson P.C. (2006). Simulating the effect of aerobic biodegradation on soil vapor intrusion into buildings: Influence of degradation rate, source concentrations. Environ. Sci. Technol. 40, 2304–2315.

Andre L., Kedziorek M.A.M., Bourg A.C.M., Haeseler F., Blanchet D. (2009). A novel experimental procedure to investigate the biodegradation of NAPL under unsaturated conditions. Journal of Hydrology 370, 1–8.

API (2000). Non-Aqueous Phase Liquid (NAPL) Mobility Limits in Soil. American Petroleum Institute. Prepared by Brost E.J.; DeVaull G.E.

API (2001a). Predicting the Effect of Hydrocarbon and Hydrocarbon-Impacted Soil on Groundwater. American Petroleum Institute. Prepared by O'Reilly K.T.; Magaw R.I.; Rixey W.G.

API (2001b). Risk-Based Methodologies for Evaluating Petroleum Hydrocarbon Impacts. American Petroleum Institute. Publication 4709.

API (2009). BioVapor, A 1-D Vapor Intrusion Model with Oxygen-Limited Aerobic Biodegradation. American Petroleum Institute.

Aronson D., Citra M., Shuler K., Printup H., Howard P.H. (1998). Aerobic Biodegradation of Organic Chemicals in Environmental Media: A Summary of Field and Laboratory Studies. US Environmental Protection Agency, Athens, GA, USA.

Aronson D., Howard P.H. (1997). Anaerobic Biodegradation of Organic Chemicals in Groundwater: A Summary of Field and Laboratory Studies. Final Report. Prepared for the American Petroleum Institute, Washington, D.C.

Asante-Duah D.K. (1993). Hazardous Waste Risk Assessment. Lewis Publishers.

ASTM (1995). Standard Guide for Risk- Based Corrective Action Applied at Petroleum Release Sites. American Society for Testing and Materials, West Conshohocken, PA, E 1739–95 (1995, Re-approved 2002).

ASTM (1999). RBCA Fate and Transport Models: Compendium and Selection Guidance. American Society for Testing and Materials, West Conshohocken PA.

ASTM (2000). Standard Guide for Risk-Based Corrective Action. American Society for Testing and Materials. Standard E2081-00. West Conshohocken, PA.

Azadpour-Keeley A., Keeley J.W., Russell H.H., Sewell G.W. (2007). Monitored natural attenuation of contaminants in the subsurface: Applications. Ground Water Monit. Rem. 21 136 – 143.

Baciocchi R., Berardi S., D'Aprile L., Marella G., Musmeci L. (2005) Health risk analysis associated with contaminated sites: Italian guidelines. Proceedings of the 9th International FZK/TNO Conference on Soil-Water Systems, Bordeaux (France) October 3-7, 2005. p. 61-71.

Bekins B.A., Hostettler F.D., Herkelrath W.N., Delin G.N., Warren E., Essaid H.I. (2005). Progression of methanogenic degradation of crude oil in the subsurface. Environ. Geosci. 12, 139–152.

Blum P., Hunkeler D., Weede M., Beyer C., Grathwohl P., Morasch B. (2009). Quantification of biodegradation for o-xylene and naphthalene using first order decay models, Michaelis-Menten kinetics and stable carbon isotope. J Contam Hydrol. 105, 118-30.

Bockelmann A., Ptak T., Teutsch G. (2001). An analytical quantification of mass fluxes and natural attenuation rate constants at a former gasworks site. Journal of Contaminant Hydrology 53, 429–453.

Boopathy R. (2004). Anaerobic biodegradation of no. 2 diesel fuel in soil: a soil column study. Bioresource Technol. 94, 143–151.

Bozkurt O., Pennell K.G., Suuberg E.M. (2009). Simulation of the vapor intrusion process for nonhomogeneous soils using a three-dimensional numerical model. Ground Water Monit. Rem. 29, 92–104.

Brauner J.S., Widdowson M.A., Novak J.T., Love N.G. (2002). Biodegradation of a PAH Mixture by Native Subsurface Microbiota. Bioremediation Journal 6, 9-24.

Christensen T.H., Bjerg P.L., Kjeldsen P. (2000). Natural Attenuation: A Feasible Approach to Remediation of Ground Water Pollution at Landfills?. Ground Water Monit. Rem. 20, 69-77.

Clement T.P. (1997). A Modular Computer Code for Simulating Reactive Multispecies Transport in 3-Dimensional Groundwater Systems. PNNL-11720.

Cozzarelli M., Bekins B.A., Baedecker M.J., Aiken G.R, Eganhouse R.P., Tuccillo M.E. (2001). Progression of natural attenuation processes at a crude-oil spill site: I. Geochemical evolution of the plume. J. Contam. Hydrol. 53, 369-385.

D.Lgs. 04/08 (2008). Ulteriori disposizioni correttive ed integrative del decreto legislativo 3 aprile 2006, n. 152, recante norme in materia ambientale. Pubblicato nella Gazzetta Ufficiale n. 24 del 29 Gennaio 2008, Supplemento Ordinario n.24.

D.Lgs. 152/06 (2006). Norme in materia ambientale. Pubblicato nella Gazzetta Ufficiale N.88 del 14 Aprile 2006, Supplemento Ordinario n.96.

D.M. 471/99 (1999). Regolamento recante criteri, procedure e modalità per la messa in sicurezza, la bonifica e il ripristino ambientale dei siti inquinati, ai sensi dell'art.17 del D.Lgs. 5 febbraio 1997 n.22 e successive modificazioni e integrazioni.

D'Aprile L., Berardi S., Baciocchi R. (2008). Development of site-specific target levels for contaminated sites: Italian guidelines. Proceedings of the 10th FKZ/TNO conference on contaminated soils. Milan (Italy), June 2-6 2008.

D'Aprile L., Bonci L., Berardi S., Baciocchi R., Musmeci L. (2006). I nuovi criteri metodologici per l'applicazione dell'analisi di rischio. Convegno Internazionale "La bonifica dei siti contaminati: normative e tecnologie a confronto", Milano, 23-24 Novembre 2006.

Davis G.B., Patterson B.M., Tefry M.G. (2009). Evidence for instantaneous oxygen-limited biodegradation of petroleum hydrocarbon vapors in the subsurface. Ground Water Monit. Rem. 29, 126-137.

Dawson H.E., McAlary T. (2009). A compilation of statistics for VOCs from Post-1990 indoor air concentration studies in North American residences unaffected by subsurface vapor intrusion. Ground Water Monit. Rem. 29, 60–69.

DeVaull G. (2007). Indoor vapor intrusion with oxygen-limited biodegradation for a subsurface gasoline source. Environ. Sci. Technol. 41, 3241–3248.

DeVaull G., Ettinger R.A., Salanitro J.P., Gustafson J. (1997). Benzene, toluene, ethylbenzene and xylenes degradation in vadose zone soils during vapor transport: first-order rate constants. Proceedings of 1997 Petroleum Hydrocarbons and Organic Chemicals in Ground Water, APIrNGWA, Houston, Texas, November, pp. 365–379.

DeVaull G.E., Ettinger R.A., Gustafson J.B. (2002). Chemical vapor intrusion from soil or groundwater to indoor air: Significance of unsaturated zone biodegradation of aromatic hydrocarbons. Soil Sediment. Contam. 11, 625-641.

Domenico P.A. (1987). An analytical model for multidimensional transport of a decaying contaminant species. J. Hydrol. 91, 49 –58.

Dou J., Liu X., Hu Z., Deng D. (2008). Anaerobic BTEX biodegradation linked to nitrate and sulfate reduction. J. Hazard. Mater. 151, 720-729.

Ferguson C., Darmendrail D., Freier K., Jensen B.K., Jensen J., Kasamas H., Urzelai A., Vegter J. (1998). Risk Assessment for Contaminated Sites in Europe. Volume 1. Scientific Basis. LQM Press, Nottingham.

Fischer M.L., Bentley A.J., Dunkin K.A., Hodgson A.T., Nazaroff W.W., Sextro R.G., Daisey J.M. (1996). Factors affecting indoor air concentrations of volatile organic compounds at a site of subsurface gasoline contamination. Environ. Sci. Technol. 30, 2948-2957.

Foght J. (2008). Anaerobic biodegradation of aromatic hydrocarbons: pathways and prospects. J. Mol. Microb. Biotech. 15, 93-120.

Garbesi K., Sextro R.G. (1989). Modeling and field evidence of pressure driven entry of soil gas into a house through permeable belowgrade walls. Environ. Sci. Technol. 23, 1481–1487.

Gray N.D., Sherry A., Hubert C., Dolfing J., Head I.M. (2010). Methanogenic degradation of petroleum hydrocarbons in subsurface environments remediation, heavy oil formation, and energy recovery. Adv. Appl. Microbiol. 72, 137-61.

Green W.H., Ampt G.A. (1911). Studies on soil physics, part 1. The flow of air and water through soils. J. Agric. Sci. 4, 1-24.

Grillo G. (2003). L'analisi del rischio. in "La bonifica biologica di siti inquinati da idrocarburi", II edizione, a cura di EniTecnologie ed Eni Corporate University, ed. Hoepli, Milano, p. 31 (2003).

Grillo G., Pedroni P. (2007). Pollution processes in soil and water, monitoring and risk analysis. Encyclopaedia of Hydrocarbons Vol. III. Istituto della enciclopedia italiana fondata da Giovanni Treccani.

GSI (2003). RBCA tool kit for chemical releases. Houston (TX), GSI (Groundwater Service Inc.).

Haeseler F., Behar F., Garnier D., Chenet P.Y. (2010). First stoichiometric model of oil biodegradation in natural petroleum systems Part I – The BioClass 0D approach. Org. Geochem. 41, 1156–1170.

Harbaugh A.W., Banta E.R., Hill M.C., McDonald M.G. (2000). MODFLOW-2000, the U.S. Geological Survey modular ground-water model - User guide to modularization concepts and the Ground-Water Flow Process, U.S. Geological Survey. Open-File Report 00-92.

Hers I., Atwater J., Li L., Zapf-Gilje R. (2000). Evaluation of vadose zone biodegradation of BTX vapours. J. Contam. Hydrol. 46, 233–264.

Hers I., Zapf-Gilje R., Johnson P.C., Li L. (2003). Evaluation of the Johnson and Ettinger model for prediction of indoor air quality. Ground Water Monit. Rem. 23, 119-133.

Hohener P., Duwig C., Pasteris G., Kaufmann K., Dakhel N., Harms H. (2003). Biodegradation of petroleum hydrocarbon vapors: Laboratory studies on rates and kinetics in unsaturated alluvial sand. J. Contam. Hydrol. 66, 93-115.

ISPRA (2008). Methodological Criteria for Absolute Risk Analysis Application at Contaminated Sites. Italian Environmental Protection Agency and Technical Services. Available at: www.isprambiente.it.

ISS-ISPESL (2009). ISS/ISPESL Database. “Proprietà chimico-fisiche e tossicologiche dei contaminanti”.

Johnson P.C., Ettinger R.A. (1991). Heuristic model for predicting the intrusion rate of contaminant vapors into buildings. Environ. Sci. Technol. 25, 1445-1452.

Johnson P.C., Ettinger R.A., Kurtz J., Bryan R., Kester J.E. (2002). Migration of soil gas vapors to indoor air: determining vapor attenuation factors using a screening-level model and field data from the CDOT-MTL Denver, Colorado site. API Technical Bulletin No. 16, American Petroleum Institute: Washington, DC.

Johnson P.C., Kemblowski M.W., Johnson R.L. (1998). Assessing the significance of subsurface contaminant migration to enclosed spaces. Site-specific alternatives to generic estimates. API Publication 4674.

Johnson P.C., Lundegard P., Liu Z. (2006). Source zone natural attenuation at petroleum hydrocarbon spill sites—i: site-specific assessment approach. Ground Water Monit. Rem. 26, 82-92.

Kao C.M., Prosser J. (2001). Evaluation of natural attenuation rate at a gasoline spill site. Journal of Hazardous Materials 82, 275-289.

Karapanagioti H.K., Gaganis P., Burganos V.N. (2003). Modeling attenuation of volatile organic mixtures in the unsaturated zone: codes and usage. Environmental Modelling and Software 18, 329–337.

Kastanek F., Demnerova K., Pazlarova J., Burkhard J., Maleterova Y. (1999). Biodegradation of polychlorinated biphenyls and volatile chlorinated hydrocarbons in contaminated soils and ground water in field condition. International Biodeterioration and Biodegradation 44, 39-47.

Khan F.I., Husain T. (2001). Risk-based monitored natural attenuation - A case study, J. Hazard Mater. B85, 243–272.

Kool J., Huyakorn P., Sudicky E., Saleem Z. (1994). A composite modelling approach for subsurface transport of degrading contaminants from land-disposal sites. J. Contam. Hydrol. 17, 69-90.

Krylov V.V., Ferguson C.C. (1998). Contamination of Indoor Air by Toxic Soil Vapours: the Effects of Subfloor Ventilation and Other Protective Measures. Build. Environ.33, 331-347.

Kuntz D., Grathwohl P. (2009). Comparison of steady-state and transient flow conditions on reactive transport of contaminants in the vadose soil zone. J. Hydrol. 369, 225-233.

Lahvis M.A., Baehr A.L., Baker R.J. (1999). Quantification of aerobic biodegradation and volatilization rates of gasoline hydrocarbons near the water table under natural attenuation conditions. Water Resour. Res. 35, 753-765.

Lee C.H., Lee J.Y., Cheon J.Y., Lee K.K. (2001). Attenuation of Petroleum Hydrocarbons in Smear Zones: A Case Study. J. Environ. Eng. 127, 639-647.

Lundegard P., Johnson P.C. (2006). Source zone natural attenuation at petroleum hydrocarbon spill sites II: application to a former oil field. Ground Water Monit. Rem. 26, 93-106.

Lundegard P., Johnson P.C., Dahlen P. (2008). Oxygen transport from the atmosphere to soil gas beneath a slab on-grade foundation overlying petroleum-impacted soil. Environ. Sci. Technol. 42, 5534–5540.

Luo H., Dahlen P., Johnson P.C., Peargin T., Creamer T. (2009). Spatial variability of soil-gas concentrations near and beneath a building overlying shallow petroleum hydrocarbon–impacted soils. Ground Water Monit. Rem. 29, 81-91.

McHugh T.E., De Blanc P.C., Pokluda R.J. (2006). Indoor air as a source of voc contamination in shallow soils below buildings. Soil Sediment Contam.15, 103–122.

Millington R.J., Quirk J.M. (1961). Permeability of porous solids. Trans. Faraday Soc. 57, 1200-1207.

Mills W.B., Liu S., Rigby M.C., Brenner D. (2007). Time-variable simulation of soil vapor intrusion into a building with a combined crawl space and basement. Environ. Sci. Technol. 41, 4993-5001.

Molins S., Mayer K.U., Amos R.T., Bekins B.A. (2010). Vadose zone attenuation of organic compounds at a crude oil spill site - Interactions between biogeochemical reactions and multicomponent gas transport. J. Contam. Hydrol. 112, 15-29.

Mulligan C.N., Yong R.N. (2004). Natural attenuation of contaminated soils. Environ. Int. 30, 587–601.

Nazaroff W.W. (1992). Radon Transport from Soil to Air. Rev. Geophys. 30, 137-160.

Nazaroff W.W., Lewis S.R., Doyle S.M., Moed B.S., Nero A.V. (1987). Experiments on pollutant transport from soil into residential basements by pressure-driven airflow. Environ. Sci. Technol. 5, 459-466.

Newell C.J., Connor J.A. (1998). Characteristics of Dissolved Petroleum Hydrocarbon Plumes. API.

Parker J.C. (2003). Physical processes affecting natural depletion of volatile chemicals in soil and groundwater. Vadose Zone J. 2, 222–230.

Patterson B.M., Davis G.B. (2009). Quantification of vapor intrusion pathways into a slab-on-ground building under varying environmental conditions. Environ. Sci. Technol. 43, 650-656.

Prommer H., Barry D.A., Davis G.B. (2002). Modelling of physical and reactive processes during biodegradation of a hydrocarbon plume under transient groundwater flow conditions. J. Contam. Hydrol. 59, 113-131.

Provoost J., Cornelis C. and Swartjes F. (2006), Comparison of Soil Clean-up Standards for Trace Elements Between Countries: Why do they differ?. J. Soils Sediments 6, 173-181.

Provoost J., Reijnders L., Swartjes F., Bronders J., Seuntjens P., Lijzen J. (2007). Accuracy of seven vapor intrusion algorithms for VOC in groundwater. J. Soils Sediments 9, 62–73.

Quercia F. (2008). I nuovi criteri per l'analisi di rischio dei siti contaminati introdotti dal D.Lgs n° 4/2008. Ambiente & Sviluppo, p. 332.

Ravi. V., Williams J. R. (1998). Estimation Of Infiltration Rate In The Vadose Zone: Compilation Of Simple Mathematical Models - Volume I. U.S. Environmental Protection Agency, Washington, D.C., EPA/600/R-97/128a (NTIS 98-142474).

Revzan K.L., Fisk W.J., Gadgil A.J. (1991). Modelling Radon Entry into Houses with Basements: Model Description and Verification. Indoor Air 2, 173-189.

Rifai H.S., Newell C.J., Gonzales J.R., Wilson J.T. (2000). Modeling natural attenuation of fuels with BIOPLUME III, J. Environ. Eng. 126, 428– 38.

Rivett M.O., Wealthall G.P., Dearde R.A., McAlary T.A. (2011). Review of unsaturated-zone transport and attenuation of volatile organic compound (VOC) plumes leached from shallow source zones. J. Contam. Hydrol. 123, 130–156.

Robinson A.L., Sextro R.G., Fisk W.J. (1997). Soil-gas entry into an experimental basement driven by atmospheric pressure fluctuations. Measurements, spectral analysis, and model comparison. Atmos. Environ. 31, 1477-1485.

Roggemans S., Bruce C.L., Johnson P.C., Johnson R.L. (2001). Vadose zone natural attenuation of hydrocarbon vapors: an empirical assessment of soil gas vertical profile data. American Petroleum Institute (API), No. 15.

Rugner H., Finkel M., Kaschl A., Bittens M. (2006). Application of monitored natural attenuation in contaminated land management - A review and recommended approach for Europe. Environ. Sci. Policy 9, 568 – 576.

Sager S.L. (2005). Risk Based Corrective Action (RBCA). Encyclopedia of Toxicology (2005) 733-736.

Salminen J.M., Tuomi P.M., Suortti A.M., Jørgensen K.S. (2004). Potential for aerobic and anaerobic biodegradation of petroleum hydrocarbons in boreal subsurface. Biodegradation 15, 29-39.

Schreiber M.E., Carey G.R., Feinstein D.T., Bahr J.M. (2004). Mechanisms of electron acceptor utilization: implications for simulating anaerobic biodegradation. J. Contam. Hydrol. 73, 99-127.

Shih T., Rong Y., Harmon T., Suffet M. (2004). Evaluation of the impact of fuel hydrocarbons and oxygenates on groundwater resources. Environ. Sci. Technol. 38, 42-48.

Spence L.R., Walden T. (2001). $RISC_4$ - User's Manual. British Petroleum

Thiele-Bruhn S. and Brümmer G.W. (2005). Kinetics of Polycyclic Aromatic Hydrocarbon (PAH) Degradation in Long-term Polluted Soils during Bioremediation. Plant and Soil 275, 31-42.

Tillman Jr. F.D., Weaver J.W. (2006). Uncertainty from synergistic effects of multiple parameters in the Johnson and Ettinger (1991) vapor intrusion model. Atmos. Environ. 40, 4098–4112.

Troldborg M., Binning P.J., Nielsen S., Kjeldsen P., Christensen A.G. (2009). Unsaturated zone leaching models for assessing risk to groundwater of contaminated sites. J. Contam. Hydrol. 105, 28-37.

U.S.EPA (1989). Risk Assessment Guidance for Superfund, Vol. 1: Human Health Evaluation Manual, Part A, EPA/540/1-89/002.

U.S.EPA (1996). BIOSCREEN - Natural Attenuation Decision Support System. User's Manual Version 1.3. EPA/600/R-96/087.

U.S.EPA (1999). Monitored Natural Attenuation of Petroleum Hydrocarbons. EPA/600/F-98/021.

U.S.EPA (2000). BIOCHLOR - Natural Attenuation Decision Support System. User's Manual Version 1.0. EPA/600/R-00/008.

Unlu K., Demirekler E. (2000). Modeling Water Quality Impacts of Petroleum Contaminated Soils in a Reservoir Catchment. Water Air Soil. Poll. 120, 169-193.

Vanderborght J., Vereecken H. (2007). Review of dispersivities for transport modelling in soils. Vadose Zone J. 6 (1), 29–52.

VanGenuchten M.Th. (1980). A Closed-form Equation for Predicting the Hydraulic Conductivity of Unsaturated Soils. Soil Sci. Soc. Am. J. 44, 892-898.

WASY (2006). FEFLOW 5.3: User Manual. WASY GmbH Berlin.

Yu S., Unger A.J.A., Parker B. (2009). Simulating the fate and transport of TCE from groundwater to indoor air. J. Contam. Hydrol. 107, 140-161.